



**HAL**  
open science

# Multicast and Broadcast in wireless OFDM systems

José Antonio Saavedra Navarrete

► **To cite this version:**

José Antonio Saavedra Navarrete. Multicast and Broadcast in wireless OFDM systems. Other [cond-mat.other]. Université Paris Sud - Paris XI, 2012. English. NNT : 2012PA112256 . tel-00757636

**HAL Id: tel-00757636**

**<https://theses.hal.science/tel-00757636>**

Submitted on 27 Nov 2012

**HAL** is a multi-disciplinary open access archive for the deposit and dissemination of scientific research documents, whether they are published or not. The documents may come from teaching and research institutions in France or abroad, or from public or private research centers.

L'archive ouverte pluridisciplinaire **HAL**, est destinée au dépôt et à la diffusion de documents scientifiques de niveau recherche, publiés ou non, émanant des établissements d'enseignement et de recherche français ou étrangers, des laboratoires publics ou privés.

UNIVERSITE PARIS-SUD

ÉCOLE DOCTORALE : STITS  
Laboratoire des signaux et systèmes -SUPELEC

*DISCIPLINE: PHYSIQUE*

THÈSE DE DOCTORAT

soutenue le 19/10/2012

par

José SAAVEDRA

Multidiffusion et diffusion  
dans les systèmes OFDM sans fil

**Directeur de thèse :**  
**Co-Encadrant :**

Pierre DUHAMEL  
Anthony BUSSON

Directeur de recherche (LSS - SUPELEC)  
Professeur (Université de Lyon 1)

**Composition du jury :**

*Président du jury :*  
*Rapporteurs :*

Véronique VEQUE  
Anissa MOKRAOUI  
Jean-Pierre CANCES  
Benoit GELLER  
Véronique VEQUE

Professeur (Université de Paris Sud)  
Maitre de conférences (Université Paris 13)  
Professeur (Université de Limoges)  
Professeur (ENSTA Paris-TECH)  
Professeur (Université de Paris Sud)

*Examineurs :*

UNIVERSITÉ PARIS-SUD 11UFR Sciences  
École Doctorale STITS

## THÈSE DE DOCTORAT

Présentée pour l'obtention du Grade de Docteur en Sciences  
de l'UNIVERSITÉ PARIS-SUD 11

par

José Antonio Saavedra Navarrete

## MULTICAST AND BROADCAST IN WIRELESS OFDM SYSTEMS

Soutenue le 19/10/2012 devant le jury composé de:

|                    |                    |
|--------------------|--------------------|
| Anissa Mokraoui    | Rapporteur         |
| Jean-Pierre Cancès | Rapporteur         |
| Benoit Geller      | Examineur          |
| Veronique Vèque    | Examineur          |
| Anthony Busson     | Co-encadrant       |
| Pierre Duhamel     | Directeur de thèse |

# Abstract

In an increasing number of situations, a single signal must reach several users in the same cell. Classically, in wireless communication systems, this was addressed by establishing several point to point communications, with full knowledge of the Channel State Information (CSI). In recent standard evolutions, a "broadcasting" option has been introduced, in which the given signal has the potential of addressing all users in the cell, without any information about CSI. However, there is an intermediate situation (i.e. "multicast") in which the signal is sent to a much smaller number of specific users, with full knowledge of the CSI. We are interested in providing tools for estimating the number of users constituting the frontiers between these three situations. The main tool which is used for making full use of CSI in an OFDM context is power allocation. Therefore, this thesis first concentrates on the effectiveness of the power allocation on the OFDM systems on the downlink in a "multicast" situation, and then provides some tools for an analytic tuning of a broadcast situation.

A review over the OFDM system is first made. We investigate how a single carrier transmission works and illustrate how the OFDM technique improves the transmission of high data rates on a frequency selective channel. A state of the art over the Multi-User Single Input Single Output (MU-SISO) and Multi-User Multiple Input Multiple Output (MU-MIMO) is then provided. We review the various expressions of capacity

of the cited systems, based on the availability of CSI.

In the MU-SISO OFDM system we propose an efficient algorithm to allocate the power on each subcarrier when we want to send the same modulated symbol to several users. The improvements are shown in a statistical way. In the MU-MIMO OFDM case, we propose an algorithm that exploits the well known zero forcing precoding method to share the power transmission over the subcarrier over the different antennas. Finally, we revisit the MU SISO-OFDM case in a broadcast setting, via a more analytic approach of the capacity. In a broadcast situation the target is to calculate the evaluate in an objective way the coverage of the system for a given power. This is done by using stochastic geometry: we take in account the probability density distribution (pdf) of the spatial placement of the users, model the pdf of the capacity and present numerical results on the coverage of the MU-SISO scheme.

In all the cases, we simulate the power allocation algorithm over the various scenarios and we perform many realizations of channels. The histogram and the statistics thus obtained constitute an excellent tool to compare and decide when the base station continues or not performing the power allocation (multicast) instead of uniform power allocation (broadcast).

Keywords: OFDM, Power allocation, Multi-User, Broadcast, Wireless Multicast, SISO, MIMO.

# Acknowledgments

I would like to thank several people that shared with me this unforgettable trip. First, I would like to thank my advisor Prof. Pierre Duhamel who was a clever presence during the period of my PhD development. I am grateful to have been guided by him over the subject by his noteworthy experience. I appreciate specially the opportunity to discover many aspects of the telecommunications world.

I also want to acknowledge Anissa Mokraoui and Jean Pierre Cances, the reviewers of my thesis manuscript. Their insightful comments and suggestions were very helpful for improving the final work. In the same line, I am thankful to share with Anthony Busson a part of this work. His comments and his sharp mind were very important for the discussion of different topics who have enriched my work. I do not forget Veronique Vèque and Benoît Geller whom were an active part of the jury.

A special thanks to the LSS office staff, whom were my first contact with the laboratory and helped me in many situations throughout my stay in France, from the beginning and even before my arrival. Special thoughts to Odette Leroux, Maryvonne Giron, Frederic Deprez and Frank Guimonnet.

Thank to my office-mates, Tanja Karp, Anissa Mokraoui, Zeina Mheich y Usman Ali, whom were kind companions and helped me to spread out my mind with their presence, sharing their own culture and experience on the research.

Special thoughts to Pamela Guevara, Amadou Diallo, Veronica Belmega and Elsa Dupraz whom gave me friendship, motivation and support during different moments of my stay in the laboratory. Thank you to all my friends at LSS and SUPELEC, with whom I could share more than the scientific experience, and enjoy several social activities, beer, wine, short and long discussions about almost everything...I am sure that if they read these acknowledgement, they know they are present in my thoughts and my heart.

Defeat (The Madman (1918) - Kahlil Gibran )

Defeat, my Defeat, my solitude and my aloofness,  
You are dearer to me than a thousand triumphs,  
And sweeter to my heart than all world-glory.

Defeat, my Defeat, my self-knowledge and my defiance,  
Through you I know that I am yet young and swift of foot  
And not to be trapped by withering laurels.  
And in you I have found aloneness  
And the joy of being shunned and scorned.

Defeat, my Defeat, my shining sword and shield,  
In your eyes I have read That to be enthroned is to be enslaved,  
And to be understood is to be levelled down,  
And to be grasped is but to reach ones fullness  
And like a ripe fruit to fall and be consumed.

Defeat, my Defeat, my bold companion,  
You shall hear my songs and my cries an my silences,  
And none but you shall speak to me of the beating of wings,  
And urging of seas, And of mountains that burn in the night,  
And you alone shall climb my steep and rocky soul.

Defeat, my Defeat, my deathless courage,  
You and I shall laugh together with the storm,  
And together we shall dig graves for all that die in us,  
And we shall stand in the sun with a will, And we shall be dangerous.



Défaite (Le Fou (1918) - Kahlil Gibran)

Défaite, ma défaite, ma solitude et mon isolement,  
Tu es pour moi plus chère que mille triomphes  
Et plus douce pour mon coeur que toute la gloire du monde.

Défaite, ma défaite, mon défi et ma connaissance de moi-même,  
Grâce à toi je sais que je suis encore un jeune homme au pied agile,  
Et qui ne se laisse attirer par des lauriers fanés.  
Et en toi j'ai trouvé ma solitude  
Et la joie d'être éloigné et dédaigné.

Défaite, ma défaite, mon épée brillante et mon bouclier,  
Dans tes yeux j'ai lu que celui qui cherche le trône se rend lui-même esclave,  
Et celui qui veut-être compris se ravale  
Et pour scruter le fond d'un être, il nous faut atteindre sa plénitude  
Et tel un fruit mûr tomber et être consommé.

Défaite, ma défaite, ma compagne audacieuse,  
Tu entendras mon chant, mes cris et mes silences,  
Et nul, à part toi, ne me parleras du battement d'ailes,  
Et de l'agitation des mers, et des montagnes qui brûlent dans la nuit.  
Et toi, seule, grimperas les chemins escarpés et rocheux de mon âme.

Défaite, ma défaite, mon courage immortel,  
Toi et moi rirons ensemble avec la tempête.  
Et ensemble nous creuserons des tombes pour tout ce qui meurt en nous.  
Et nous nous tiendrons face au soleil avec obstination, Et nous serons dangereux.

# Table of Contents

|  |            |
|--|------------|
| <b>Abstract</b>  | <b>i</b>   |
| <b>Acknowledgments</b>   | <b>iii</b> |
| <b>Table of Contents</b>   | <b>vii</b> |
| <b>List of Tables</b>  | <b>ix</b>  |
| <b>List of Figures</b>   | <b>x</b>   |
| <b>Chapter 1:</b>  |            |
| <b>Introduction</b> . . . . .  | <b>51</b>  |
| 1.1 Motivation . . . . .   | 51         |
| 1.2 Problems . . . . .   | 54         |
| 1.3 Objectives and Contributions . . . . .   | 57         |
| 1.4 Organization of the Thesis . . . . .   | 59         |
| 1.5 Notations . . . . .  | 60         |
| 1.5.1 Time domain, Frequency domain notations . . . . .                                  | 61         |
| 1.5.2 SISO System Model . . . . .  | 61         |
| 1.5.3 MIMO System Model . . . . .  | 62         |
| <b>Chapter 2:</b>  |            |
| <b>Concepts in wireless communications systems</b> . . . . .                             | <b>65</b>  |
| 2.1 Transmission in wireless communications . . . . .                                    | 66         |
| 2.1.1 Basic principles of OFDM . . . . .   | 67         |
| 2.1.2 MIMO communication Model . . . . .   | 79         |
| 2.2 Multi-User SISO communication system . . . . .                                       | 85         |
| 2.2.1 Channel capacity of MU-SISO broadcast channel . . . . .                            | 86         |
| 2.2.2 Channel capacity of MU-SISO multiple access channel . . . . .                      | 87         |
| 2.2.3 Duality of degraded Broadcast Channel and the Multiple Access<br>Channel . . . . . | 88         |
| 2.2.4 Discussion on Downlink and Uplink . . . . .  | 89         |

|                   |  |            |
|-------------------|--|------------|
| 2.3               | Multi-User MIMO . . . . .  | 89         |
| 2.3.1             | Channel capacity of MU-MIMO Broadcast . . . . .                    | 89         |
| 2.3.2             | Channel capacity of MU-MIMO Multiple Access Channel . . . . .      | 93         |
| 2.3.3             | MU-MIMO BC and MAC duality . . . . .                               | 94         |
| 2.3.4             | Discussion on Multi-User MIMO systems . . . . .                    | 94         |
| 2.4               | Channel modeling . . . . .   | 94         |
| 2.4.1             | Large-scale fading . . . . .                                       | 95         |
| 2.4.2             | Small-scale fading . . . . .                                       | 97         |
| 2.4.3             | Channel Model . . . . .  | 99         |
| <b>Chapter 3:</b> |  |            |
|                   | <b>Multicast or Broadcast using MU-SISO OFDM systems</b> . . . . . | <b>101</b> |
| 3.1               | System sum-capacity . . . . .                                      | 103        |
| 3.2               | SISO optimal power allocation algorithm . . . . .                  | 105        |
| 3.3               | Numerical results . . . . .  | 109        |
| 3.4               | Conclusion . . . . .   | 111        |
| <b>Chapter 4:</b> |  |            |
|                   | <b>Power allocation in MU-MIMO OFDM systems</b> . . . . .          | <b>116</b> |
| 4.1               | Notations and problem statement . . . . .                          | 117        |
| 4.2               | Block diagonalization . . . . .                                    | 119        |
| 4.3               | Sum-rate maximization . . . . .                                    | 122        |
| 4.4               | Numerical results . . . . .  | 125        |
| 4.5               | Conclusion . . . . .   | 127        |
| <b>Chapter 5:</b> |  |            |
|                   | <b>OFDM Realistic Coverage</b> . . . . .                           | <b>130</b> |
| 5.1               | OFDM coverage modeling . . . . .                                   | 131        |
| 5.1.1             | Outage probability . . . . .                                       | 135        |
| 5.1.2             | Modeling the capacity pdf . . . . .                                | 137        |
| 5.2               | Numerical results . . . . .  | 139        |
| 5.2.1             | Numerical results at 10 dB . . . . .                               | 140        |
| 5.2.2             | Numerical results at 15 dB . . . . .                               | 145        |
| 5.3               | Conclusion . . . . .   | 147        |
| <b>Chapter 6:</b> |  |            |
|                   | <b>Summary and Conclusions</b> . . . . .                           | <b>150</b> |
|                   | <b>Bibliography</b> . . . . .                                      | <b>154</b> |

# List of Tables

|     |   |     |
|-----|---|-----|
| 1   | résultats pour le schéma MU-MIMO OFDM . . . . . | 32  |
| 2.1 | Power Delay Profile Model E [41] . . . . .      | 98  |
| 2.2 | 802.11a/n Parameters . . . . .                  | 100 |
| 4.1 | Multiuser MIMO Results . . . . .                | 127 |

# List of Figures

|     |  |     |
|-----|--|-----|
| 2   | Distribution d'un canal à multi-trajets . . . . .  | 36  |
| 3   | PDF de la capacité pour un scenario donné . . . . .  | 40  |
| 1   | Histogrammes pour 5 Utilisateurs a 300 [m] de la station de base . . .   | 47  |
| 4   | Capacité moyenne, Capacité de coupure pour 95 % et moyenne de<br>Capacité sur 95 % pour un SNR 10 dB . . . . . | 48  |
| 5   | Pourcentage d'amélioration à 10 dB . . . . .   | 49  |
| 6   | Capacité optimisée et de diffusion pour un utilisateur á 10 dB . . . .   | 50  |
| 2.1 | Single Carrier Communication . . . . .   | 68  |
| 2.2 | OFDM Modulation / Demodulation . . . . .   | 73  |
| 3.1 | Histograms for 1 User at 100 [m] from access point . . . . .   | 113 |
| 3.2 | Histograms for 5 User at 100 [m] from access point . . . . .   | 114 |
| 3.3 | Histograms for 5 User at 300 [m] from access point . . . . .   | 115 |
| 4.1 | Histograms for 3 User at 200 [m] from access point . . . . .   | 129 |
| 5.1 | Multipath Distribution . . . . .   | 134 |
| 5.2 | PDF of the capacity of a given scenario . . . . .  | 139 |
| 5.3 | Mean capacity, Outage capacity for 95 % and Mean over 95 % for SNR<br>10 dB . . . . .                          | 141 |
| 5.4 | Percentage increase at 10 dB . . . . .   | 143 |
| 5.5 | Optimized and Broadcast Capacity for one user at 10 dB . . . . .   | 144 |
| 5.6 | Mean capacity, Outage capacity for 95 % and Mean over 95 % for SNR<br>15 dB . . . . .                          | 146 |
| 5.7 | Percentage increase at 15 dB . . . . .   | 149 |

# Résumé en Français

## Motivation, problèmes et contributions

Dans les dernières années l'évolution des besoins de la part des utilisateurs associée à une augmentation de l'offre des opérateurs mobiles, a entraîné une demande croissante de services sur les dispositifs mobiles. Ceci pose de nouveaux problèmes de recherche scientifique et industrielle pour offrir de meilleurs produits répondant à cette nouvelle demande. Les services les plus demandés sont liés au streaming multimédia et au téléchargement. De telles applications nécessitent une très bonne qualité de service, ce qui signifie un haut débit de données, une communication fiable et une utilisation efficace de la puissance. Le signal transmis de la station de base vers l'utilisateur subit une atténuation et propagation par trajets multiples, qui peuvent dégrader le service. Afin d'avoir un système de communication efficace, capable de faire face aux difficultés apportés par les communications sans fil, les standards récents de communications conçus pour la transmission de paquets sur les canaux sans fils (tels que : IEEE 802.16, IEEE 802.11 ou des technologies mobiles comme : 3GPP Long Term Evolution -LTE-), utilisent les modulations multi-porteuses Orthogonal Frequency Division Multiplexing (OFDM) en vue d'obtenir une communication fiable sur la liaison descendante.

Le principe de la technologie OFDM consiste à répartir le flux de données sur plusieurs sous-porteuses orthogonales [44]. Cela permet de transformer un canal sélectif en fréquence de large bande, en plusieurs canaux plats orthogonaux de bande étroite. Il est ainsi possible de traiter les sous-canaux indépendamment avec des égaliseurs et décodeurs simples. Un autre avantage est que cela permet d'effectuer la répartition de puissance sur l'ensemble des sous-canaux. On peut tirer partie de cette technologie dans les environnements difficiles comme les zones urbaines. Celles-ci produisent des retards, de l'interférence, du bruit et de l'atténuation sur le signal, ainsi que de l'interférence de entre symboles.

La technologie multi-porteuse OFDM a été initialement introduite pour les appareils munis d'une antenne, ce qui est encore la situation la plus fréquente. Les utilisateurs ont des smartphones, tablettes et netbooks qui sont pour la plupart d'entre eux équipés d'une antenne. Toutefois, une attention spéciale a été accordée dernièrement aux systèmes " Multiple Input Multiple Output (MIMO) " qui mettent en oeuvre des antennes multiples à l'émetteur et au récepteur. En effet, il a été démontré que les technologies MIMO permettent de transmettre des débits plus élevés avec la même énergie par rapport aux transmissions avec une seule antenne, également connu sous le nom de " Single Input Single Output(SISO) ".

Une utilisation classique des ressources est d'établir une liaison point à point entre la station de base et chaque utilisateur, même s'ils souhaitent recevoir le même signal. La situation de diffusion (Broadcast) peut être considérée comme un extrême opposé avec celle de multiples liaisons point a point, car il est probable que dans une station de base donnée le nombre d'utilisateurs simultanés d'un service vidéo ne sera pas trop grand. L'inconvénient de la situation de diffusion est qu'aucune connaissance

de canal n'est disponible à l'émetteur, ce qui empêche un réglage de la puissance de transmission sur des canaux réels. Nous allons considérer dans notre travail que le même service est requis par un groupe d'utilisateurs à partir de la station de base.

Ce problème est connu dans les réseaux câblés sous le nom de multidiffusion (multicast): lorsque un utilisateur souscrit aux mêmes services que d'autres personnes, le réseau répond à cette demande au moindre coût en partageant les ressources.

Dans ce travail, nous utilisons la théorie de l'information pour modéliser la situation de multidiffusion sur un système de communication sans fil OFDM. De toute évidence, un service de multidiffusion peut être modélisé comme étant une situation broadcast (ici, "broadcast" est dans le sens de la théorie de l'information). En théorie de l'information le canal de diffusion (broadcast channel) a été formalisé par Cover [16] et révisé par Van der Meulen dans [70].

Nous considérons que l'émetteur connaît la réalisation du canal (Channel State Information, CSI), de chaque utilisateur. Cela nous permet de développer des algorithmes qui optimisent la capacité, en prenant en compte que la puissance disponible à la station de base est limitée.

Dans le cas SISO [77], la technique du " bit loading " et l'allocation de puissance sur chaque sous-porteuse sont traitées, l'allocation étant faite pour un ensemble d'utilisateurs. Dans [34], les données de différents utilisateurs sont additionnées dans chaque sous-porteuse, une fonction de débit est déduite et optimisé par la méthode de Lagrange.

Dans le cas de la transmission multi-utilisateur dans un système MIMO-OFDM avec Channel State Information (CSI) à l'émetteur et au récepteur, le précodage " zéro forcing " est utilisé pour approcher la région de capacité du " dirty paper coding



” [12].

Dans cette thèse, l’allocation de puissance multi-utilisateurs pour un système OFDM-SISO et OFDM-MIMO sont étudiés tout d’abord, ce qui permet d’effectuer une étude statistique de la couverture de chaque schéma sur un canal réaliste. Ce travail apporte les outils nécessaires pour comparer les communications point à point, point à multipoints avec CSI connus, et point à multipoints avec CSI inconnus.

Pour le modèle multi-utilisateurs-SISO-OFDM nous proposons un algorithme efficace pour l’allocation de puissance sur chaque sous-porteuse, dans le cas où l’on veut envoyer le même bitstream imbriqué (”scalable”) modulé à chaque utilisateur. Les améliorations sont mises en évidence de manière statistique, basée sur les histogrammes.

Dans le cas multi-utilisateur-MIMO-OFDM, nous proposons une extension du travail de Kaviani [38] basé sur une approche du precodage ” Zero Forcing ” déjà étudié par [60, 13, 27, 12]. Enfin, nous fournissons des moyens de réglage pour la zone de couverture du cas classique de diffusion sans recourir à un grand nombre de simulations, au moyen d’outils de géométrie stochastique.

Dans tous les cas, nous simulons l’algorithme d’allocation de puissance sur les différents scénarios et effectuons de nombreuses réalisations de canaux. L’histogramme et les statistiques sont un outil pour comparer et décider du nombre d’utilisateurs à partir duquel la station de base continue ou non d’effectuer de l’allocation de puissance au lieu de la répartir uniformément sur tous les canaux.

## Background

La croissance du trafic de données demandé par les appareils mobiles a posé un grand défi pour l'industrie et le monde de la science. La flexibilité de l'OFDM permet de développer des algorithmes pratiques d'allocation de ressources. Notre objectif est de comparer l'efficacité de cette technique par rapport à celle à une seule porteuse. Nous étendons notre analyse au cas MIMO. Apparue en Décembre 1966, le papier précurseur de Chang [11] présente les principes de multiplexage orthogonal sur des données transmises sur multicanaux, pour une bande limitée. Cette technique a d'abord été mise en oeuvre par le biais de filtres analogiques, mais Weinstein [75] propose un algorithme numérique basé sur la transformée de fourier rapide (Fast Fourier Transform, FFT) et comprenant un intervalle de garde pour prévenir le chevauchement dans le domaine temporel. En 1980, Peled [52] introduit une extension cyclique dans le schéma numérique proposé par Weinstein [75]. Cela permet que la séquence reçue comporte exactement une période de la convolution cyclique de la séquence d'entrée par le canal ce qui permet à la FFT de diagonaliser exactement le canal. Ceci annule les interférences entre sous canaux.

La transmission sur une porteuse est fortement perturbée par l'interférence entre symboles (Inter Symbol Interference, ISI) lorsque le débit des données augmente. Il est possible de contourner ce problème avec des méthodes qui respectent le critère de Nyquist, mais la complexité de l'égaliseur augmente due au haut débit et le coût associé à la transmission devient prohibitif [12]. La transmission sur un canal sélectif en fréquence peut être combattue à l'aide de techniques multi-porteuses. Modulée sur des fréquences différentes, le canal peut être divisé en plusieurs sous-canaux plats à bande étroite. Puisque le débit total est partagé entre les sous-canaux, l'égalisation

est moins complexe. Cette configuration assure également une faible distorsion de la transmission de données dans le cas où l'orthogonalité entre les sous-porteuses est maintenu [12, 4, 44], ce qui est le cas en OFDM.

Le développement des techniques numériques permet actuellement d'effectuer cette décomposition et sa reconstruction via les algorithmes IFFT et FFT à l'aide d'un seul modulateur analogique haute fréquence. [75].

Des détails sur le fonctionnement de l'OFDM se trouvent dans le chapitre 2 dans la sous-section 2.1. Nous nous intéresserons aux résultats de capacité du canal lorsque nous considérons l'utilisation de cette technologie avec un intervalle de garde qui garantit l'orthogonalité des sous porteuses.

## SISO OFDM Capacité

Dans le cadre de la théorie de l'information, tous les signaux d'entrée sont supposés être gaussiens, car il est bien connu que ce choix maximise la capacité. Par conséquent, les résultats correspondants doivent être considérés comme des bornes supérieures des taux de transmission atteignables. Puisque dans le domaine fréquentiel les gains des canaux d'un système OFDM correspondent à un symbole modulé transmis, une transmission point à point peut être modélisée comme:

$$\mathbf{y} = \mathbf{H}\mathbf{x} + \mathbf{z} \tag{1}$$

Don  $\mathbf{y} = (y^{(1)}, \dots, y^{(N)})$  est le vecteur de bande de base complexe reçu. La matrice  $\mathbf{H}$  est la matrice de canal orthogonale, c'est une matrice diagonale dont les éléments représentent le gain complexe sur chaque sous-porteuse, comme indiqué ci-dessous:

$$\mathbf{H} = \begin{bmatrix} h^{(1)} & 0 & \dots & 0 \\ 0 & h^{(2)} & \ddots & \vdots \\ \vdots & \ddots & \ddots & 0 \\ 0 & \dots & 0 & h^{(N)} \end{bmatrix} \quad (2)$$

Le symbole transmis est  $\mathbf{X} = (x^{(1)}, \dots, x^{(N)}) \sim \mathbb{C}\mathcal{N}(0, S_x)$ , où  $S_x$  est la matrice de covariance diagonale du vecteur  $\mathbf{X}$ , les éléments de la diagonale sont les puissances mise sur chaque symbole modulé. Tels que:

$$S_x = \begin{bmatrix} p_1 & 0 & \dots & 0 \\ 0 & p_2 & \ddots & \vdots \\ \vdots & \ddots & \ddots & 0 \\ 0 & \dots & 0 & p_N \end{bmatrix} \quad (3)$$

Le signal reçu est affecté par un bruit blanc additif gaussien complexe  $Z \sim \mathbb{C}\mathcal{N}(0, S_z)$ . La matrice de covariance du bruit,  $S_z$ , pour ce modèle de canal parallèle, est diagonale puisque les canaux sont orthogonaux. L'information mutuelle  $I(\mathbf{x}; \mathbf{y})$  entre l'ensemble des signaux d'entrée et ceux reçus s'exprime comme suit:

$$I(\mathbf{x}; \mathbf{y}) = \frac{1}{N} \sum_{n=1}^N \log \left( 1 + \frac{|h^{(n)}|^2 p_n}{\sigma_z^2} \right) \quad \text{bits/s/Hz} \quad (4)$$

La somme des puissances sur les sous-porteuses doit satisfaire la contrainte sur la puissance :  $\sum_{n=1}^N p_n \leq P$ , où  $P$  est la puissance totale disponible à la station de base. Afin de maximiser l'information mutuelle, le problème est mis sous la forme d'un problème d'optimisation convexe[6]:

$$\min_{p_n} \left\{ -\frac{1}{N} \sum_{n=1}^N \log \left( 1 + \frac{|h^{(n)}|^2 p_n}{\sigma_z^2} \right) \right\} \quad (5)$$

$$\text{Subject to } \begin{cases} \sum_{n=1}^N p_n = P \\ -p_n \leq 0 \end{cases} \quad (6)$$

En faisant une optimisation Lagrangienne nous obtenons:

$$\frac{-1}{p_n + \frac{\sigma_z^2}{|h^{(n)}|^2}} + \lambda = 0 \quad (7)$$

En utilisant la positivité de la puissance mise sur chaque sous-porteuse, on obtient la formulation de l'algorithme "waterfilling". [17]:

$$p_n = \left( \frac{1}{\lambda} - \frac{\sigma_z^2}{|h^{(n)}|^2} \right)^+ \quad (8)$$

La fonction  $(\cdot)^+$  est :

$$(x)^+ = \begin{cases} x, & x \geq 0 \\ 0, & \text{otherwise} \end{cases} \quad (9)$$

La simplicité de cet algorithme permet une allocation optimale de la puissance, en supposant que l'état du canal est connu à l'émetteur.

## Modèle MIMO

La configuration Multiple Input Multiple Output (MIMO), permet d'augmenter le débit par rapport au cas SISO, en exploitant deux caractéristiques principales: le multiplexage et la diversité [29, 76]. Le multiplexage exploite la structure du gain du

canal pour augmenter le taux de données, car des flux de données indépendants sont transmis en parallèle en utilisant les différentes antennes. Les techniques de diversité visent à exploiter les informations de l'état du canal à l'émetteur ou au récepteur, ou les deux pour améliorer la fiabilité de transmission. Le modèle habituel présenté dans la littérature est le suivant:

$$\begin{pmatrix} y_1 \\ \vdots \\ y_R \end{pmatrix} = \begin{pmatrix} h_{11} & \dots & h_{1T} \\ \vdots & \ddots & \vdots \\ h_{R1} & \dots & h_{RT} \end{pmatrix} \begin{pmatrix} x_1 \\ \vdots \\ x_T \end{pmatrix} + \begin{pmatrix} z_1 \\ \vdots \\ z_R \end{pmatrix} \quad (10)$$

Ou simplement:

$$\mathbf{y} = \bar{\mathbf{H}}\mathbf{x} + \mathbf{z} \quad (11)$$

Où  $\mathbf{y}$  est un vecteur complexe qui modélise le récepteur avec  $R$  antennes. L'émetteur est modélisé par le vecteur complexe  $\mathbf{x}$ , de taille  $T$ . Le signal transmis est envoyé sur le canal représenté par la matrice  $\bar{\mathbf{H}}$  de taille  $R \times T$ .

Les possibilités offertes par ce schéma MIMO sont différentes si nous disposons de l'information sur l'état du canal à l'émetteur (CSIT) et/ou au niveau du récepteur (CSIR). Les premiers résultats en théorie de l'information sur le canal MIMO ont été publiés par Telatar et Foschini [65, 23]. Dans ces publications, l'information mutuelle pour des canaux statiques est donnée par:

$$I(\mathbf{x}; \mathbf{y}) = \log_2 \det \left( \mathbf{I}_R + \frac{1}{\sigma_z^2} \bar{\mathbf{H}}\mathbf{S}_x\bar{\mathbf{H}}^H \right) \quad (12)$$

où  $\mathbf{S}_x$  est la matrice de covariance du vecteur  $\mathbf{x}$ . L'information mutuelle  $I(\mathbf{x}; \mathbf{y})$  est optimale lorsque le vecteur d'entrée est gaussien complexe circulaire symétrique

de moyenne nulle [65]. La capacité est obtenue en maximisant l'information mutuelle sur les matrices de covariance  $\mathbf{S}_x$  qui satisfont les contraintes de puissance. C'est à dire:

$$C_{MIMO} = \max_{\mathbf{S}_x: \text{Tr}(\mathbf{S}_x) \leq P} \log_2 \det \left( \mathbf{I}_R + \frac{1}{\sigma_z^2} \bar{\mathbf{H}} \mathbf{S}_x \bar{\mathbf{H}}^H \right) \quad (13)$$

Une valeur optimale de la capacité  $C_{MIMO}$  sera conditionnée à la connaissance ou non de l'état du canal à l'émetteur. Nous verrons quelques résultats, mais de plus amples détails peuvent être trouvés dans [68, 65, 50, 29, 27, 23, 24].

### MIMO avec CSIT et CSIR

Supposons que l'état du canal est connu à l'émetteur et au récepteur, l'émetteur peut préparer la transmission sur la base de cette connaissance. Ceci est obtenu par l'intermédiaire d'une décomposition en valeurs singulières du canal:

$$\bar{\mathbf{H}} = \mathbf{U} \Sigma \mathbf{V}^H \quad (14)$$

où  $\mathbf{U} \in \mathbb{C}^{R \times R}$  and  $\mathbf{V} \in \mathbb{C}^{T \times T}$  sont des matrices unitaires, et  $\Sigma \in \mathbb{C}^{R \times T}$  est une matrice diagonale contenant les valeurs singulières du canal (la racine carrée des valeurs propres):  $\sqrt{\gamma_1} \geq \dots \geq \sqrt{\gamma_J}$ ,  $J = \text{Rank}(\bar{\mathbf{H}})$ . Les colonnes de  $\mathbf{U}$  sont les vecteurs propres de  $\bar{\mathbf{H}} \bar{\mathbf{H}}^H$ , tandis que les colonnes de  $\mathbf{V}$  sont les vecteurs propres de  $\bar{\mathbf{H}}^H \bar{\mathbf{H}}$ . Si l'on remplace dans l'équation correspondante, nous obtenons:

$$I(\mathbf{x}; \mathbf{y}) = \log_2 \det \left( \mathbf{I}_R + \frac{1}{\sigma_z^2} \Sigma \mathbf{Q} \Sigma \right) \quad (15)$$

La matrice  $\mathbf{Q} = \mathbf{V}^H \mathbf{S}_x \mathbf{V}$ . Dans [65], L'auteur observe que  $\mathbf{Q}$  est une matrice

semi-définie positive et donc l'inégalité d'Hadamard peut être utilisé:

$$\det \left( \mathbf{I}_R + \frac{1}{\sigma_z^2} \Sigma \mathbf{Q} \Sigma \right) \leq \prod_j \left( 1 + \frac{Q_{jj} \gamma_j}{\sigma_z^2} \right) \quad (16)$$

En remplaçant dans (12), il résulte que l'information mutuelle est optimale quand  $\mathbf{Q}$  est une matrice diagonale, donc:

$$C = \sum_{j=1}^J \log_2 \left( 1 + \frac{Q_{jj} \gamma_j}{\sigma_z^2} \right) \quad (17)$$

Il est aussi observé que la capacité croit linéairement avec  $\text{Rank}(\bar{\mathbf{H}})$  [65, 23].

L'équation (17) peut être maximisée pour obtenir une répartition adéquate de la puissance sur chaque valeur propre [65, 29]:

$$\max_{P_j: \sum_{j=1}^J P_j \leq P} \sum_{j=1}^J \log_2 \left( 1 + \frac{P_j \gamma_j}{\sigma_z^2} \right) \quad (18)$$

Après une maximisation Lagrangienne nous avons:

$$P_j = \left( \frac{1}{\lambda} - \frac{\sigma_z^2}{\gamma_j} \right)^+ \quad (19)$$

L'allocation de puissance sur les valeurs propres du canal est aussi l'algorithme du waterfilling, cette fois ci sur le schéma MIMO.

En l'absence de CSIT, l'allocation optimale est obtenue en répartissant de façon égale la puissance sur les antennes. La matrice de covariance devient  $\mathbf{S}_x = \frac{P}{\sigma_z^2 T} \mathbf{I}_T$ . En remplaçant par la matrice de covariance à répartition uniforme de puissance, l'équation (12) devient:



$$I(\mathbf{x}; \mathbf{y}) = \log_2 \det \left( \mathbf{I}_R + \frac{P}{\sigma_z^2 T} \bar{\mathbf{H}} \bar{\mathbf{H}}^H \right) \quad (20)$$

Utilisant la décomposition en valeurs singulières, nous avons:

$$I(\mathbf{x}; \mathbf{y}) = \sum_{j=1}^{N_Z} \log_2 \left( 1 + \frac{P}{\sigma_z^2 T} \gamma_j \right) \quad (21)$$

Dans la conception de systèmes de diffusion ou de multidiffusion, une quantité utile est la probabilité de coupure, définie comme suit:

$$\mathbb{P}_{out} = \mathbb{P} \left( \bar{\mathbf{H}} : \log_2 \det \left( \mathbf{I}_R + \frac{P}{\sigma_z^2 T} \bar{\mathbf{H}} \bar{\mathbf{H}}^H \right) < C_{out} \right) \quad (22)$$

La capacité  $C_{out}$  représente le débit nécessaire à l'obtention de certains services. Une mesure appropriée de l'efficacité d'un schéma donné est la probabilité que le débit obtenu est plus petit que celui requis (c'est à dire que le canal est en "outage" ou coupure). C'est la définition de la probabilité de coupure, comme définie par [48, 65, 29].

### Capacité MIMO OFDM

Le système MIMO OFDM peut être représenté dans le domaine fréquentiel en tant que  $N$  systèmes MIMO indépendants avec des matrices de taille  $R \times T$ , si l'on considère que le préfixe cyclique est suffisamment long [29, 63]. Une explication détaillée peut se trouver dans [63]. Si le système OFDM est bien conçu, une sous-porteuse du système MIMO OFDM est décrite comme suit:

$$\begin{pmatrix} y_1^{(n)} \\ \vdots \\ y_R^{(n)} \end{pmatrix} = \begin{pmatrix} h_{11}^{(n)} & \dots & h_{1T}^{(n)} \\ \vdots & \ddots & \vdots \\ h_{R1}^{(n)} & \dots & h_{RT}^{(n)} \end{pmatrix} \begin{pmatrix} x_1^{(n)} \\ \vdots \\ x_T^{(n)} \end{pmatrix} + \begin{pmatrix} Z_1^{(n)} \\ \vdots \\ Z_R^{(n)} \end{pmatrix} \quad (23)$$

ou simplement:

$$\mathbf{y}_{(n)} = \mathbf{H}_{(n)}\mathbf{x}_{(n)} + \mathbf{z}_{(n)} \quad (24)$$

où  $\mathbf{y}_{(n)}$  est un vecteur complexe qui correspond aux  $R$  signaux reçus par les antennes à la réception sur la sous-porteuse  $n$ . L'émetteur envoie le vecteur complexe  $\mathbf{y}_{(n)}$  sur ses  $T$  antennes. Le signal transmis est envoyé sur le canal représenté par la matrice  $\mathbf{H}_{(n)}$  de taille  $R \times T$ . Donc, sous les hypothèses mentionnées ci-dessus, la structure est semblable à (10) et (11); les formules développées dans la section ci-dessus sont pleinement valides.

## Le cas multi-utilisateurs sur la voie descendante ou Broadcast Channel

Cette section passe en revue les modèles utilisés pour le cas multi-utilisateurs (SISO-OFDM et MIMO-OFDM) ainsi que les principaux résultats disponibles dans ce contexte. On distingue deux situations principales, en fonction de la direction de la communication. Si la communication se fait à partir de la station de base vers les utilisateurs, on parle de la liaison descendante. A l'inverse, si la communication se fait depuis les utilisateurs vers la station de base on parle de liaison montante. En théorie de l'information la liaison descendante est connue sous le nom de canal de

diffusion ou Broadcast Channel (BC) et la liaison montante est connue sous le nom de canal d'accès multiple ou Multiple Access Channel (MAC). Dans ce résumé on mettra l'accent sur la voie descendante, celle-ci étant principalement abordée dans cette thèse. La bibliographie sur la voie montante et la dualité BC-MAC se trouve dans les sections 2.2 et 2.3.

## La voie descendante pour le cas multi-utilisateurs SISO-OFDM

Le canal de diffusion est décrit dans [17], en termes de canaux à évanouissement plats. Dans le contexte OFDM, en raison de l'orthogonalité entre les sous-porteuses, nous avons  $N$  canaux de diffusion indépendants. Le modèle mathématique pour l'OFDM sur chaque sous-porteuse est:

$$y^{(\ell,n)} = h^{(\ell,n)}x^{(n)} + z^{(\ell,n)} \quad (25)$$

où  $y^{(\ell,n)} \in \mathbb{C}$  est le signal de bande de base reçu sur la sous-porteuse  $n$  de l'utilisateur  $\ell$ . Le signal à diffuser est  $x^{(n)} \in \mathbb{C}$ , le symbole modulé complexe en bande base, sur la sous-porteuse  $n$ .

Dans un contexte SISO, ce signal atteint l'utilisateur  $\ell$  après avoir passé par  $h^{(\ell,n)} \in \mathbb{C}$ , qui est la transformée de Fourier de la réponse impulsionnelle du canal à temps invariant de l'utilisateur  $\ell$  sur la sous-porteuse  $n$ . Le symbole est contraint en puissance par:  $E \{|x^{(n)}|^2\} \leq P_n$ .

Dans son livre [17], Cover stipule que dans le but d'envoyer une information commune à tous les utilisateurs on peut tout simplement transmettre le même signal à une puissance permettant d'atteindre la capacité de l'utilisateur avec le pire canal. Une autre situation se présente quand on veut envoyer des signaux différents à chaque

utilisateur. Cela peut être fait par l'utilisation de codes superposés [17]. Le modèle plus simple permettant de résoudre ce problème, c'est la diffusion sur canal dégradé [25]. étant donné une fonction de permutation  $\pi(\cdot)$  qui permet de trier les canaux par l'amplitude de leurs gain d'atténuation dans un ordre décroissant, la diffusion sur canal dégradé est défini dans la situation où le signal d'émission est physiquement dégradé entre le canal et le premier récepteur et se dégrade plus encore au deuxième récepteur et ainsi de suite, formant une chaîne de Markov:

$$x^{(n)} \rightarrow y^{(\pi(1),n)} \dots \rightarrow y^{(\pi(L),n)} \quad (26)$$

On dit aussi que les canaux à diffusion sont stochastiquement dégradés, lorsque les canaux sont stochastiquement équivalents à une diffusion physiquement dégradé. Cela veut dire, qu'il existe une distribution de  $x^{(n)}$  vers  $y^{(L,n)}$  tel que :

$$p(y^{(1,n)}, \dots, y^{(L,n)} | x^{(n)}) = p(y^{(\pi(1),n)} | x^{(n)}) \prod_{\ell=2}^L p(y^{(\pi(\ell),n)} | y^{(\pi(\ell-1),n)}) \quad (27)$$

La région de capacité du canal à diffusion dégradé est bien connu [17, 25]. En prenant en compte que les gains des canaux des utilisateurs on été ordonnées du pire au meilleur utilisateur, avec un ordre de décodage:  $|h^{(\pi(1),n)}|^2 > \dots > |h^{(\pi(L),n)}|^2$  et une contrainte de puissance  $P_n$  sur la sous-porteuse  $n$ , la région de capacité est

$$C_{BC} = \bigcup_{\sum_{\ell}^L p_{(\ell),n} = P_n} \left\{ R : R_{\pi(\ell)} \leq \log_2 \left( 1 + \frac{|h^{(\pi(\ell),n)}|^2 p_{(\pi(\ell),n)}}{\sigma_{\mathbf{z}^{(\ell)}}^2 + |h^{(\pi(\ell),n)}|^2 \sum_{j < \ell} p_{(\pi(j),n)}} \right) \right\} \quad (28)$$

Les points de la région de capacité peut être obtenus avec un codage à superposition et décodage successif [17, 25]. Dans ce contexte dégradé, il faut noter que les Bons utilisateurs (ceux avec un bon SNR) peuvent également recevoir les signaux

qui sont destinées aux utilisateurs qui ont des SNR moins bons. En d'autres termes, pour une source codée hiérarchiquement, les bons utilisateurs vont recevoir des signaux de bonne qualité, tandis que les mauvais utilisateurs recevront un signal, mais de moindre qualité.

## La voie descendante pour le cas multi-utilisateurs MIMO-OFDM

Suite à la sous-section précédente, nous faisons un aperçu de la voie descendante pour le cas multi-utilisateur MIMO et les principaux résultats du domaine.

Le schéma de ce cas pour l'utilisateur  $\ell$  sur la sous-porteuse  $n$  est modélisé de la façon suivante :

$$\mathbf{y}_{(\ell,n)} = \mathbf{H}_{(\ell,n)}\mathbf{x}_{(n)} + \mathbf{z}_{(\ell,n)} \quad (29)$$

Le vecteur  $\mathbf{y}_{(\ell,n)} = (y_1^{(\ell,n)T} \dots y_R^{(\ell,n)T})^T$  modélise le récepteur avec  $R$  antennes. Le signal transmis est  $\mathbf{x}_{(n)} = (x_1^{(n)T} \dots x_T^{(n)T})^T \sim \mathcal{CN}(0, S_{\mathbf{x}_{(n)}})$ , où  $S_{\mathbf{x}_{(n)}}$  est la matrice de covariance du signal à transmettre, qui est soumis à une contrainte de puissance :  $Tr(S_{\mathbf{x}_{(n)}}) \leq P_n$ , où  $P_n$  est la puissance totale dans la sous-porteuse  $n$ . Ce signal est diffusé à tous les utilisateurs et contient les informations pour chaque utilisateurs dans la sous-porteuse  $n$ .

Le canal de diffusion MIMO n'est pas dégradé en général. Par conséquent, le codage par superposition n'est pas utilisé pour atteindre la capacité. Une technique souvent utilisée est celle développée par Costa [15], le " Dirty Paper Coding " (DPC). En 2001, une région atteignable a été déduite par Yu et Cioffi [79]. La base de cette

méthode consiste à décomposer le canal de diffusion en une série de canaux individuels par utilisateurs avec des informations non-causales disponibles à l'émetteur et à utiliser une méthode de précodage basée sur la méthode de précodage de Tomlinson-Harashima [66, 31, 22]. Également basé sur le DPC, Caire et Shamaï [7, 8, 9] ont développé une approche MIMO avec  $T$  antennes à l'émetteur et  $L$  utilisateurs, chacun avec une seule antenne. Ils explorent la possibilité de transmettre une information indépendante à l'aide d'une station de base avec des antennes multiples vers des utilisateurs avec une antenne. L'émetteur décompose le canal dans un ensemble ordonné de canaux à interférence, puisque cette opération est faite avant d'effectuer la transmission elle est connue sous le nom de technique non-causale, comme dans [15]. Les informations des utilisateurs sont successivement codées sur la base de la connaissance non-causale du canal. Les auteurs expliquent également que le cas à deux utilisateurs est une version spéciale de la région de capacité de Marton [40], qui peut atteindre la somme des capacités du système. D'une autre part, Goldsmith présente un aperçu des progrès sur le sujet jusqu'en 2003 [30]. En 2006 Weingarten et al. proposent une région de capacité atteignable pour le canal de diffusion [73], en utilisant DPC. Considérant un codage arbitraire  $\pi(\cdot)$ , où l'utilisateur  $\pi(1)$  est codé en premier, jusqu'à l'utilisateur  $\pi(L)$ , la capacité est l'union des bornes des débits atteignables qui composent le vecteur  $\mathbf{R} = (R_1, \dots, R_L)$  sur l'ensemble  $\mathcal{S} = \left\{ S_{\mathbf{x}(\ell,n)} \succeq 0, \forall \ell \in \mathcal{L} : \text{Tr}(\sum_{\ell=1}^L S_{\mathbf{x}(\ell,n)}) \leq P_n \right\}$ , qui contient les matrices de covariances  $S_{\mathbf{x}(\ell,n)}$  de chaque utilisateurs, et qui respectent les contraintes de puissance:

$$C_{BC}(H, P_n) = \bigcup_s \left\{ \mathbf{R} : R_\ell \leq \log_2 \frac{\det \left( \mathbf{I} + \mathbf{H}_{(\pi(\ell),n)} \left( \sum_{j \geq \ell} S_{\mathbf{x}^{(\ell),n}} \right) \mathbf{H}_{(\pi(\ell),n)}^H \right)}{\det \left( \mathbf{I} + \mathbf{H}_{(\pi(\ell),n)} \left( \sum_{j > \ell} S_{\mathbf{x}^{(\ell),n}} \right) \mathbf{H}_{(\pi(\ell),n)}^H \right)} \right\} \quad (30)$$

Du point de vue de Gesbert et al. [27], on peut comprendre que les résultats sur le schéma multi-utilisateurs MIMO sont principalement obtenus en utilisant le SDMA (Space Division Multiple Access), avec un précodage à l'émetteur. Evaluer combien d'utilisateurs peuvent obtenir un certain service implique un problème d'allocation de ressources. Le multiplexage spatial de flux de données peut être fait lorsque les utilisateurs ont une seule antenne, mais cette situation peut avoir un problème de dimension (rank problem) lorsque LOS est présent. La difficulté d'avoir pleinement du CSIT, fait sortir la nécessité d'étudier le cas CSIT-partiel.

L'allocation de ressources du schéma multi-utilisateur-MIMO tire parti de la CSIT en attribuant correctement la puissance  $P_{(\ell,n)}$  qui sera dédié à l'utilisateur  $\ell$  sur la sous-porteuse  $n$ . Le gain de multiplexage est de rang limitée à  $T$ , ce qui signifie que le nombre d'utilisateurs servis avec  $P_n$  à tout moment est lié au nombre d'antennes à la station de base. Dans [78], Yu et Rhee expliquent que le nombre optimal d'utilisateurs avec  $P_{(\ell,n)}$  est borné supérieurement par  $T^2$ .

Lorsque une technique précodage linéaire est utilisée, le nombre d'utilisateurs est limité par le nombre de degrés de liberté à la station de base, i.e.  $T$  [27]. Les métriques généralement optimisées par les schedulers sont principalement la somme des débits du système ou un débit spécifique par utilisateur, tout en minimisant la puissance d'émission.

La maximisation de la somme des débits sur le canal de diffusion peut être obtenue

par DPC [73], mais elle est difficile à mettre en pratique. Deux méthodes de précodage sont principalement employées, linéaire ou non linéaire.

Le précodage linéaire est une généralisation du schéma SDMA. Il est fait à la station de base, de telle sorte que le récepteur ne décode que le signal prévu pour lui. Le signal reçu est:

$$\mathbf{y}^{(\ell,n)} = \mathbf{H}^{(\ell,n)} \sum_{j=1}^L \mathbf{W}_{(j,n)} \mathbf{u}_{(j,n)} + \mathbf{z}^{(\ell,n)} \quad (31)$$

$$\mathbf{y}^{(\ell,n)} = \mathbf{H}^{(\ell,n)} \mathbf{W}_{(\ell,n)} \mathbf{u}_{(\ell,n)} + \mathbf{H}^{(\ell,n)} \sum_{\substack{j=1 \\ j \neq \ell}}^L \mathbf{W}_{(j,n)} \mathbf{u}_{(j,n)} + \mathbf{z}^{(\ell,n)} \quad (32)$$

Le signal transmis,  $\mathbf{x}^{(n)} = \sum_{j=1}^L \mathbf{W}_{(j,n)} \mathbf{u}_{(j,n)}$ , est composé de l'ensemble de signaux des utilisateurs  $\{\mathbf{u}_{(j,n)}\}_{\ell=1}^L$ , celui-ci préfiltré par l'ensemble de filtres  $\{\mathbf{W}_{(\ell,n)}\}_{\ell=1}^L$ . Ici  $\mathbf{u}_{(\ell,n)} \in \mathbb{C}^{S \times 1}$ , est un vecteur où  $S$  est le nombre de signaux pour l'utilisateur  $\ell$  et  $\mathbf{W}_{(\ell,n)} \in \mathbb{C}^{T \times S}$ .

Le signal à transmettre est  $\mathbf{x}^{(n)} \in \mathbb{C}^{T \times 1}$ . L'objectif est de concevoir le filtre  $\mathbf{W}_{(\ell,n)}$ , de telle sorte que la partie de la somme de (32) soit nulle et que finalement l'utilisateur ne puisse 'voir' que le signal qui lui est destiné:

$$\mathbf{y}^{(\ell,n)} = \mathbf{H}^{(\ell,n)} \mathbf{W}_{(\ell,n)} \mathbf{u}_{(\ell,n)} + \mathbf{z}^{(\ell,n)} \quad (33)$$

Un exemple de précodage par zero forcing amplement connu est la diagonalisation par bloc, qui annule l'interférence à la station de base [60] [37]. Les méthodes de précodage non-linéaires sont basées sur la méthode de perturbation [51] ou sur l'extension spatiale du précodage Tomlinson-Harashima [27]. Ces méthodes ne seront pas examinées dans cette thèse.



## Contributions

### Multidiffusion ou diffusion dans un système multi-utilisateur SISO-OFDM

La situation où le même signal doit être envoyé à un certain nombre de récepteurs se pose de plus en plus souvent, en raison de l'utilisation croissante de l'Internet sans fil y compris pour la télévision. Les services sont souvent délivrés soit par communication point à point, soit par la diffusion de ceux-ci. Les deux solutions sont cependant sous-optimales du point de vue de la gestion de la puissance disponible à la station de base. L'une assure une communication fiable mais avec un gaspillage d'énergie, tandis que l'autre économise de l'énergie mais n'assure pas une communication trop fiable. Ceci pourrait être évité si l'émetteur connaissait les canaux des utilisateurs demandeurs du service, dans une situation similaire à la multidiffusion ou "multicast". Ce chapitre fournit les outils nécessaires à l'évaluation de l'amélioration de la performance apportée par la multidiffusion sans fil (Wireless multicast) par rapport à la diffusion classique. Nous fournissons aussi les résultats de simulation numérique pour le cas de la transmission sur des modèles réalistes de canaux OFDM. Nous proposons aussi des moyens de déterminer les cas où la multidiffusion serait utile dans les systèmes OFDM sans fil. On montre que cela dépend fortement du nombre d'utilisateurs, ce qui était attendu, mais aussi de leurs distances à l'émetteur. La définition précédente de la multidiffusion sans fil, est proche de celle des canaux à diffusion (Broadcast Channels) bien connus en théorie de l'information. Il y a cependant une différence entre les deux situations : Le canal à diffusion en théorie de l'information permet de modéliser le problème de codage qui a pour but d'envoyer des informations différentes

à chaque utilisateur présent dans le système.

Nous abordons donc une situation intermédiaire. Un signal commun doit-être transmis, mais lorsque certains utilisateurs disposent d'un débit supplémentaire, ce débit peut être utilisé pour leur permettre d'obtenir une meilleure qualité de signal source grâce à un système de codage en couches [61]. Cela peut par exemple être utile pour de la vidéo. Pour aborder ce problème, nous avons choisi la somme des débits de tous les récepteurs en tant que critère d'optimisation, en proposant un algorithme d'allocation de puissance qui maximise ce critère du système multi-utilisateur SISO-OFDM. Nous illustrons à l'aide de simulations numériques les résultats du fonctionnement de l'algorithme d'allocation de puissance sur des scénarios différents et pour de nombreuses réalisations de canaux.

Nous ferons plusieurs réalisations de canal et nous travaillerons les statistiques des améliorations des capacités de ceux-ci via des histogrammes. On disposera donc des histogrammes de capacité de diffusion, de capacité optimisée et de pourcentage d'amélioration. Ce dernier est calculé en faisant le rapport entre la capacité de diffusion et la capacité de multidiffusion pour chaque échantillon. Ceci nous permet d'avoir un outil pour comparer et pouvoir ainsi décider si la multidiffusion est vraiment d'intérêt par rapport à la diffusion.

Le système étudié est constitué d'un émetteur et de  $L > 1$  récepteurs. Nous supposons que tous les récepteurs son équipés d'une antenne. Notre objectif est d'étudier le problème d'allocation de puissance lorsque l'émetteur utilise  $N$  sous-porteuses orthogonales pour envoyer des messages aux récepteurs. Le signal reçu par l'utilisateur  $\ell \in \{1, \dots, L\}$  peut être exprimé comme:

$$\mathbf{y}_\ell = \mathbf{H}_\ell \mathbf{x} + \mathbf{z}_\ell, \quad (34)$$

Où  $\mathbf{x} = (x^{(1)}, \dots, x^{(N)}) \sim \mathbb{C}\mathcal{N}(0, S_{\mathbf{x}})$  représente le vecteur d'entrée avec des symboles repartis sur  $N$  sous-porteuses OFDM, et  $S_{\mathbf{x}}$  est la matrice de covariance du vecteur  $\mathbf{x}$ . Cette matrice est une matrice diagonale  $S_{\mathbf{x}} = \text{diag}\{p_n\}$ ,  $n \in \{1, \dots, N\}$ , et  $p_n$  représente la puissance allouée à la sous-porteuse  $n$ . La puissance totale qui s'exprime comme la somme des puissances des sous-porteuses, doit respecter:

$$\sum_{n=1}^N p_n \leq P.$$

La matrice  $\mathbf{H}_\ell$  de taille  $N \times N$  représente le canal. Elle est diagonale et ses éléments sont la transformée de Fourier de la réponse impulsionnelle du canal, comme expliqué dans le chapitre de background, ( $\mathbf{H}_\ell = \text{diag}\{h^{(\ell, n)}\}$ ). Elle est supposée connue de l'émetteur. Le vecteur  $\mathbf{z}$ , est le bruit additif complexe gaussien à la réception, noté  $\mathbf{z}_\ell \sim \mathbb{C}\mathcal{N}(0, S_{\mathbf{z}})$  (on suppose que tous les récepteurs ont la même variance de bruit).

Puisque nous voulons transmettre la même information à des récepteurs multiples en respectant une contrainte de puissance au récepteur, nous cherchons à maximiser l'information mutuelle entre l'émetteur et les  $L$  récepteurs. D'après les résultats du chapitre 3, le critère à considérer est la somme des informations mutuelles de chaque utilisateur:

$$I(\mathbf{x}; (\mathbf{y}_1, \dots, \mathbf{y}_L)) = \sum_{\ell=1}^L I(\mathbf{x}; \mathbf{y}_\ell) \quad (35)$$

La capacité du système est donnée par l'information mutuelle (35), que l'on maximise sur l'ensemble des vecteurs  $\mathbf{x}$  qui respectent les contraintes d'allocation de puissance:

$$C = \max_{\mathbf{x}: \text{Tr}(S_{\mathbf{x}}) \leq P} \sum_{\ell=1}^L I(\mathbf{x}; \mathbf{y}_{\ell}) \quad (36)$$

Ce problème peut être réécrit sous la forme d'un problème d'optimisation convexe avec des contraintes linéaires :

$$\min_{\{p_n\}_n} \left\{ - \sum_{\ell=1}^L \sum_{n=1}^N \log \left( \frac{p_n}{\gamma_n^{(\ell)}} + 1 \right) \right\} \quad (37)$$

$$\text{Avec } \begin{cases} \sum_{n=1}^N p_n = P \\ -p_n \leq 0, \end{cases} \quad (38)$$

$$(39)$$

Avec  $\gamma_n^{(\ell)} = \frac{\sigma_z^2}{|h^{(\ell,n)}|^2}$  pour tout  $n$  et pour tout  $\ell$ .

Par optimisation lagrangienne, on constate que la répartition de puissance optimale dépend d'un paramètre  $\lambda \geq 0$ :

$$\forall n, \sum_{\ell=1}^L \frac{-1}{p_n + \gamma_n^{(\ell)}} + \lambda = 0 \quad (40)$$

où  $\lambda$  est choisi de telle sorte que la contrainte de puissance soit respectée:  $\sum_{n=1}^N p_n^* = P$ .

Nous pouvons voir que si  $L = 1$ , la solution de (40) est le water-filling. En revanche, dans le cas multi-utilisateurs, il n'existe pas de solution explicite pour l'allocation de puissance. Cependant une solution peut-être est obtenue par l'intermédiaire d'une méthode numérique, comme on le verra par la suite.

On définit tout d'abord les fonctions suivantes:

$$f(\lambda) = \sum_{n=1}^N p_n(\lambda) - P \quad (41)$$

et

$$\forall n, F_n(p_n, \lambda) = \sum_{\ell=1}^L \frac{-1}{p_n + \gamma_n^{(\ell)}} + \lambda \quad (42)$$

On cherche la solution du système:

$$\left\{ \begin{array}{l} f(\lambda) = 0 \\ \forall n, F_n(p_n(\lambda), \lambda) = 0 \end{array} \right. \quad (43)$$

On doit donc résoudre une équation du type  $F_n(p_n(\lambda), \lambda) = 0$ . Pour cela, nous commençons par calculer la dérivée partielle de  $F_n(p_n(\lambda), \lambda)$  par rapport à  $p_n$ .

$$\frac{\partial F_n(p_n, \lambda)}{\partial p_n} = \sum_{\ell=1}^L \frac{1}{(p_n + \gamma_n^{(\ell)})^2}; \quad (44)$$

Nous analysons ensuite la fonction  $F_n(p_n, \lambda)$  intervalle par intervalle, par rapport à  $p_n$ . Nous devons d'abord trouver les points critiques des fonctions  $F_n(\cdot)$ , c.a.d. l'ensemble des points où la fonction tend vers l'infini. Le seul intervalle sur lequel on peut vérifier que  $p_n > 0$ , est l'intervalle:  $] - \gamma_n^{(1)}, +\infty[$ .

Puisque la dérivée est strictement positive dans tout l'intervalle, la fonction est monotone croissante et par conséquent si la fonction tend vers 0 ( $F_n(p_n, \lambda) \rightarrow 0$ ) pour une valeur de  $p_n$ , cette valeur est unique.

### simulations numériques MU-SISO OFDM et Conclusions

L'outil que nous utilisons pour comparer la multidiffusion et la diffusion classique (à allocation de puissance égale) est l'histogramme obtenu à partir de la l'optimisation de la somme des débits. Cela nous permet de comparer la fréquence (statistique) des valeurs de capacité optimisés et non optimisés, sur un grand nombre d'échantillons (5000). Nous avons établi un modèle de canal (Chap.2.4.3), fixé les caractéristiques

des utilisateurs (distance à l'émetteur, nombre d'utilisateurs) et généré aléatoirement des échantillons. Nous commençons par des échantillons avec un utilisateur dans le système et puis en augmentant le nombre d'utilisateurs, nous obtenons des histogrammes pour toutes les situations. Nous présentons ici les résultats pour 300 [m]. Plus de résultats sont disponibles dans le chapitre 3. Avec 1 utilisateur dans le système, le pourcentage d'amélioration est, en moyenne, de près de 107.26 % à 0.2 *bit/s/Hz*. Quand on passe de 2 à 5 utilisateurs le pourcentage d'amélioration se situe entre 61,47 % et 28,01 %, avec diminution de la capacité de 0.17 à 0.15 *bit/s/Hz* en moyenne. Si nous avons 10 utilisateurs dans le système, l'allocation de puissance a 14.96 % de pourcentage d'amélioration, avec 0,14 % *Bit/s/Hz*. Avec 15 utilisateurs, le pourcentage d'amélioration est de 9,95% et la capacité optimisée est de 0.14 *Bit/s/Hz*. Nous pouvons voir sur la Fig. 1(a), l'histogramme du pourcentage d'amélioration et sur la Fig. 1(b) la répartition de la capacité optimisée par utilisateur dans ce scénario.

Dans cette première contribution, nous avons dérivé un algorithme d'allocation de puissance qui permet de répartir la puissance de manière optimale sur les symboles OFDM transmis, ceci dans le cas multi-utilisateurs. Les résultats des simulations montrent que notre algorithme permet des améliorations en terme de capacité par rapport à une répartition uniforme de la puissance. Évidemment, lorsque le nombre d'utilisateurs augmente, l'optimisation sera de moins en moins utile. Cependant, il peut être observé que des améliorations notables sont obtenues pour les utilisateurs les moins avantagés dans une cellule (ceux qui sont loin du point d'accès) avec une limite d'environ 5 utilisateurs. Au-delà de ce nombre, la répartition uniforme de puissance semble être le choix le plus simple.

Dans la suite nous explorons le schéma Multiuser-Multiple Input Multiple Output OFDM (MU-OFDM), et nous verrons si les techniques de transmission actuelles nécessitent d'adopter une optimisation sur la puissance transmise ou bien une répartition égale de celle-ci sur toutes les sous-porteuses.

## Allocation de puissance dans un système MU-MIMO OFDM

La section précédente a abordé le cas MU-SISO OFDM, où l'émetteur et le récepteur ont une antenne unique et plusieurs sous-porteuses. Nous nous intéressons maintenant au cas MIMO-OFDM (Multiple Input Multiple Output - OFDM), pour lequel nous avons plusieurs antennes et plusieurs sous-porteuses tantôt à l'émetteur qu'au récepteur.

Nous avons choisi de travailler sur la situation où l'émetteur dispose de la CSIT pour effectuer un précodage linéaire, ce qui apporte de fortes contraintes sur le nombre d'antennes à l'émetteur et au récepteur. Par conséquent, l'ensemble des situations possibles est limité, mais les résultats montrent clairement des améliorations apportées par la CSIT dans tous les cas possibles.

Dans cette section nous définissons  $t = 1, \dots, T$  comme l'index d'une antenne d'émission,  $T$  étant le nombre total d'antennes à l'émission. L'index  $r = 1, \dots, R$  est l'index d'une antenne au récepteur, et  $R$  est le nombre total d'antennes de réception. Le système MIMO est modélisé comme ce qui suit. Pour l'utilisateur  $\ell$  dans la sous-porteuse  $n$ , le signal reçu est:

$$\mathbf{y}_{(\ell,n)} = \mathbf{H}_{(\ell,n)} \mathbf{x}^{(n)} + \mathbf{z}_{(\ell,n)} \quad (45)$$

où  $\mathbf{y}_{(\ell,n)} = (y_1^{(\ell,n)T} \dots y_R^{(\ell,n)T})^T$  est le vecteur reçu sur l'ensemble des  $R$  antennes

de réception. Le signal à transmettre est  $\mathbf{x}^{(n)} = (x_1^{(n)T} \dots x_T^{(n)T})^T \sim \mathbb{CN}(0, S_{\mathbf{x}^{(n)}})$ , où  $S_{\mathbf{x}^{(n)}}$  est la matrice de covariance du signal. Celle-ci doit respecter une contrainte de puissance  $Tr(S_{\mathbf{x}^{(n)}}) \leq P_n$  ; où  $P_n$  est la puissance totale dans la sous-porteuse  $n$ . Ce signal est diffusé à tous les utilisateurs sur la sous-porteuse  $n$ .

Pour transmettre sur la voie descendante, nous avons choisi une méthode de précodage (ou préfiltrage) par zero-forcing, la diagonalisation par bloc [60, 13, 27, 38, 12].

La méthode est appliquée à la station de base sur chaque sous-porteuse et pour tous les utilisateurs du système. Le signal à diffuser est construit de la façon suivante :

$$\mathbf{x}^{(n)} = \mathcal{W}^{(n)} \mathbf{u}^{(n)} \quad (46)$$

où  $\mathbf{x}^{(n)} \in \mathbb{C}^{T \times 1}$ ,  $\mathcal{W}^{(n)} \in \mathbb{C}^{T \times LS}$  et  $\mathbf{u}^{(n)} \in \mathbb{C}^{LS \times 1}$ . La super-matrice  $\mathcal{W}^{(n)} = (\mathbf{W}_{(1,n)} \dots \mathbf{W}_{(L,n)})$ , contient l'ensemble de matrices de préfiltrage  $\{\mathbf{W}_{(\ell,n)}\} \in \mathbb{C}^{T \times S}$  et le super-vecteur  $\mathbf{u}^{(n)} = (\mathbf{u}_{(1,n)}^T \dots \mathbf{u}_{(L,n)}^T)^T$ , contient la concaténation des vecteurs de symboles  $\{\mathbf{u}_{(\ell,n)}\} \in \mathbb{C}^{S \times 1}$  de dimension  $S$ , qui seront transmis aux  $L$  utilisateurs.

La matrice de canal MIMO qui relie la station de base à l'utilisateur  $\ell$  sur la sous-porteuse  $n$  est :

$$\mathbf{H}_{(\ell,n)} = \begin{pmatrix} h_{11}^{(\ell,n)} & \dots & h_{1T}^{(\ell,n)} \\ \vdots & \ddots & \vdots \\ h_{R1}^{(\ell,n)} & \dots & h_{RT}^{(\ell,n)} \end{pmatrix} \quad (47)$$

Les éléments  $h_{rt}^{(\ell,n)}$  sont les coefficients d'atténuation entre l'antenne d'émission  $t$  et l'antenne de réception  $r$ . L'atténuation est modélisée suivant le modèle présenté



dans la section 2.4.3.

Le vecteur  $\mathbf{z}_{(\ell,n)} = (z_1^{(\ell,n)T} \dots z_R^{(\ell,n)T})^T \sim \mathcal{CN}(0, S_{\mathbf{z}^{(n)}})$  est le vecteur de bruit blanc additif gaussien présent à la réception. On considère que le bruit entre les antennes et les utilisateurs est decorrélié. La matrice de covariance du bruit est donc diagonale :  $S_{\mathbf{z}^{(n)}} = \sigma^2 \mathbf{I}_R$ . Nous simplifions en normalisant (45) par la variance du bruit  $\sigma$ . Grâce à cela, nous obtenons un système normalisé avec une matrice de covariance de bruit  $\mathbf{I}_R$  et une matrice de canal  $\mathbf{H}_{(\ell,n)} = \frac{1}{\sigma} \mathbf{H}_{(\ell,n)}$ .

La diagonalisation par bloc est expliquée en détail dans le chapitre 4. Sachant que le vecteur transmis vers tous les utilisateurs (46), contient des symboles qui ne concernent pas forcément l'utilisateur  $\ell$  en question, le signal reçu par l'utilisateur  $\ell$  dans la soup-porteuse  $n$  peut être exprimé comme:

$$\mathbf{y}_{(\ell,n)} = \mathbf{H}_{(\ell,n)} \mathbf{W}_{(\ell,n)} \mathbf{u}_{(\ell,n)} + \mathbf{H}_{(\ell,n)} \sum_{\substack{j=1 \\ j \neq \ell}}^L \mathbf{W}_{(j,n)} \mathbf{u}_{(j,n)} + \mathbf{z}_{(\ell,n)} \quad (48)$$

Pour que l'utilisateur  $\ell$  puisse récupérer ses données, nous avons besoin que la partie somme de (48), soit égale à zéro.

Si  $\mathbf{W}_{(\ell,n)}$  est judicieusement choisi cette équation devient:

$$\mathbf{y}_{(\ell,n)} = \mathbf{H}_{(\ell,n)} \mathbf{W}_{(\ell,n)} \mathbf{u}_{(\ell,n)} + \mathbf{z}_{(\ell,n)} \quad (49)$$

Les contraintes de conception du préfiltrage sont données par le nombre d'antennes à l'émetteur et au récepteur, par le nombre d'utilisateurs et par la taille des vecteurs de symboles à transmettre. Dans notre cas, la longueur du vecteur de symboles à transmettre est fixée à  $S$  pour tous les utilisateurs. Puisque nous précodons avec  $\mathcal{W}^{(n)}$  pour rassembler tous les symboles sur  $\mathbf{x}^{(n)}$ , nous avons besoin de  $LS$  precodeurs

linéairement indépendants, qui doivent être appliqués au niveau des  $T$  antennes d'émission. La condition est que  $T \geq LS$ . Pour un nombre  $T$  d'antennes, la matrice de precodage  $\mathbf{W}_{(\ell,n)}$  doit mapper les signaux vers le canal  $\mathbf{H}_{(\ell,n)}$ . Le produit  $\mathbf{H}_{(\ell,n)}\mathbf{W}_{(\ell,n)}$  a donc besoin de  $R$  filtres linéairement indépendants pour transmettre les  $S$  symboles concernés. La condition est que  $R \geq S$ . Pour concevoir  $\mathbf{W}_{(\ell,n)}$  nous définissons la super-matrice  $\mathbf{H}_{(\bar{\ell},n)} \in \mathbb{C}^{(L-1)R \times T}$  qui regroupe toutes les matrices de canal du système, en excluant celle de l'utilisateur  $\ell$ . Si nous voulons que la partie de la somme de l'équation (48) soit égale à zéro, la condition  $\mathbf{W}_{(\ell,n)} \in \text{Kern}(\mathbf{H}_{(\bar{\ell},n)})$  doit être vérifiée.

La décomposition en valeurs singulières (SVD) de  $\mathbf{H}_{(\bar{\ell},n)}$  est définie comme:

$$\mathbf{H}_{(\bar{\ell},n)} = \mathbf{U}_{(\bar{\ell},n)} \mathbf{\Sigma}_{(\bar{\ell},n)} [\mathbf{V}_{(\bar{\ell},n)}^{(1)} \mathbf{V}_{(\bar{\ell},n)}^{(0)}]^T \quad (50)$$

Les colonnes de  $\mathbf{V}_{(\bar{\ell},n)}^{(0)} \in \mathbb{C}^{T \times T - \text{Rank}(\mathbf{H}_{(\bar{\ell},n)})}$  forment une base dans le noyau de  $\mathbf{H}_{(\bar{\ell},n)}$ . N'importe quelle combinaison linéaire de  $\mathbf{V}_{(\bar{\ell},n)}^{(0)}$  peut donc être utilisée pour construire  $\mathbf{W}_{(\ell,n)}$ , par exemple:

$$\mathbf{W}_{(\ell,n)} = \mathbf{V}_{(\bar{\ell},n)}^{(0)} \boldsymbol{\sigma}_{(\ell,n)} \quad (51)$$

où  $\boldsymbol{\sigma}_{(\ell,n)} \in \mathbb{C}^{T - \text{Rank}(\mathbf{H}_{(\bar{\ell},n)}) \times S}$ , est une matrice arbitraire qui respecte les contraintes de puissance du vecteur de symbole  $\mathbf{u}_{(\ell,n)}$ , de façon que  $\mathbf{P}_{(\ell,n)} = \boldsymbol{\sigma}_{(\ell,n)} \boldsymbol{\sigma}_{(\ell,n)}^H$ . Dans ce cas  $\mathbf{P}_{(\ell,n)} \in \mathbb{C}^{T - \text{Rank}(\mathbf{H}_{(\bar{\ell},n)}) \times T - \text{Rank}(\mathbf{H}_{(\bar{\ell},n)})}$ .

À la réception l'équation (49) peut être réécrite de la manière suivante:

$$\mathbf{y}_{(\ell,n)} = \mathbf{H}_{(\ell,n)} \mathbf{V}_{(\bar{\ell},n)}^{(0)} \boldsymbol{\sigma}_{(\ell,n)} \mathbf{u}_{(\ell,n)} + \mathbf{z}_{(\ell,n)} \quad (52)$$

En prenant en compte tous les utilisateurs sur toutes les sous-porteuses et en

considérant  $\mathbf{G}_{(\ell,n)} = \mathbf{H}_{(\ell,n)} \mathbf{V}_{(\bar{\ell},n)}^{(0)}$  [38], nous cherchons à maximiser la somme des capacités du système, qui s'exprime de la manière suivante:

$$\begin{aligned} \max \quad & \sum_{\ell=1}^L \sum_{n=1}^N \log |\mathbf{G}_{(\ell,n)} \mathbf{P}_{(\ell,n)} \mathbf{G}_{(\ell,n)}^H + \mathbf{I}_R| \\ \text{t.q.} \quad & \sum_{\ell=1}^L \sum_{n=1}^N \text{Tr}(\mathbf{P}_{(\ell,n)}) \leq P \\ & \mathbf{P}_{(\ell,n)} \succeq 0; \quad \ell = \{1, \dots, L\}, n = \{1, \dots, N\}. \end{aligned} \quad (53)$$

Il s'agit d'un problème d'optimisation convexe, donc les conditions KKT sont nécessaires et suffisantes pour caractériser une solution [81] [6].

L'application de conditions KKT nous mène à l'expression suivante pour la matrice de puissance associé aux symboles:

$$\mathbf{P}_{(\ell,n)} = (\lambda \mathbf{I}_{T-\text{Rank}(\mathbf{H}_{(\bar{\ell},n)})} + \mathbf{Q}_{(\ell,n)})^{-1} - \mathbf{G}_{(\ell,n)}^{-1} \mathbf{G}_{(\ell,n)}^{-H} \quad (54)$$

Comme les matrices  $\mathbf{G}_{(\ell,n)} \mathbf{G}_{(\ell,n)}^H \in \mathbb{C}^{J \times J}$  et  $\mathbf{Q}_{(\ell,n)} \in \mathbb{C}^{J \times J}$  sont des matrices commutantes, elles peuvent partager les mêmes vecteurs propres ( $J = T - \text{Rank}(\mathbf{H}_{(\bar{\ell},n)})$ ). Si  $\mathbf{U}_{(\ell,n)}$  est une matrice de vecteurs propres, nous faisons une décomposition en valeurs propres tel que :  $\mathbf{G}_{(\ell,n)} \mathbf{G}_{(\ell,n)}^H = \mathbf{U}_{(\ell,n)} \Gamma_{(\ell,n)} \mathbf{U}_{(\ell,n)}^H$  et  $\mathbf{Q}_{(\ell,n)} = \mathbf{U}_{(\ell,n)} \Delta_{(\ell,n)} \mathbf{U}_{(\ell,n)}^H$ . En appliquant les conditions KKT nous obtenons ainsi:

$$\begin{aligned} \mathbf{P}_{(\ell,n)} = \\ \mathbf{U}_{(\ell,n)} \text{diag} \left[ \left( \frac{1}{\lambda} - \frac{1}{\gamma_{(\ell,n)_1}} \right)^+, \dots, \left( \frac{1}{\lambda} - \frac{1}{\gamma_{(\ell,n)_J}} \right)^+ \right] \mathbf{U}_{(\ell,n)}^H \end{aligned} \quad (55)$$

où  $(x)^+ = \max(x, 0)$  est une fonction qui prend en compte uniquement la partie

positive. En remplaçant cette dernière équation dans la contrainte de puissance, nous obtenons :

$$\sum_{\ell=1}^L \sum_{n=1}^N \sum_{j=1}^J \left( \frac{1}{\lambda} - \frac{1}{\gamma_{(\ell,n)_j}} \right)^+ \leq P \quad (56)$$

qui est l'expression du waterfilling sur les valeurs propres pour les  $L$ -utilisateurs, sur les  $N$ -sous porteuses et les  $J$ -modes de transmission, pour un precodage zero-forcing. Ceci est une conséquence des travaux précédents de [60, 38].

### simulations numériques MU-MIMO OFDM et Conclusions

Comme on l'a vu, la conception d'un precodage zero-forcing pour un système MIMO multi-utilisateurs implique beaucoup de contraintes que nos simulations respectent. Le nombre d'antennes à la réception est égale à la dimension du signal transmis sur la sous-porteuse  $n$ , c.a.d.  $R = S$ . On considère un scénario réaliste avec  $T = 8$ . Les contraintes que posent les dimensions des matrices nous conduisent à séparer le système en sous-systèmes comparables, en termes de nombre d'utilisateurs et de nombre d'antennes de réception. Le tableau 1 résume les résultats pour des utilisateurs sur des distances moyennes à l'émetteur de 100, 200 et 300 mètres. Le tableau est divisé en fonction de sous-systèmes comparables. Lorsque les utilisateurs disposent d'une antenne, la station de base peut assurer jusqu'à 8 utilisateurs avec un precodage zero-forcing. Si l'on ajoute une antenne aux récepteurs, le système MIMO multi-utilisateurs peut recevoir jusqu'à 4 utilisateurs en respectant les contraintes. Lorsque le récepteur possède 3 ou 4 antennes, le système peut accepter jusqu'à 2 utilisateurs. Nous exposons les résultats en pourcentage d'amélioration, par rapport au cas uniforme, sur le tableau suivant et de bits par sous porteuses.

Table 1: résultats pour le schéma MU-MIMO OFDM

| $\ell$ Ant | 100 meters |        | 200 meters |        | 300 meters |        |
|------------|------------|--------|------------|--------|------------|--------|
|            | % Inc.     | B\S.c. | % Inc.     | B\S.c. | % Inc.     | B\S.c. |
| 1 1        | 269,40     | 24,31  | 581,58     | 7,49   | 787,73     | 0,37   |
| 2 1        | 317,45     | 17,59  | 775,74     | 5,21   | 1121,57    | 0,26   |
| 3 1        | 370,57     | 13,92  | 941,15     | 3,98   | 1404,39    | 0,20   |
| 4 1        | 428,16     | 11,39  | 1113,37    | 3,13   | 1690,82    | 0,16   |
| 5 1        | 504,42     | 9,13   | 1310,71    | 2,37   | 2005,65    | 0,12   |
| 6 1        | 607,15     | 7,20   | 1573,75    | 1,82   | 2418,25    | 0,09   |
| 7 1        | 765,68     | 5,46   | 1981,08    | 1,35   | 3067,02    | 0,07   |
| 8 1        | 1108,16    | 3,49   | 2868,99    | 0,84   | 4497,37    | 0,04   |
| 1 2        | 160,64     | 18,00  | 337,29     | 4,97   | 458,05     | 0,47   |
| 2 2        | 208,00     | 12,01  | 500,40     | 3,19   | 724,26     | 0,31   |
| 3 2        | 279,49     | 8,23   | 700,74     | 2,14   | 1042,34    | 0,21   |
| 4 2        | 431,87     | 5,03   | 1099,58    | 1,27   | 1657,00    | 0,12   |
| 1 3        | 112,14     | 14,90  | 242,09     | 3,93   | 333,08     | 0,55   |
| 2 3        | 169,61     | 8,73   | 415,45     | 2,25   | 603,27     | 0,32   |
| 1 4        | 84,10      | 13,01  | 190,59     | 3,39   | 265,98     | 0,64   |
| 2 4        | 157,54     | 6,89   | 389,57     | 1,76   | 567,50     | 0,33   |

Pour le système MIMO avec 8 antennes d'émission et 1 antenne de réception, aussi appelé MISO (Multiple Input Single Output), nous pouvons immédiatement constater que le pourcentage d'amélioration est beaucoup plus grand que celui obtenu dans le cas de communications SISO. A titre d'exemple, avec 5 utilisateurs l'amélioration est de 504,42% , avec la possibilité d'allouer 9,13 bits par sous-porteuse à une distance de 100 mètres en moyenne. Cela est due à la configuration MIMO. On constate donc que par la stratégie d'allocation de puissance uniforme est loin d'être optimale. Quand le nombre d'utilisateurs augmente, la capacité en bits par porteuse diminue car l'énergie doit être partagée entre l'ensemble des utilisateurs qui arrivent dans le système. D'autre part, lorsque la distance augmente, le pourcentage d'amélioration due à l'allocation de puissance augmente également, mais la capacité diminue en conséquence. Ce phénomène a déjà été observé dans le cas SISO.

Pour un système avec 8 antennes d'émission et 2 à la réception, les contraintes font

que dans ce schéma le système peut accepter jusqu'à 4 utilisateurs. Le pourcentage d'augmentation en capacité est inférieure en relation à la même quantité d'utilisateurs du cas précédent. À 300 mètres, même si le pourcentage d'amélioration est inférieur, la méthode assure plus de bits en moyenne par sous-porteuse.

En résumé et en conclusion le chapitre 4, est une extension du travail effectué par Kaviani [38], du schéma MU-MIMO au MU-MIMO OFDM. L'algorithme développé est basé sur le precodage zero-forcing et présente beaucoup de contraintes lorsqu'il s'agit d'incorporer des utilisateurs disposant de plusieurs antennes dans le système. On observe que l'amélioration est assez importante dans la plupart des cas. Ce genre de "broadcast" est toujours plus efficace que la mise en place de plusieurs liens de communications points à point, même si l'on tient compte du fait que dans le cas multi-utilisateurs, l'optimisation est moins efficace que dans le cas mono-utilisateur.

## **Couverture réaliste d'un système OFDM**

En pratique, l'estimation de la couverture d'un point d'accès ou d'une station de base peut se faire via un grand nombre de simulations. Mais récemment, des techniques de "géométrie stochastique" [62] ont été introduites. Elles permettent de résoudre analytiquement ces problèmes dans des cas simples. Nous visons donc à étendre ces techniques pour les canaux OFDM. Nous montrerons que les solutions analytiques obtenues ne sont pas tout à fait faciles à gérer. En revanche des solutions numériques sont obtenues. Nous faisons l'hypothèse que les utilisateurs sont répartis autour de la station de base selon une loi uniforme, à partir de laquelle nous déduisons la fonction de distribution de la capacité. Ensuite, pour un utilisateur typique, nous calculons une zone de couverture pour laquelle une capacité minimale est assurée

avec une certaine probabilité, dite de coupure. Cette probabilité de coupure peut aussi être interprétée comme la proportion d'utilisateurs pour lesquels cette valeur de capacité fixe est assurée. Il s'agit précisément du critère de conception requis pour les transmissions par diffusion.

L'objectif est de trouver une expression analytique pour calculer la couverture, et d'obtenir un critère pour déterminer si l'optimisation lors de la multidiffusion est toujours utile quand on considère que les utilisateurs ont une répartition spatiale donnée, pour un débit de coupure fixé. La probabilité,  $\mathbb{P}(C \geq C_{out})$ , que la capacité  $C$  d'un utilisateur quelconque soit plus grande qu'une valeur prédéterminée  $C_{out}$  est nommée probabilité de coupure [29, 68]. Si on fixe une capacité à garantir  $C_{out}$  et une probabilité de coupure, on peut calculer la couverture maximale, c'est à dire la distance maximale où les utilisateurs peuvent être distribués et statistiquement répondre à ces deux contraintes.

Pour obtenir cette capacité nous devons disposer de la distribution de probabilité de la capacité. L'expression de la capacité en considérant le path loss et les multitrajets est la suivante :

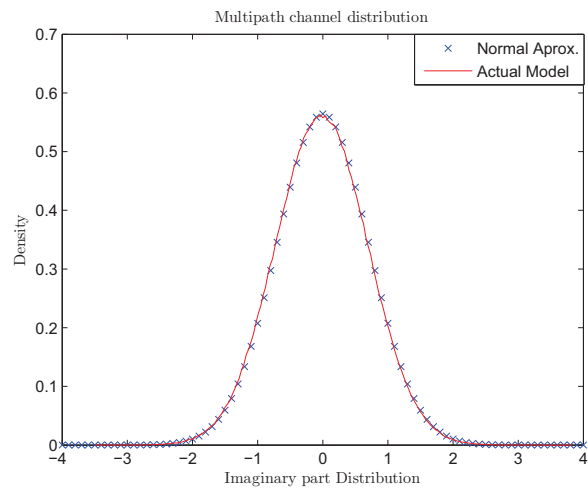
$$C = \frac{1}{N} \sum_{n=1}^N \log \left( 1 + \frac{1}{L(D)} |g^{(n)}|^2 \frac{P_n}{\sigma_z^2} \right) \quad \text{bits/s/Hz} \quad (57)$$

Le path loss  $L(D)$  et la perte par multitrajets  $g^{(n)}$  sont données dans [21],[57],[56],[53] et expliquées dans la sous-section 2.4.3. Pour caractériser l'équation de la fonction de distribution de la capacité, nous approximons la perte de multitrajets par une fonction de distribution Gaussienne complexe, en considérant les valeurs des variances du modèle E décrit dans [41] :

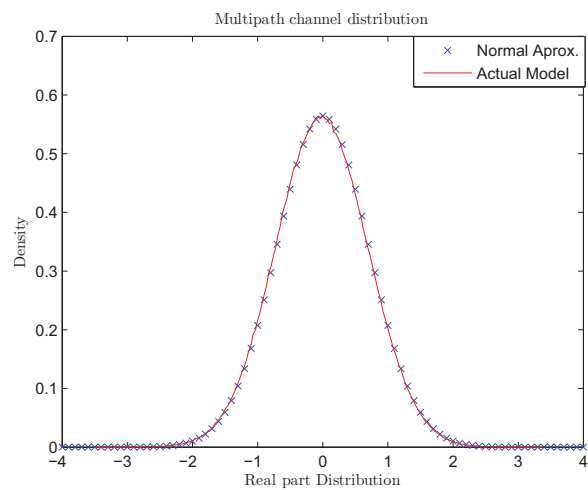
$$f_{g^{(n)}}(z) = \frac{1}{\pi \sum_{i=1}^I \sigma_i^2} \exp \left\{ -\frac{\bar{z}z}{\sum_{i=1}^I \sigma_i^2} \right\} \quad (58)$$

Nous pouvons montrer par simulations que cette approximation est suffisamment précise. Nous avons illustré dans la Figure 2 on the next page, la partie réelle et imaginaire de l'équation de distribution précédente. Nous voyons en rouge la distribution empirique du modèle et en bleu la courbe faite avec notre approximation.





(a) Partie imaginaire de la distribution multi-trajets



(b) Partie réelle de la distribution multi-trajets

Figure 2: Distribution d'un canal à multi-trajets

L'autre variable aléatoire qui influe sur la capacité est la distance  $D$ . Entre l'utilisateur et la station de base, qui paramétrise le path-loss. Nous considérons que les utilisateurs sont indépendamment et uniformément distribués dans une boule de rayon  $R$  avec la fonction de distribution suivante :

$$f_D(d) = \frac{2d}{R^2} \quad (59)$$

avec  $d \in [0, R]$ .

Malheureusement, le calcul analytique de la distribution de probabilité de la capacité n'est pas possible pour ce modèle. A la place, nous cherchons à l'approcher avec une distribution connue. Les paramètres de cette distribution seront déduits de l'espérance et la variance de la capacité.

L'espérance de la capacité est donnée par :

$$\mathbb{E}[C] = \frac{1}{N} \sum_{n=1}^N \mathbb{E} \left[ \log_2 \left( 1 + \frac{1}{L(D)} |g^{(n)}|^2 \frac{P_n}{\sigma_z^2} \right) \right] \quad (60)$$

$$= \frac{1}{N} \sum_{n=1}^N \int_0^R \int_{\mathbb{C}} \log_2 \left( 1 + \frac{1}{L(d)} |z|^2 \frac{P_n}{\sigma_z^2} \right) f_{g^{(n)}}(z) f_D(d) dz dd \quad (61)$$

et la variance par :

$$Var(C) = \sum_{n=1}^N Var(C_n) + 2 \sum_{n=1, i>n}^{N-1, N} Cov(C_i, C_n) \quad (62)$$

Où  $C_n$  est la capacité sur une sous-porteuse.

Etant donné que les canaux peuvent avoir une corrélation entre les sous-porteuses, les covariances ne sont pas nulles. La covariance a la forme suivante :

$$Cov(C_i, C_n) = \int_0^R \int_{\mathbb{C}} \int_{\mathbb{C}} c_n(z^n, d) c_i(z^i, d) f_{g^{(n)}, g^{(i)}}(z^{(n)}, z^{(i)}) f_D(d) dz^{(n)} dz^{(i)} dd \quad (63)$$

Dans la formule précédente,  $c_n(z^n, d)$  représente la capacité pour la sous-porteuse  $n$  pour une réalisation de la variable aléatoire  $g^n$  (égale à  $z^n$ ) et pour une réalisation  $d$  de la variable aléatoire  $D$ . La fonction  $f_{(g^{(n)}, g^{(i)})}(z^{(n)}, z^{(i)})$ , est la distribution de

probabilité jointe des variables aléatoires  $(g^n, g^i)$ .

Si nous faisons l'hypothèse que le vecteur aléatoire  $(g^n, g^i)$  est Gaussien complexe, la distribution jointe est donnée par:

$$f_{(g^n, g^i)}(z^{(n)}, z^{(i)}) = \frac{1}{\pi^2 \det(\Gamma)} \exp \left\{ \frac{\sum_{i=1}^I \sigma_i^2}{\det(\Gamma)} \left( z^{(n)} \overline{z^{(n)}} + z^{(i)} \overline{z^{(i)}} \right) - 2\text{Re}(\gamma_{n,i} z^{(i)} \overline{z^{(n)}}) \right\} \quad (64)$$

avec  $\det(\Gamma) = \left( \sum_{i=1}^I \sigma_i^2 \right)^2 - |\gamma_{n,i}|^2$  et

$$\gamma_{n,i} = \sum_{u=1}^l \sigma_u^2 \exp \{ -j2\pi(f_n - f_i)\tau_u \} \quad (65)$$

La distribution jointe est obtenue sous l'hypothèse que le vecteur aléatoire  $(g^n, g^i)$  est normal complexe [69, 54].

Les intégrales qui composent la moyenne et la variance sont difficiles à développer sous une forme explicite. Nous les calculons donc numériquement.

Une fois que l'on obtient les valeurs numériques de la moyenne et de la variance, on peut paramétrer une fonction usuelle et la comparer avec la distribution empirique de la capacité. Soit  $f(E[C], Var[C], x)$ , la densité de probabilité paramétrée avec la moyenne  $E[C]$  et la variance  $Var[C]$ . Pour calculer la probabilité de coupure dans une situation donnée, nous utilisons la formule suivante:

$$\begin{aligned} \mathbb{P}(C \geq C_{out}) &= 1 - \mathbb{P}(C \leq C_{out}) \\ &= 1 - \int_0^{C_{out}} f(E[C], Var[C], x) dx \end{aligned} \quad (66)$$

Pour  $f(E[C], Var[C], x)$ , on peut choisir par exemple la distribution log-normale:

$$f(E[C], Var[C], x) = \frac{1}{x\sigma_V} \exp - \left( \frac{(\ln(x) - \mu_E)^2}{2\sigma_V} \right) \quad (67)$$

$$\text{où } \mu_E = \ln \left( \frac{E[C]^2}{\sqrt{Var[C] + E[C]^2}} \right) \quad (68)$$

$$\sigma_V = \ln \left( \frac{Var[C]}{E[C]^2} + 1 \right) \quad (69)$$

On voit que les paramètres  $\mu_E$  et  $\sigma_V$  de cette fonction sont déduits à partir de la moyenne et de la variance de la capacité. Pour des utilisateurs distribués uniformément sur une boule de rayon  $R = 200$  on obtient  $E[C] = 0.4529$  et  $Var[C] = 0.8827$ .

D'autre part, pour vérifier ces résultats, nous avons effectué des tirages aléatoires issus de valeurs empiriques. On obtient une moyenne empirique  $E[C] = 0.4525$  et une variance empirique  $Var[C] = 0.9996$ . La différence est essentiellement due aux itérations nécessaires pour effectuer les intégrations. La distribution log-normale est ensuite paramétrée avec cette moyenne et cette variance. Les distributions empiriques et log-normale sont tracées sur la Figure on the next page.

La courbe *bleu* est la distribution empirique, obtenue avec un grand nombre d'échantillons. La courbe *magenta* est la distribution log-normale paramétrée avec les valeurs empiriques de la moyenne et la variance. La courbe en *noir* représente la fonction log-normale paramétrée avec les valeurs calculées théoriquement, par intégration numérique.

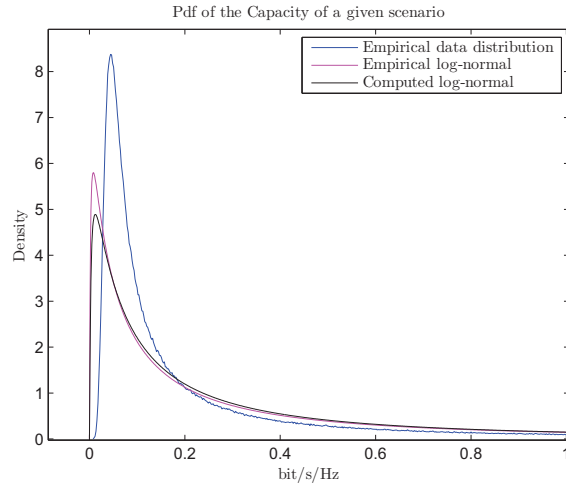


Figure 3: PDF de la capacité pour un scénario donné

Pour finir, la formule (66) peut être utilisée de différentes manières. Elle donne la distribution de probabilité de capacité pour un système de diffusion, lorsque l'on connaît les paramètres du canal. Mais elle peut aussi être utilisée pour paramétrer un système pour garantir une certaine qualité de service avec une certaine probabilité.

### Simulations numériques pour une couverture réaliste SISO-OFDM

Nous présentons des résultats pour deux niveaux de bruit différents, en considérant que les utilisateurs sont distribués uniformément sur un cercle de diamètre  $R = 200$ . Pour un SNR cible de 10 dB, la puissance du bruit est fixée à  $1.0 \times 10^{-12}[W]$ . Et pour un SNR cible de 15 dB, elle est fixée à  $1.0 \times 10^{-13}[W]$ . Dans ce résumé, nous présentons les résultats pour un SNR cible de 10 dB. On fixe une probabilité de coupure de 95%, c.a.d.  $\mathbb{P}(C \geq C_{out}) = 0.95$  puis on calcule  $C_{out}$ .

L'objectif est de vérifier si le critère d'optimisation (la capacité somme) coïncide avec le critère de diffusion (capacité de coupure). Nous verrons aussi si l'extrapolation de la distribution de probabilité de la capacité avec une distribution de probabilité

connue est utile pour établir un critère de conception pour une transmission par diffusion.

La Figure 4 montre les résultats des simulation pour des scenarios réalistes et théoriques. Les concepts présentés sont les suivants:

- Capacité de coupure  $C_{out}$  pour une probabilité de coupure à de 95% dans un schéma de diffusion, Cercle-Marron.
- Capacité de coupure  $C_{out}$  pour une probabilité de coupure à de 95% dans un schéma de multidiffusion, Etoile-Rouge foncé.
- Capacité moyenne de diffusion quand la probabilité de coupure est supérieure à 95 %, Croix-Cyan.
- Capacité moyenne de multidiffusion quand la probabilité de coupure est supérieure à 95 % , Carré-Rose.
- Capacité moyenne de diffusion (100 %), Triangle-Jaune.
- Capacité moyenne de multidiffusion (100 %), Losange-Bleu.
- Capacité de coupure calculée avec une distribution log-normale théorique, Plus-Bleu-Vert.
- Capacité de coupure calculée avec une distribution log-normale empirique, Tiret-Rouge.

Tout d'abord, on peut voir que le gain en capacité est faible en moyenne. Sur la Figure 4, on peut voir 20% d'augmentation pou un seul utilisateur et 13 % lorsque il y en a 2. La moyenne du sous-ensemble qui est sur le 95 % de probabilité est

égale à celle qui considère le 100% des échantillons. La moyenne de la capacité de multidiffusion montre une amélioration faible entre 1 et 8 utilisateurs. La valeur empirique de la capacité de coupure est proche de 0.03 [*bits/s/Hz*]. On cherche à approcher la distribution réelle avec une distribution log-normale. Quand on paramétrise la distribution log-normale avec la moyenne et la variance des échantillons, la capacité de coupure empirique est 0.0103 [*bits/s/Hz*]. Et quand on paramétrise avec la moyenne et la variance obtenus par nos calculs, c.a.d.  $E[C] = 0.4529$  et  $Var[C] = 0.8827174$ , la capacité de coupure théorique basée sur la log-normale est 0.0127 [*bits/s/Hz*].

D'autre part, nous nous intéressons au *pourcentage d'amélioration* (Figure 5). Nous le calculons pour tous les échantillons avec la formule:

$$\left( \frac{Capacite\ Optimisee}{Capacite\ de\ Diffusion} - 1 \right) \cdot 100$$

La Figure 5 montre la distribution du pourcentage d'amélioration. Un pourcentage d'amélioration de 0 % signifie que la capacité optimisée et de diffusion sont les mêmes (le rapport est de 1).

Nous pouvons observer que pour environ 30 % des échantillons, on observe un pourcentage d'amélioration supérieur à 100 %, ce qui signifie que la capacité optimisée est au moins deux fois supérieure à la capacité de diffusion. En outre, il convient de noter que pour un seul utilisateur le pourcentage d'amélioration, est en moyenne de 72 %. La différence avec les résultats présentés dans la Figure 4, peut s'expliquer par le fait que ces améliorations concernent principalement les utilisateurs à faible capacité mais qui gardent une capacité moyenne constante. On peut le constater en comparant les histogrammes de la Figure 5.5, pour un seul utilisateur. Il apparaît clairement que la distribution de la capacité est différente de la première partie (environ pour

une capacité de moins de 0.5 bits/s/Hz, voir figure 4), et de même pour des capacités supérieures.

Plus précisément, pour un utilisateur, la capacité moyenne optimisée est de 0.55 bits/s/Hz alors que la capacité moyenne de diffusion est de 0.46 bits/s/Hz. Si l'on compare les moyennes, nous avons 20 % d'augmentation. Pour 2, 3, 4 et 5 utilisateurs ce rapport donne 13 %, 8.7 %, 8.8 % et 6.66 % respectivement.

Pour conclure, dans ce chapitre on a exploité la capacité SISO-OFDM avec de nouveaux éléments. L'utilisateur est placé uniformément sur une balle à rayon fixe par rapport à la station de base. Avec l'idée de caractériser la probabilité de coupure, nous trouvons des expressions pour l'espérance et la variance de la capacité. Ces valeurs peuvent être utilisées pour faire une extrapolation de la distribution de la capacité. En utilisant cette distribution, la transmission par diffusion peut être utilisée pour assurer une certaine qualité de service. Par exemple, le système peut être réglé pour assurer qu'un certain pourcentage d'utilisateurs ait sur un rayon donné une certaine capacité. La comparaison entre la capacité optimisée et la capacité de diffusion montre qu'il n'y a pas d'amélioration significative en moyenne. La capacité moyenne croît 20 % pour un utilisateur et décroît lentement avec une augmentation des utilisateurs. Néanmoins, une étude plus approfondie montre que cette amélioration est importante pour une grande partie des utilisateurs. Mais, il s'agit d'utilisateurs à faible capacité. Ce qui explique une pauvre amélioration en moyenne, et est compatible avec les travaux effectués dans les chapitres précédents.

Une extension logique de ce travail peut consister à comparer l'amélioration en capacité sur des distributions spatiales différentes. Puisqu'il est clair que la distance entre les utilisateurs et la station de base joue énormément sur la capacité.



## Conclusions

Le sujet principal de cette thèse porte sur l'utilité de l'allocation de puissance sur la voie descendante d'un système OFDM où l'on vise à transmettre un signal commun à tous les utilisateurs.

Nous examinons d'abord les systèmes SISO et MIMO OFDM, avec un regard particulier sur l'orthogonalité et leur capacité. Notre objectif est d'obtenir des conclusions pour des situations concrètes à travers la modélisation de canal, ceci en considérant des paramètres réalistes. Nous proposons tout d'abord une allocation de puissance à l'émetteur dans le cas MU-SISO OFDM et nous étendons notre étude au cas MU-MIMO OFDM en utilisant un précodage linéaire. Finalement, nous revenons sur le schéma MU-SISO OFDM et nous incorporons des éléments de géométrie stochastique, en essayant de trouver une expression pour évaluer zone de couverture d'une station de base. On veut garantir un débit minimum dit capacité de coupure, en considérant une contrainte de probabilité de coupure.

Nos contributions développent trois aspects, et sont l'extension de résultats connus d'allocation de ressources au cas multi-utilisateurs.

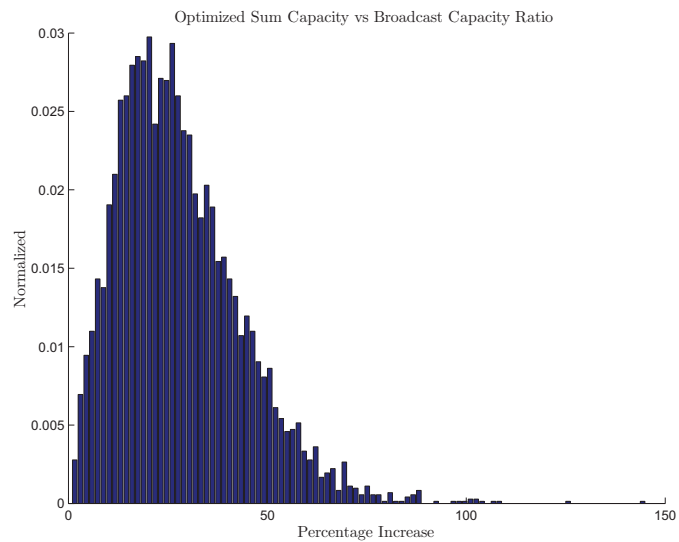
Pour le cas MU-SISO OFDM, nous proposons un algorithme d'allocation de puissance. Cet algorithme n'a pas une forme explicite comme le waterfilling, mais a une structure très simple et garantie une convergence. Les simulations montrent que notre algorithme apporte une amélioration substantielle par rapport à une allocation de puissance uniforme. Nous faisons une étude statistique en utilisant des histogrammes de la capacité des utilisateurs par rapport à leur distance du point d'accès. Nous observons qu'au fur et à mesure que des utilisateurs intègrent le système, l'optimisation

n'apporte pas beaucoup plus d'amélioration en termes de capacité et une allocation de puissance uniforme est la meilleure option. Sinon, pour 5 utilisateurs des améliorations appréciables sont obtenues sur l'optimisation de la somme des capacités. Il est observé que les meilleures améliorations sont obtenues par les utilisateurs ayant les moins bon canaux.

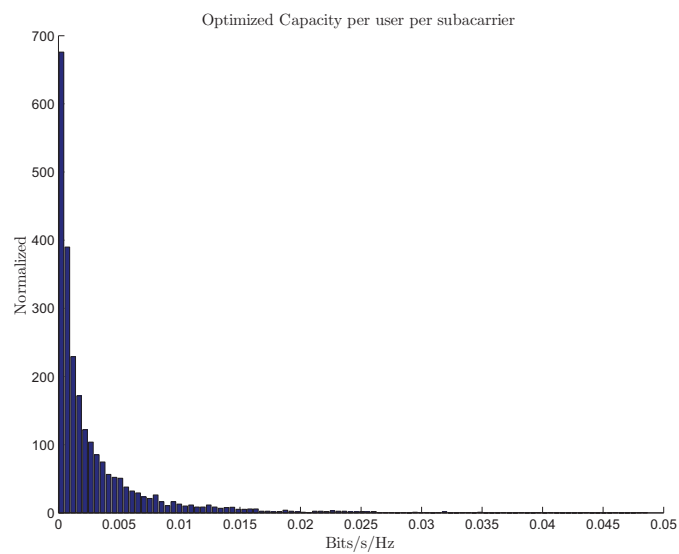
Le cas MU-MIMO OFDM présente des contraintes qui rendent difficile la prise en main du sujet. Le gain de diversité et de multiplexage sont de vastes sujets sur le domaine. Nous étudions ces sujets dans le chapitre 2, puis nous choisissons d'étendre le travail de Kaviani [38] au cas OFDM. Nous développons un algorithme d'allocation de puissance sous les contraintes que l'émetteur implémente un precodeur par zero forcing. Les contraintes données par les dimensions des matrices qui participent du schéma MIMO, limitent le nombre d'utilisateurs que l'on peut servir. Malgré ces contraintes, pour les situations possibles, l'algorithme d'allocation de puissance donne des améliorations substantielles par rapport à celle d'une allocation de puissance uniforme.

La question de la couverture du système MU-MIMO OFDM est abordée dans la dernière contribution. La densité de probabilité de la distance de l'utilisateur par rapport à la station de base et celle du canal est prise en compte. Le but étant d'obtenir une expression pour la distribution de probabilité de la capacité et pouvoir ainsi calculer la capacité de coupure en ayant une probabilité de coupure comme contrainte. On obtient les expressions pour l'espérance et la variance de la capacité sur le scénario étudié. Nous paramétrons une distribution connue qui pourrait s'approcher de la distribution empirique. Ceci permet une évaluation rapide du débit qui peut être transmis sur un scénario donné, ceci seulement avec deux paramètres. Les simulations

numériques confirment les résultats précédents: le débit moyen n'est pas sensiblement augmenté car les meilleurs utilisateurs (dominants dans la moyenne) n'ont pas d'amélioration sensible, alors que ce sont les plus mauvais utilisateurs (les plus lointains) qui bénéficient de l'optimisation. On peut donc s'attendre à une couverture plus grande avec une optimisation de type "multicast".



(a) Pourcentage d'amélioration



(b) Capacité en Bit/s/Hz

Figure 1: Histogrammes pour 5 Utilisateurs a 300 [m] de la station de base

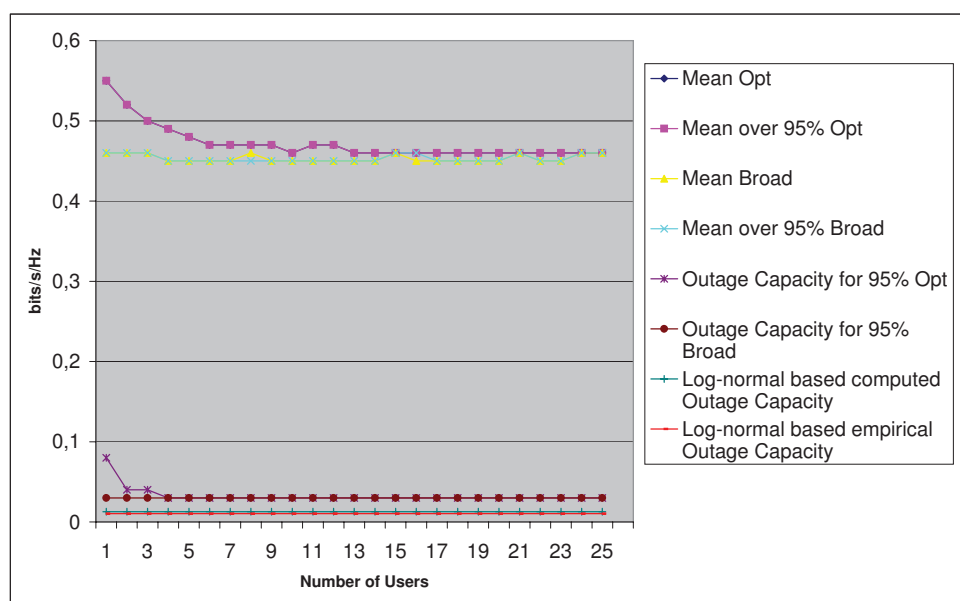
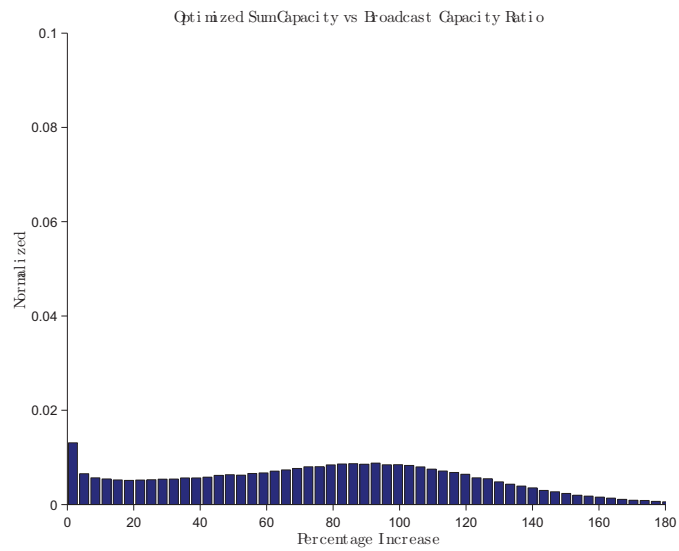
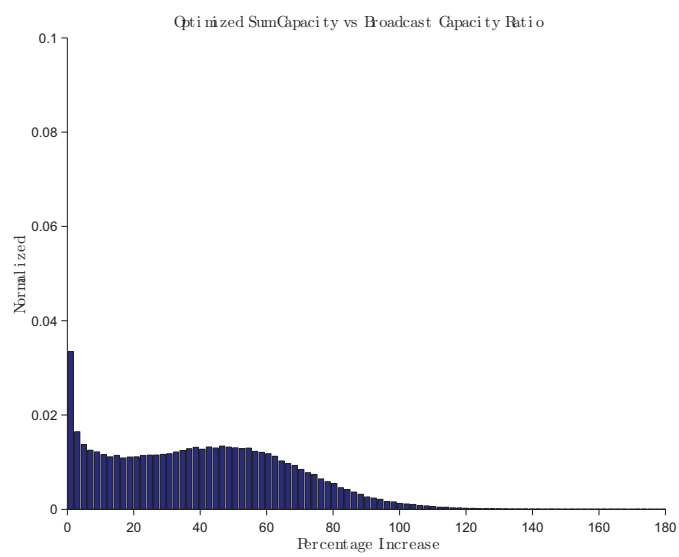


Figure 4: Capacité moyenne, Capacité de coupure pour 95 % et moyenne de Capacité sur 95 % pour un SNR 10 dB

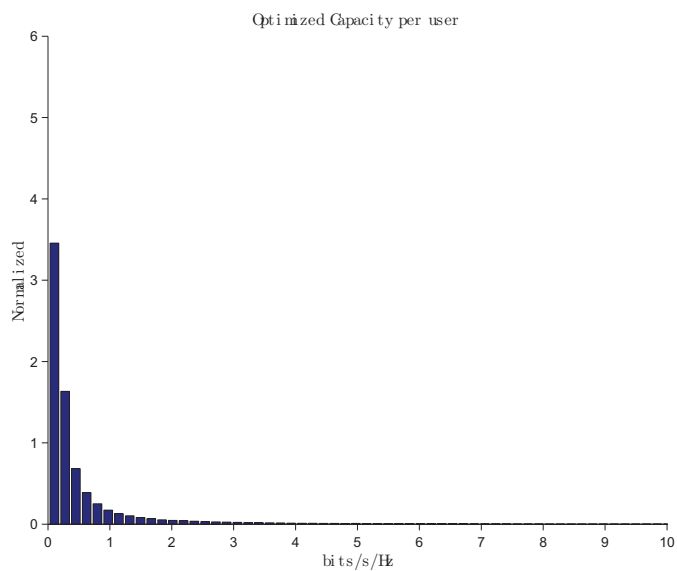


(a) 1 Utilisateur

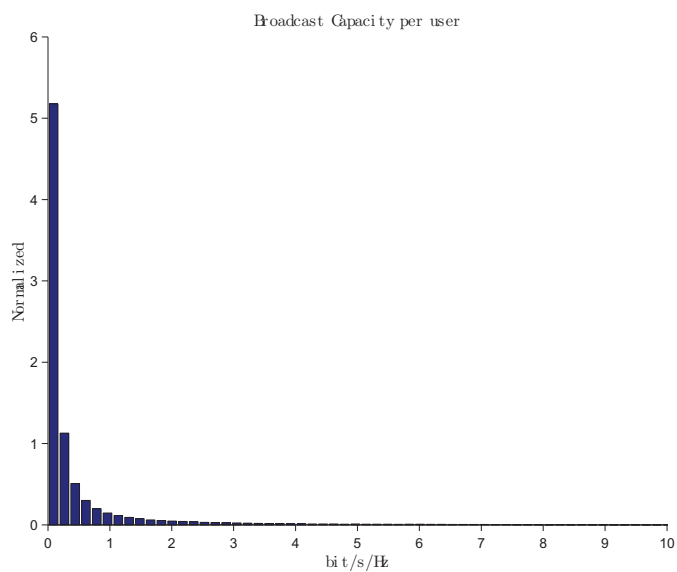


(b) 2 Utilisateur

Figure 5: Pourcentage d'amélioration à 10 dB



(a) Capacité optimisée pour un utilisateur



(b) Capacité de diffusion pour un utilisateur

Figure 6: Capacité optimisée et de diffusion pour un utilisateur à 10 dB

# Chapter 1

## Introduction

### 1.1 Motivation

In the last years the evolution of user needs combined with an increasing offer from mobile operators has resulted in an ever increasing demand on mobile devices and services, which in turn raises new research problems so that the industry can offer better products meeting this new demand. These recent services more and more frequently asked from mobile devices are linked to multimedia streaming or downloading, since video on demand (VOD), video conference, news consultation, clip downloading are becoming an increasing part (close to majority) of the occupancy of mobile networks. The main technical problem lies in the wireless link, which is currently the bottleneck of the system: if too many users try to download video from a base station or an access point, the cell capacity can quickly be reached. Globally, such a situation requires a very good quality of the service, meaning high data rate, reliable communication and efficient use of the power. The last points offer challenging topics because of the characteristics of the wireless data transmission. The transmission of the data for a



specific service never happens in ideal conditions, the signal from the base station to the user experiences attenuation and multipath propagation that can degrade the service.

In order to have an efficient communication system able to cope with the impairments brought by wireless links, most recent telecommunications standards designed for packet transmission on wireless channels, such as IEEE 802.16, IEEE 802.11 or from mobile technologies like 3GPP Long Term Evolution (LTE), use Orthogonal Frequency Division Multiplexing (OFDM) multi-carrier systems to obtain reliable communication on downlink. This technology was adopted because it allows high data rate over multipath and scattered environment. The idea behind OFDM technology is to spread the data stream on several orthogonal sub-carriers [44]. Another presentation of OFDM is that it permits to transform a wideband frequency-selective channel into several and orthogonal narrowband frequency-flat fading channels, thus allowing to process the subchannels independently with simple equalizers and decoders. Moreover, working on a set of subchannels gives a chance to perform simple and efficient power allocation. In fact if we can have a knowledge of the channel, we can use optimization tools in order to use the energy available at the base station in an efficient manner. This leads to the so called "waterfilling" algorithm.

Multicarrier OFDM was initially introduced for devices that have a single antenna, which is still the most common situation. The users having smartphones, tablets and netbooks are for most of them equipped with a single antenna. However, a special attention has been paid to Multiple Input Multiple Output (MIMO) systems that implement multiple antennas at the transmitter and the receiver sides. Indeed, it has been shown that MIMO technologies allow to transmit higher data rates with the

same energy compared to single antenna transmission, also known as Single Input Single Output (SISO) situation. The arrival of this new technology poses challenging problems in order to develop algorithms that can support the target tasks, i.e. high data rate, reliable communication and power energy consumption.

A somewhat new aspect in terms of wireless networks lies in the fact that in some downlink situations, the same signal is of interest to several users in the same neighbourhood. This is the case for example of TV channels disseminated via mobile networks, clips, news, and so on... In such cases, it is clearly a waste of resources to establish point to point links from the base station to each final end user. Recent mobile communication standards recognized this problem and standardized "broadcast" situations. This broadcast situation can be considered as an extreme opposite with respect to the many point to point ones, since it is likely that in a given cell the number of simultaneous users of a given video service is not too large. The corresponding drawback of the broadcast situation is that no channel knowledge is possible at the transmitter, which prevents a good tuning of the transmission parameters to the actual channels (the "waterfilling" above). Moreover, since the number of final users can be very large, no "acknowledgment" procedure is feasible, which clearly has an impact on the resulting performance.

This is the motivation for our work: we consider the situation where the same service is required from a base station by a group of users of reasonable size. This problem is known in wired networks as a "multicast", where the user subscribes the same services as other people, the network managing to respond to this demand at the smallest cost by pooling the resources. This also allows savings in the wireless situation as well as increased quality of service, because the transmitter can now

make full use of each channel knowledge, and some ARQ are feasible if the number of subscribers is not too large. This ARQ problem is not addressed in this work, and we concentrate on the power allocation part of the problem. First results on ARQ in a multicast situation can however be found in [5].

## 1.2 Problems

Data transmission through wireless channels at high data rate while ensuring a good quality of service is the main goal of all service providers. The most challenging environment that can be met in this context is urban areas: the propagation channels are impacted by buildings, trees, cars and many obstacles that produce delay, interference, noise and attenuation of the signal, as well as intersymbol interference. Since data rates have quickly increased one must deal with highly frequency selective channels. The solution to this problem is the OFDM technology, that splits the channel in many narrowband subchannels. By doing so, the high data rate can be split into a lower data rate per subchannel. This is our choice for the transmitter, following a trend in the wireless system design.

Our objective is to transmit an OFDM signal from the base station to several receivers. The signal carries the same information to all receivers like an old fashioned broadcast-tv. In wired networks, this type of transmission is named *Multicast*, where a group of users subscribed to a service and receive the same information from the network [64].

We will use information theory to model the multicast situation over an OFDM wireless communication system. Obviously, a multicast service from the base station to a known number of users can be modeled as being a broadcast channel situation

(here, "broadcast" is not used in its information theoretic terminology, since we are interested mostly in the "common" part of the signal). In information theory the *broadcast channel* has been formalized by Cover in [16] and reviewed by Van der Meulen in [70]. In this understanding, "broadcast" means that each user is interested in its own message, plus a possible common signal. The capacity region of the general broadcast channel is not known [18] and is still a theoretical challenge. However, specific cases are well described as the degraded broadcast channel. The degraded broadcast situation is anyway exactly what is needed in our SISO case: the "good" receivers (the ones that have good channels) can receive a good quality signal, assuming that the additional part of the bitstream received by the "good" users complements the signal received by the "bad" users (the ones that have poor transmission conditions).

This situation, where each user receives the best possible information, given its channel, requires the source signal to be designed in a "scalable" or even "embedded" form: the bitstream can be cut at any place while still being "understood" by the source decoder and providing a video (for example) with the best possible quality corresponding to the size of the bitstream. This comes in contrast with what could be a multicast situation with a strict understanding, where we would be interested only in the capacity to send common information through the channel. The situation where we transmit only a common information through the channel is a max-min problem [17] where we compute the mutual information between the transmitter and each user then we choose the worst value and we maximize at the base station this mutual information with a power constraint. In our case, the sum-rate capacity will be of interest.

We consider that the transmitter knows the realization of the Channel State Information (CSI) since the users are individually known at the transmitter. This allows us to develop algorithms that maximize the capacity, given a limited power available at the base station.

The Multi-User case of SISO systems is a difficult problem to address. Many power allocation schemes were proposed using existing modulation and coding schemes, allowing an improved throughput by means of an optimal power assignment to the Sub-Carriers. In [77], bit loading and power over each sub carrier are optimized, the allocation being made for a set of users. In [34], the data to various users are summed in each Sub-Carrier, a rate function is deduced and optimized by Lagrange method.

The scheme of MIMO broadcast channel can also be modeled as a compound channel. A "compound" channel corresponds to the case where the transmitter does not know the exact realization of the channel, but knows that it belongs to a given set. This would be a non CSI case, where only the common signal would be of interest. This situation was addressed by Weingarten, Shamai and Kramer in [74] in an abstract setting. In the case of Multi-User MIMO-OFDM transmission with CSI at the transmitter and the receiver, the zero-forcing precoding method is used to approach the dirty paper coding capacity region [12]. In [60], the author proposes zero-forcing methods for the Multi-User MIMO systems and [38] performs an optimal power allocation over the scheme.

In this work, Multi-User power allocation schemes for OFDM-SISO and OFDM-MIMO schemes are first investigated, which allows to perform a statistical investigation of the coverage of each scheme based on a realistic channel model. When compared with the classical "broadcast" situation (i.e. one to many unknown users),

this will allow to decide for which number of users some power allocation is useful or not. In other words, this work brings the tools that are necessary for deciding on the best frontiers between the one to one communications, the one to many known users, and one to many unknown users.

### 1.3 Objectives and Contributions

As explained above, one of the main objective of the thesis is to estimate the moment where the optimization of the power allocation for given channels does not improve the capacity of the network over a uniform power allocation over the Sub-Carriers. The study is made on the Multi-User SISO-OFDM and the Multi-User MIMO-OFDM schemes. We begin by investigating how a single carrier transmission works, and we justify the use of the OFDM technique that allows an easy tuning of the system in terms of capacity.

Once we know how the OFDM system works, we will see how it can be used in the SISO and MIMO contexts. The capacity formulas are deduced under the assumption that CSI is known at the transmitter (base station) in the SISO case, and when CSI is known at both the transmitter and the receiver sides in the MIMO case.

We then analyze how the schemes are modified when the Multi-User situation is introduced in the SISO and MIMO cases.

Since we are interested in realistic situations, the channel gains are modeled with realistic parameters. We have chosen to work under the WIFI context, and we use the same channel parameters that are classically used to evaluate WIFI systems.

This background allows a better understanding of the problem and will be useful for the presentation of the results described in the next chapters.

For Multi-User SISO-OFDM model we propose an efficient algorithm to allocate the power on each Sub-Carrier when we want to send the same modulated embedded bitstream to each user. The improvements are demonstrated in a statistical way, based on histograms. We evaluate the sum-rate capacity of many realizations of the channels and we perform the corresponding histograms of the optimized capacity and the uniform power allocation capacity. We compare the shapes of both histograms in terms of percentage of capacity improvements and we discuss the results.

In the Multi-User MIMO-OFDM case, we investigate the transmission schemes available at the moment. The MIMO multicast case is still under development and practical transmission schemes are not fully mature. We propose an extension of the work of Kaviani [38] based on the zero forcing approach already studied by [60, 13, 27, 12].

Finally, we provide means of tuning the coverage region in a classical broadcast situation without resorting to a huge number of simulations, by means of stochastic geometry. We consider the Multi-User SISO-OFDM case. In this line we obtain a more analytic approach over the capacity. We take in account the probability density distribution of the spatial placement of the users and model the corresponding probability density distribution of the capacity. This allows to present numerical results over the coverage of the MU-SISO scheme.

In all cases, we simulate power allocation algorithms over different scenarios and perform many realizations of channels. The histogram and the statistics permits to give an excellent tool to compare and decide when the base station continues or not performing the power allocation instead of uniform power allocation.

## 1.4 Organization of the Thesis

Chapter I is a general introduction, where we develop the main ideas and objective of the thesis. Chapter 2 provides an introduction to OFDM transmission. Through the analysis of the SISO-OFDM model we explain how the orthogonality works and derive the capacity of the SISO-OFDM scheme. We then concentrate on the MIMO transmission setting and present the model that will be used in the MIMO-OFDM situation. We also review the Multi-User case, providing the available results over those schemes. Finally, since we want to evaluate the systems in a realistic manner, we briefly review the channel models and realistic parameters for data transmission over WIFI systems.

Chapter 3 deals with the Multi-User SISO-OFDM case, and we present an algorithm for allocating optimally the power among each Sub-Carrier at the base station in order to transmit the same signal to multiple users. We derive the system sum-rate capacity and we use Lagrangian optimization to obtain an optimal power distribution over the frequencies. We perform numerical simulations with realistic channel models and provide the channel capacity histograms for many channel realizations. This allows to answer until how much users the optimization is useful. Clearly the optimization is useful for a single user, useless for an infinite number, we are looking for the frontier.

A waterfilling power allocation algorithm is presented in Chapter 4, for the MIMO-OFDM case. We review how the zero forcing method is applied in order to send different information to users, given that send common information is still an unsolved problem for this scheme. With the obtained algorithm we perform numerical simulations over different MIMO schemes, which surge from characterization of the model



itself, and constraints over dimensionality of the matrices appears. The results are analyzed over schemes that respect those dimensionality constraints.

Chapter 5 aims at providing an efficient tool for estimating the coverage of a broadcast system, given the probability density function of the users locations. The coverage problem is addressed for the MU-SISO-OFDM case. In this chapter the spatial distribution of the users is taken into account to calculate the coverage, the outage probability being used as a design criterion. Our aim is to compute the maximum rate that can be transmitted in a Multi-User scenario, with the constraint that a given percentage of the users should have a capacity higher than this rate. This leads us to characterize the probability density distribution (among the users) of the available capacities. Given the channel model of chapter 2, we obtain the pdf of the channel model and derive expressions for the mean and the variance of the capacity. A closed-form expression for the pdf is not found, but approximations are performed, and justified by numerical simulations.

Finally, Chapter 6 concludes and outlines future work.

## 1.5 Notations

To avoid confusion between the classical notations used in telecommunications and mathematical notations used in matrix theory, we first describe the main notations used in this thesis. Usually in telecommunications lower case characters are used for time domain variables and upper case characters are used for frequency domain variables, but on matrix theory lower case variable are elements of a matrix, and for this one upper case characters are used. We propose the following notations in order to avoid the confusion over this issue.

### 1.5.1 Time domain, Frequency domain notations

These notations will be used mainly to explain how the orthogonal frequency division multiplexing works. It appears mainly on the Background on the subsection *OFDM Transmission*, until the subsubsection *SISO OFDM Capacity*. From there after 1.5.2 and 1.5.3 are used.

- $y(t)$  : Time domain continuous variable.
- $Y(f)$  : Frequency domain continuous variable.
- $y_k$  : Discrete time domain variable.
- $Y_n$  : Discrete frequency domain variable.
- $n$  : Frequency domain discrete index.
- $k$  : Time domain discrete index.

### 1.5.2 SISO System Model

These notations are used for the Single Input Single Output (SISO) part.

- $\mathbf{Y}$ : Matrices are denoted by boldface upper case symbols.
- $\mathbf{y}$ : Vectors are denoted by boldface lower case symbols.
- $y$ : Elements of matrices or vectors are denoted by simple non-boldface symbols.
- $y^{(n)}$ : Complex valued element affected to the Sub-Carrier  $n$ .
- $\ell$ : Index of the user.

- $\mathbf{Y}_\ell$ : Matrix affected to the user  $\ell$ .
- $\mathbf{y}_\ell$ : Vectors affected to the user  $\ell$ .
- $y^{(\ell,n)}$ : Complex valued element affected to the user  $\ell$ , on the Sub-Carrier  $n$ .
- $p(\mathbf{x})$  Probability density function (p.d.f.) of the random vector  $\mathbf{x}$ .
- $\mathbf{x} \sim \mathcal{CN}(0, S_{\mathbf{x}})$ : Complex random variable normally distributed with zero mean and covariance matrix  $S_{\mathbf{x}}$
- $S_{\mathbf{x}}$ : Covariance matrix of the sent signal subject to a power constraint such that  $Tr(S_{\mathbf{x}}) \leq P$ .
- $P$ : Total power on the Sub-Carrier.
- $p_n$ : The power affected to the Sub-Carrier  $n$ .
- $L$  Total users receivers.
- $N$ : Number of orthogonal Sub-Carriers.

### 1.5.3 MIMO System Model

These notations are used for the Multiple Input Multiple Output part.

- $t$ : Index for the transmit antenna,  $t = \{1, \dots, T\}$ .
- $T$ : Total number of transmit antenna.
- $r$ : Index for the receiver antenna,  $r = \{1, \dots, R\}$ .
- $R$ : Total number of receive antenna.

- $\mathbf{Y}_{(n)}$ : Matrix affected to the Sub-Carrier  $n$ .
- $\mathbf{y}_{(n)}$ : Vector affected to the Sub-Carrier  $n$ .
- $y_r^{(n)}$ : Complex valued element affected to the Sub-Carrier  $n$ , at the receiver antenna  $r$ .
- $\mathbf{H}_{(n)}$ : MIMO-channel matrix from the base station to the user  $\ell$  on the sub-carrier  $n$ .

$$\mathbf{H}_{(n)} = \begin{pmatrix} h_{11}^{(n)} & \dots & h_{1T}^{(n)} \\ \vdots & \ddots & \vdots \\ h_{R1}^{(n)} & \dots & h_{RT}^{(n)} \end{pmatrix} \quad (1.1)$$

- $\mathbf{y}_{(\ell,n)}$ : Vector affected to the user  $\ell$  at the Sub-Carrier  $n$ .
- $\mathbf{y}_{(\ell,n)} = (y_1^{(\ell,n)T} \dots y_R^{(\ell,n)T})^T$ : Received vector over the  $R$  antennas.
- $\mathbf{x}_{(n)} = (x_1^{(n)T} \dots x_T^{(n)T})^T \sim \mathcal{CN}(0, S_{\mathbf{x}_{(n)}})$ : The sent signal  $\mathbf{x}_{(n)} \in \mathbb{C}^{A_t \times 1}$ , on the Sub-Carrier  $n$ .
- $S_{\mathbf{x}_{(n)}}$ : Covariance matrix of the sent signal subject to a power constraint such that  $Tr(S_{\mathbf{x}_{(n)}}) \leq P_n$ . Where  $Tr(\cdot)$  is the trace of the referred matrix
- $P_n$  is the total power on the sub-carrier  $n$ .
- $\mathcal{W}^{(n)} \in \mathbb{C}^{A_t \times LS}$ : The super-matrix  $\mathcal{W}^{(n)} = (\mathbf{W}_{(1,n)} \dots \mathbf{W}_{(L,n)})$ , contains the set of matrix pre-filters  $\{\mathbf{W}_{(\ell,n)}\} \in \mathbb{C}^{A_t \times S}$
- $\mathbf{u}^{(n)} \in \mathbb{C}^{LS \times 1}$ : The super-vector  $\mathbf{u}^{(n)} = (\mathbf{u}_{(1,n)}^T \dots \mathbf{u}_{(L,n)}^T)^T$ , contains the stacked intended S-symbols vector  $\{\mathbf{u}_{(\ell,n)}\} \in \mathbb{C}^{S \times 1}$  to be sent to the L-users.

- $\mathbf{H}_{(\ell,n)}$ : MIMO-channel matrix from the base station to the user  $\ell$  on the sub-carrier  $n$ , is given by

$$\mathbf{H}_{(\ell,n)} = \begin{pmatrix} h_{11}^{(\ell,n)} & \dots & h_{1T}^{(\ell,n)} \\ \vdots & \ddots & \vdots \\ h_{R1}^{(\ell,n)} & \dots & h_{RT}^{(\ell,n)} \end{pmatrix} \quad (1.2)$$

- $h_{rt}^{(\ell,n)}$ : Composed fading coefficient from the transmit antenna  $t$  to the receiver antenna  $r$ .
- $|\mathcal{A}|$ : Determinant of  $\mathcal{A}$ ,  $(\cdot)^H$  is the hermitian operator and  $(\cdot)^T$  is the transpose operator.

# Chapter 2

## Concepts in wireless communications systems

The growing of high data traffic demand by mobile devices has put a big challenge to the industry and the science world. The orthogonal frequency division multiplexing (OFDM) technique is an efficient mean to fight the impairments of the wireless channel. The flexibility of the OFDM technology permits to develop practical resource allocation algorithms. In this chapter we describe the elements to understand the constraints that appear when we try to send information simultaneously to multiple users over a wireless medium. The OFDM is first introduced. Our aim is to understand the efficiency of this technique compared to the single carrier transmission in scattered SISO environments and to derive the corresponding system capacity. We extend these results to the MIMO case. A state of the art of the multiuser case in SISO-OFDM and MIMO-OFDM is then presented. Finally we review the main characteristics of the wireless channel and present the model that will be used in the simulations.

## 2.1 Transmission in wireless communications

This section briefly describes the Orthogonal Frequency Division Multiplexing (OFDM) technology and the various transmission schemes used to send information over a wireless channel. The SISO model is the more simple scheme where the transmitter sends information to a single user via a single antenna, the user also disposes of a single antenna. Many wireless technologies and standards were developed based on this technology. It is still of great scientific and industrial interest, since small and cheap devices can be constructed, integrating many features and services. Since the work of Winters, Foschini and Telatar [76, 24, 23, 65]; a growing interest was put in MIMO systems, due to the results that showed an increment of the capacity using the same amount of power (compared to a SISO system). On the other hand, recent telecommunications standards designed for packet transmission wireless networks like IEEE 802.16 [1], IEEE 802.11 [3] or from mobile technologies like 3GPP Long Term Evolution (LTE) [2], use OFDM multi-carrier systems to provide reliable downlink communication. Appeared in december 1966, the seminal paper of Chang [11] brings the principles of orthogonal multiplexing for multichannel data over a band-limited channel. This interesting technique was first implemented by the means of analog filters, but Weinstein [75] proposes digital Fast Fourier Transform algorithm including a Guard Interval to prevent the overlapping in time domain. In 1980, Peled [52] introduces a Cyclic Extension used in a digital implementation of the work of Weinstein [75]; allowing the transmitted sequence to appear periodic, in that way the circular convolution properties hold. OFDM is now present in various standards, in SISO and MIMO variants.

### 2.1.1 Basic principles of OFDM

Transmission over a single carrier is highly impacted by Inter Symbol Interference (ISI) when the data rate increases. This problem is faced by equalization methods that respect the Nyquist criterion, but the complexity of the equalizer increases (in the receiver) with the data rate and the cost of high data rate transmission becomes prohibitive [12]. The frequency selective channel can be fought using multi-carrier transmission. Modulated in different frequencies, the channel can be split in multiple flat fading narrowband sub-channels. Since the overall data rate is shared among the sub-channels, the equalizer is less complex. This situation also ensures low distortion data transmission if the orthogonality among the sub-carriers is kept [12, 4, 44], which is the case in OFDM.

OFDM is a type of multi-carrier transmission, where the communication is split over " $N \geq 1$ " orthogonal sub-carriers. The implementation cost is maintained to a reasonable level because the whole set of sub-bands can be implemented with a single Radio Frequency chain, the decomposition being performed via IFFT and FFT algorithms [75].

Given that, OFDM translates the wideband frequency selective channel into an equivalent set of narrowband flat fading channels spread in frequency. Even if the attenuations of these channels are not independent (they depend on a small number of time frequency coefficients), this allows to adapt the power put on the different frequencies with an algorithm well known as water-filling or water-pouring [59, 17]. In that way, frequency diversity can be used.



### Drawback of SISO Communication model using single carrier transmission

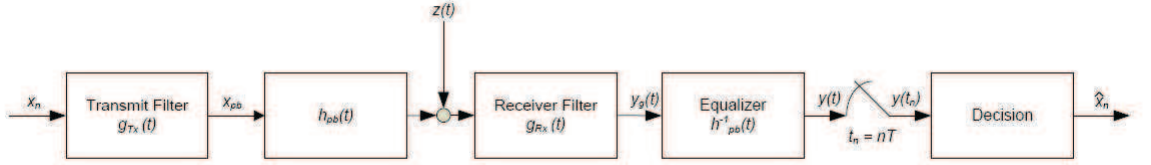


Figure 2.1: Single carrier communication model

The transmission scheme to be used in the sequel is the complex baseband equivalent model that is an abstraction of the real valued bandpass model [56, 55]. Consider the baseband transmission model depicted in Figure 2.1, where  $h_{pb}(t)$  is a bandlimited channel with bandwidth  $W$ . At the transmitter side, the transmit filter  $g_{Tx}(t)$  is used to adapt the digital symbol  $x_k$  to a passband waveform to be sent through the bandwidth limited channel. At the receiver side, the receiver filter  $g_{Rx}(t)$  detects the transmitted signal, and the equalizer  $h_{pb}^{-1}(t)$  that compensates the attenuation of the channel. The signal after the equalization is given by the following equation:

$$y(t) = \sum_{m=-\infty}^{\infty} x(mT_s)h(t - mT_s) + z(t) \quad (2.1)$$

where  $h(t) = g_{Tx}(t) * h_{pb}(t) * g_{Rx}(t) * h_{pb}^{-1}(t)$ , is the impulse response of the overall baseband equivalent system.

From this simple model one can obtain the constraints that allow to configure a single carrier transmission. We have  $h(t)$ , the baseband equivalent channel with bandwidth  $W$ .  $x(mT_s) = x(m) = x_m$  is the transmitted symbols are  $x_k$ , which are complex and sent with a data rate of  $R = \frac{1}{T_s}$ , where  $T_s$  is the symbol period. The

transmit filter  $g_{T_x}(t)$  shapes the symbols at rate  $R$  over a single carrier frequency and the corresponding signal is sent over the channel. If we sample this signal  $t_k = kT_s$  and isolate symbol  $k$ , we have:

$$y_k = x_k h(0) + \sum_{m=-\infty, m \neq k}^{\infty} x_m h((k-m)T_s) + z(t) \quad (2.2)$$

If  $h((k-m)T_s) \neq 0$ , the second part of the equation represents an Inter Symbol Interference (ISI) which has to be taken into account in order to detect  $x_k$ . If the rate  $R$  increases, the symbol period  $T_s$  approaches zero,  $(k-m)T_s \rightarrow 0$  and ISI becomes important.

The symbol  $x_k$  is digital modulated, usual modulation schemes are BPSK, QPSK, 16-QAM or 64-QAM. These different modulations permits link adaptation, i.e., if the channel presents good conditions we can select a high data rate modulation scheme in the communication system [45, 29].

OFDM increases the symbol duration of the sub-carriers, while decreasing accordingly their bandwidth. This represents a compromise between time-frequency use [55, 43]. The next section introduces more precisely the OFDM scheme, that has strong characteristic to face a high data rate.

### Multicarrier transmission, OFDM

When we increase the data rate on the traditional schemes, intersymbol interference appears. To overcome this situation, the OFDM technique splits the data rate into several lower data rate symbols. Each symbol is put on an orthogonal sub-carrier. This section shows how this is feasible.

**Orthogonality** :

The orthogonality of the OFDM transmission is based on an *orthogonal basis function* argument. Let the following set  $\Phi = \{\varphi_0(t), \dots, \varphi_{N-1}(t)\}$ , we say that this set is said to be an orthogonal basis function if the inner product between each element is null, that is:

$$\langle \varphi_i(t), \varphi_k(t) \rangle = \int_D \varphi_i(t) \varphi_k(t) dt = 0, \text{ if } k \neq i \in \mathbb{N} \quad (2.3)$$

where  $D$  is the domain of the inner product.

An example of one of these orthogonal basis functions is the *Fourier basis functions* made of complex exponentials as follows:

$$\varphi_n = e^{j2\pi f_n t} \quad (2.4)$$

If we define orthogonal signals with set of  $N$  functions  $\Phi_F = \{e^{j2\pi f_0 t}, \dots, e^{j2\pi f_{N-1} t}\}$  in the period  $t \in [0, T_{sym}]$ , those signals are orthogonal if the inner product in the fundamental period is zero. That is:

$$\frac{1}{T_{sym}} \int_0^{T_{sym}} e^{j2\pi f_i t} e^{j2\pi f_k t} dt = 0, \text{ if } k \neq i \in \mathbb{N} \quad (2.5)$$

Taking the discrete samples at  $t = mT_s$ , where  $T_s = \frac{T_{sym}}{N}$  is the modulated symbol period and  $T_{sym}$  is the oversampled period (OFDM symbol period). With  $m$  the index of the discrete time, we have:

$$\frac{1}{N} \sum_{m=0}^{N-1} e^{j2\pi \frac{i}{T_{sym}} mT_s} e^{j2\pi \frac{k}{T_{sym}} mT_s} = 0, \text{ if } i \neq k \in \mathbb{N} \quad (2.6)$$

which is the discrete time expression of orthogonality and is an important condition for the OFDM signal.

**OFDM Modulation and Demodulation** From the last section we saw that with a Fourier basis we can have an orthogonality between the functions of the basis. In this section we apply this property in order to transmit various symbols over orthogonal parallel channels.

Let  $X_{s,n}$  be the  $s$ -th symbol (QAM or QPSK) at the  $n$ -th sub-carrier of the OFDM system. Consider that those elements are defined in the frequency domain, therefore, they must be translated in the time domain in order to allow transmission. We use an orthogonal basis  $\Phi = \{\varphi_{s,1}(t), \dots, \varphi_{s,N-1}(t)\}$  defined by:

$$\varphi_{s,n}(t) = \begin{cases} e^{j2\pi f_n(t-sT_{sym})} & \text{if } 0 < t \leq T_{sym}, \\ 0 & \text{otherwise} \end{cases}$$

The OFDM bandpass signal in the continuous time domain is:

$$x(t) = \text{Re} \left\{ \frac{1}{T_{sym}} \sum_{s=0}^{\infty} \left\{ \sum_{n=0}^{N-1} X_{s,n} \varphi_{s,n}(t) \right\} \right\} \quad (2.7)$$

The base band OFDM signal is:

$$x(t) = \sum_{s=0}^{\infty} \sum_{n=0}^{N-1} X_{s,n} e^{j2\pi f_n(t-sT_{sym})} \quad (2.8)$$

In order to recover the  $s$ -th symbol OFDM, we must sample the signal at  $t = sT_{sym} + kT_s$ .

Where  $T_s = \frac{T_{sym}}{N}$ ,  $f_n = \frac{n}{T_{sym}}$ . With this sampling, we obtain the discrete OFDM symbol:

$$x_{s,k} = \sum_{n=0}^{N-1} X_{s,n} e^{j2\pi \frac{nk}{N}} \text{ for } k = 0, 1, \dots, N_{FFT} \quad (2.9)$$

This expression is similar to the  $N$ -point ( $N = N_{FFT}$ ) IDFT of  $\{X_{s,n}\}$ :

$$x_{s,k} = \frac{1}{N_{FFT}} \sum_{n=0}^{N_{FFT}-1} X_{s,n} e^{j2\pi \frac{nk}{N_{FFT}}} \text{ pour } k = 0, 1, \dots, N_{FFT} \quad (2.10)$$

and can be implemented using very efficient algorithms, as IFFT [47].

Consider for a while that the transmission channel is noiseless. The received base band OFDM signal is:

$$y_s(t) = \sum_{i=0}^{N_{FFT}-1} X_{s,i} e^{j2\pi f_i(t-sT_{sym})}, \quad \text{with } sT_{sym} \leq t \leq sT_{sym} + kT \quad (2.11)$$

If we sample the received OFDM signal at  $t = sT_{sym} + kT$ , we obtain the discrete time OFDM symbol as:

$$y_{s,k} = \frac{1}{N_{FFT}} \sum_{i=0}^{N_{FFT}-1} X_{s,i} e^{j2\pi \frac{ik}{N_{FFT}}}, \quad sT_{sym} \leq t \leq sT_{sym} + kT \quad (2.12)$$

On the other hand, in the frequency domain the OFDM symbol at the  $n$ -th sub carrier is given as follows:

$$Y_{s,n} = \sum_{k=0}^{N_{FFT}-1} y_{s,k} e^{-j2\pi \frac{kn}{N_{FFT}}} \text{ for } n = 0, 1, \dots, N_{FFT} - 1 \quad (2.13)$$

Replacing (2.12) in (2.13) we have:

$$Y_{s,n} = \frac{1}{N_{FFT}} \sum_{k=0}^{N_{FFT}-1} \sum_{i=0}^{N_{FFT}-1} X_{s,i} e^{j2\pi \frac{(i-n)k}{N_{FFT}}} \quad (2.14)$$

Here the orthogonality between the frequencies holds and we can see that  $Y_{s,n} = X_{s,n}$  if  $i = n$ , like (2.6).

The figure 2.2 on the next page shows the OFDM modulation and demodulation scheme. The bits enters the mapper and digital modulated symbols are generated

(QAM/PSK). The symbols are put in the subcarriers at different frequencies, this operation is made by the IFFT algorithm. The sent signal is bi-orthogonal, over the time and over the frequency domain. The signal is recovered by adapted filter in each frequency, and parallel serial converted in order to be sent to the demapper and recover de bitstream.

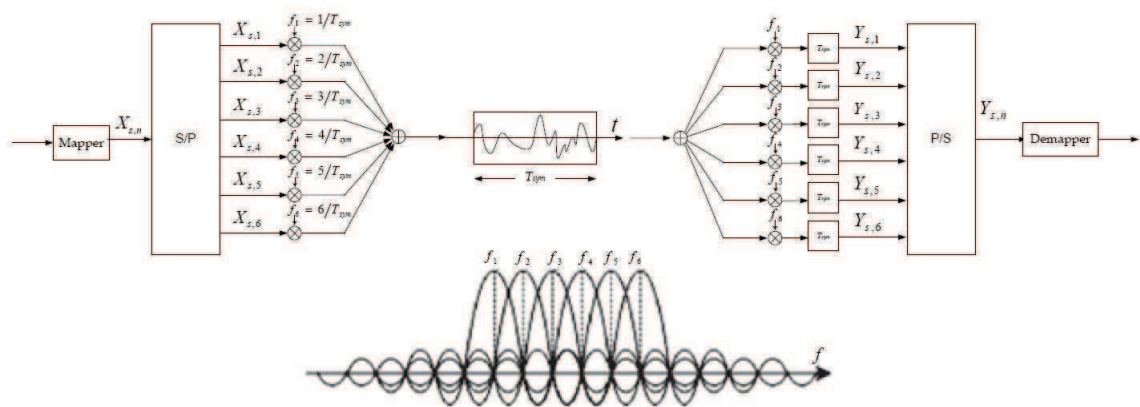


Figure 2.2: OFDM Modulation / Demodulation

**Linear and cyclic convolutions** The sampled signal is converted to an analog signal that undergoes convolution by the channel. Even if the bandwidth of each sampled signal is narrow, and, as a consequence the symbol period becomes large, the channel convolution still enlarges the received signal, and if the next OFDM symbol follows immediately, inter-symbol interference will take place. To solve this problem a guard interval is added to the signal. In this case, no ISI will take place. Moreover, if the transmit symbol is extended by a cyclic prefix, this solution ensures orthogonality between the transmitted OFDM symbols. This is explained below.

If we transmit the OFDM signal  $x_s(t)$  over a channel with impulse response  $h_s(t)$ ,

the receiver sees  $y_s(t)$  which is the linear convolution:

$$y_s(t) = x_s(t) * h_s(t) + z_s(t) = \int_0^{\infty} h_s(t)x_s(t - \tau)d\tau + z_s(t) \quad (2.15)$$

If we sample both this received signal and the transmit signal at times  $kT_s = k\frac{T_{sym}}{N_{FFT}}$ , the discrete version of the linear convolution is expressed as:

$$y_{s,k} = x_{s,k} * h_{s,k} + z_{s,k} = \sum_{m=0}^{\infty} h_{s,k}x_{s,k-m} + z_{s,k} \quad (2.16)$$

On another hand, we know that for two finite periodic sequences  $\{x'_{s,k}\}$  and  $\{h'_{s,k}\}$ , the Fourier transform of those type of sequences is a periodic sequence over the frequency domain, with period  $N_{FFT}$  [47]. The  $N_{FFT}$ -point discrete Fourier transform, of those sequences are:

$$DFT_{N_{FFT}} [\{x'_{s,k}\}] = X'_{s,n} \quad (2.17)$$

$$DFT_{N_{FFT}} [\{h'_{s,k}\}] = H'_{s,n} \quad (2.18)$$

Due to the periodicity (or circularity) of the discrete Fourier transform, the circular convolution is defined by:

$$x'_{s,k} \odot h'_{s,k} = \sum_{m=0}^{N_{FFT}-1} h'_{s,k}x'_{s,(k-m)_{N_{FFT}}} \quad (2.19)$$

where  $\odot$  denotes the operator for circular convolution and  $(\cdot)_N$  is the modulo- $N$  operator defined by:

$$(k - m)_{N_{FFT}} = \begin{cases} (k - m) & \text{if } (k - m) \geq N_{FFT} \\ N_{FFT} - (k - m) & \text{if } (k - m) < N_{FFT} \end{cases}$$

A property of the circular convolution is that

$$DFT_{N_{FFT}} [\{x'_{s,k} \odot h'_{s,k}\}] = X'_{s,n} H'_{s,n} \quad (2.20)$$

But we want to calculate *the linear convolution* given by the equation (2.16). In 1980 Peled [52] proposed a solution which consist to add a prefix over one of those sequences (i.e. append the beginning of the sequence at its end), in such a way that the output of the linear filter provides exactly the same samples as those that would be provided by the periodic (or cyclic) convolution over one period. It is the origin of the name, Cyclic Prefix (CP).

Consider and define the channel samples of length  $L_h$ , as :

$$h'_{s,k} = \begin{cases} h_{s,k} & \text{if } 0 \leq k \leq L_h - 1 \\ 0 & \text{otherwise} \end{cases}$$

The sent signal is composed by the extension of the signal that comes from the IDFT and the desired signal itself, as:

$$x_{s,k} = \begin{cases} x'_{s,k} & \text{if } 0 \leq k \leq N_{FFT} \\ x'_{s,N+k} & \text{if } -L_h < k \leq 0 \end{cases}$$

Taking up (2.16) and considering the length of the channel  $L_h$  and replacing by the upper definitions we have:

$$y_{s,k} = x_{s,k} * h_{s,k} = \sum_{m=0}^{L_h-1} h_{s,k} x_{s,k-m} \quad (2.21)$$

$$= \sum_{m=0}^{L_h-1} h_{s,k} x'_{s,(k-m)_{N_{FFT}}} = x'_{s,k} \odot h'_{s,k} \quad (2.22)$$

The interested point is that the CP allows the transmit signal to be circularly



convolved with the channel samples. So the cyclic property of (2.20) holds:

$$Y_{s,n} = \sum_{k=0}^{N_{FFT}-1} (x'_{s,k} \odot h'_{s,k}) e^{-j2\pi \frac{kn}{N_{FFT}}} \quad (2.23)$$

$$= X'_{s,n} H'_{s,n} \quad (2.24)$$

In other words the string of transmitted symbols is received as if it would have gone through a set of parallel channels. The only cost is the duration of the guard interval, which has to be small compared with the duration of the OFDM symbol. This is the reason why, in order to maintain a good spectral efficiency, OFDM systems with guard interval usually involve a large number of sub-carriers. In what follows, since we are comparing only OFDM systems, the corresponding loss of spectral efficiency is considered as being negligible.

### SISO OFDM Capacity

In this section, based on an information theoretic framework, all input signals are assumed to be Gaussian, since it is well known that this choice maximizes capacity. Therefore, the corresponding results should be considered as upper bounds of the attainable transmission rates.

Since, in frequency domain, OFDM is equivalent to individual channel gains per transmitted symbol, the system of a point to point transmission can be modelled as:

$$\mathbf{y} = \mathbf{H}\mathbf{x} + \mathbf{z} \quad (2.25)$$

where  $\mathbf{y} = (y^{(1)}, \dots, y^{(N)})$  is the complex baseband received vector. Matrix  $\mathbf{H}$  is the orthogonal channel matrix, a diagonal matrix whose elements represents the complex

gain on each sub-carrier, as shown below:

$$\mathbf{H} = \begin{bmatrix} h^{(1)} & 0 & \dots & 0 \\ 0 & h^{(2)} & \ddots & \vdots \\ \vdots & \ddots & \ddots & 0 \\ 0 & \dots & 0 & h^{(N)} \end{bmatrix} \quad (2.26)$$

The transmitted symbol is denoted  $\mathbf{X} = (x^{(1)}, \dots, x^{(N)}) \sim \mathbb{C}\mathcal{N}(0, S_x)$ .  $S_x$  is a diagonal covariance matrix of the vector  $\mathbf{X}$ , which elements are the power that is put on the symbol. Such that:

$$S_x = \begin{bmatrix} p_1 & 0 & \dots & 0 \\ 0 & p_2 & \ddots & \vdots \\ \vdots & \ddots & \ddots & 0 \\ 0 & \dots & 0 & p_N \end{bmatrix} \quad (2.27)$$

The received signal is affected by a complex additive white Gaussian noise  $Z \sim \mathbb{C}\mathcal{N}(0, S_z)$ , and the noise covariance matrix in the parallel channel model is diagonal since the channels are orthogonal.

The mutual information  $I(\mathbf{x}; \mathbf{y})$  between the set of input signals and the received ones is expressed as follows:

$$I(\mathbf{x}; \mathbf{y}) = \frac{1}{N} \sum_{n=1}^N \log_2 \left( 1 + \frac{|h^{(n)}|^2 p_n}{\sigma_z^2} \right) \quad \text{bits/s/Hz} \quad (2.28)$$

The above mutual information depends heavily on the power allocation on each sub-carrier, and since the power available at the base station is constrained, it is important to optimize the mutual information in terms of the individual sub-carrier

powers, in order to obtain the capacity of the system. The sum of the powers on the subcarriers must satisfy  $\sum_{n=1}^N p_n \leq P$ , where  $P$  is the total available power.

In order to maximize the mutual information, we formulate the following convex optimization problem [6]:

$$\min_{p_n} \left\{ -\frac{1}{N} \sum_{n=1}^N \log \left( 1 + \frac{|h^{(n)}|^2 p_n}{\sigma_z^2} \right) \right\} \quad (2.29)$$

$$\text{Subject to } \begin{cases} \sum_{n=1}^N p_n = P \\ -p_n \leq 0 \end{cases} \quad (2.30)$$

The Lagrangian optimization provides the following:

$$\frac{-1}{p_n + \frac{\sigma_z^2}{|h^{(n)}|^2}} + \lambda = 0 \quad (2.31)$$

Using the positiveness of the power put on each carrier (2.33), we obtain the well known waterfilling result [17]:

$$p_n = \left( \frac{1}{\lambda} - \frac{\sigma_z^2}{|h^{(n)}|^2} \right)^+ \quad (2.32)$$

where  $(\cdot)^+$  denotes the function:

$$(x)^+ = \begin{cases} x, & x \geq 0 \\ 0, & \text{otherwise} \end{cases} \quad (2.33)$$

The nice form of this algorithm allows an optimal power allocation, assuming that the channel state information is known at the transmitter.

### Discussion on the SISO Model

The full band SISO model has clear drawbacks in terms of complexity when the data rate increases, this can be overcome with a multi-carrier modulation such as OFDM. In the point to point model, OFDM allows to divide the full band frequency selective channel in a number of parallel flat fading subchannels. This allows an efficient and easy use of power allocation algorithms at the transmitter among the various subchannels, namely the waterfilling algorithm.

### **2.1.2 MIMO communication Model**

The Multiple Input Multiple Output (MIMO) scheme, allows to increase data rates compared to the SISO case, by exploiting two main characteristics: Multiplexing and Diversity [29, 76]. Under specific conditions, the MIMO channel capacity increases by a factor proportional to the rank of the channel matrix, without using additional transmit power or spectral bandwidth [12, 29]. Multiplexing exploits the structure of the channel gain to increase data rate, because independent data streams are transmitted over the antenna array. Diversity techniques exploit the channel state information at the transmitter or at the receiver, or both to improve the transmission reliability. This improvement is based on the fact that a deep fading is unlikely to appear on all channels at the same time or frequency, allowing smart techniques to be applied at the transmission or the reception to have a reliable connection [12, 29, 50]. The cost to implement this solution is to increase the number of antennas properly located. Keeping the added complexity required by the corresponding signal processing to a reasonable amount is a challenge in order to design component elements and algorithms compatible with energy-saving philosophy. The papers that are commonly

cited on this subject are [76, 65, 23, 24] .

The usual model presented in the literature is as follows:

$$\begin{pmatrix} y_1 \\ \vdots \\ y_R \end{pmatrix} = \begin{pmatrix} h_{11} & \dots & h_{1T} \\ \vdots & \ddots & \vdots \\ h_{R1} & \dots & h_{RT} \end{pmatrix} \begin{pmatrix} x_1 \\ \vdots \\ x_T \end{pmatrix} + \begin{pmatrix} z_1 \\ \vdots \\ z_R \end{pmatrix} \quad (2.34)$$

or simply:

$$\mathbf{y} = \mathbf{H}\mathbf{x} + \mathbf{z} \quad (2.35)$$

Where  $\mathbf{y}$  is a complex vector that models the receiver with  $R$  receive antennas. The transmitter is modeled by the complex vector  $\mathbf{x}$  of size  $T$ , the number of antennas. The transmitted signal is sent through the channel represented by matrix  $\mathbf{H}$  of size  $R \times T$ . Different configurations can be distinguished depending on the number of antennas at the transmitter or the receiver depending on whether we want to have maximum data rate or a reliable transmission. In MIMO systems the Channel State Information has a crucial influence on the capacity of the system. The improvement over the SISO situation can be different if we have Channel State Information available at the Transmitter (CSIT) and/or at the receiver (CSIR). We review these different situations in the next sections.

The first results in information theory over MIMO channel are the results of Telatar and Foschini [65, 23]. In those papers the mutual information for the static channel is obtained and is:

$$I(\mathbf{x}; \mathbf{y}) = \log_2 \det \left( \mathbf{I}_R + \frac{1}{\sigma_z^2} \mathbf{H}\mathbf{S}_x\mathbf{H}^H \right) \quad (2.36)$$

where  $\mathbf{S}_x$  is the covariance matrix of the vector  $\mathbf{x}$ . The mutual information  $I(\mathbf{x}; \mathbf{y})$  is optimal when the input vector is zero-mean circularly-symmetric complex gaussian [65]. The capacity is obtained by maximizing the mutual information over the covariance matrices  $\mathbf{S}_x$  that satisfies the power constraints. That is:

$$C_{MIMO} = \max_{\mathbf{S}_x: \text{Tr}(\mathbf{S}_x) \leq P} \log_2 \det \left( \mathbf{I}_R + \frac{1}{\sigma_z^2} \mathbf{H} \mathbf{S}_x \mathbf{H}^H \right) \quad (2.37)$$

An optimal value of the capacity  $C_{MIMO}$  will be conditioned by the knowledge or not of the Channel State Information (CSI). We will review some results, but further details can be found in [68, 65, 50, 29, 27, 23, 24].

### MIMO channel capacity with CSIT and CSIR

The CSIR can be obtained by the use of a training sequence before transmitting data. The CSIT can be obtained by assuming some feedback from the receiver, which can forward its own estimations of the channel. Usually, since this is a very small piece of information, this is assumed to be obtained at a negligible cost. Assume that the channel state information is known at the transmitter and the receiver, the transmitter can prepare the transmission based on this knowledge. This is obtained via a Singular Value Decomposition (SVD) of the channel, i.e.:

$$\mathbf{H} = \mathbf{U} \mathbf{\Sigma} \mathbf{V}^H \quad (2.38)$$

where  $\mathbf{U} \in \mathbb{C}^{R \times R}$  and  $\mathbf{V} \in \mathbb{C}^{T \times T}$  are unitary matrices, and  $\mathbf{\Sigma} \in \mathbb{C}^{R \times T}$  is a diagonal matrix contains singular values of the channel (the square root of the eigenvalues):  $\sqrt{\gamma_1} \geq \dots \geq \sqrt{\gamma_J}$ , whit  $J = \text{Rank}(\mathbf{H})$ . The columns of  $\mathbf{U}$  are the eigen-vectors of  $\mathbf{H} \mathbf{H}^H$ , while the columns of  $\mathbf{V}$  are the eigen-vectors of  $\mathbf{H}^H \mathbf{H}$ . If we replace the SVD

in (2.36), we have:

$$I(\mathbf{x}; \mathbf{y}) = \log_2 \det \left( \mathbf{I}_R + \frac{1}{\sigma_z^2} \Sigma \mathbf{Q} \Sigma \right) \quad (2.39)$$

where  $\mathbf{Q} = \mathbf{V}^H \mathbf{S}_x \mathbf{V}$ . In [65], the author observes that  $\mathbf{Q}$  is a positive semidefinite matrix, and the Hadamard inequality can be used in the determinant part, resulting in:

$$\det \left( \mathbf{I}_R + \frac{1}{\sigma_z^2} \Sigma \mathbf{Q} \Sigma \right) \leq \prod_j \left( 1 + \frac{Q_{jj} \gamma_j}{\sigma_z^2} \right) \quad (2.40)$$

Replacing the later in (2.36), the mutual information is optimal when  $\mathbf{Q}$  is a diagonal matrix, the deterministic channel capacity is given as follows:

$$C = \sum_{j=1}^J \log_2 \left( 1 + \frac{Q_{jj} \gamma_j}{\sigma_z^2} \right) \quad (2.41)$$

Also it can be observed that the capacity grows linearly as  $\text{Rank}(\mathbf{H})$  increases [65, 23].

**MIMO waterfilling** When we have CSIT and CSIR, matrix  $\mathbf{Q}$  plays the same role as the covariance matrix  $\mathbf{S}_x$ , that is diagonal and which elements on the diagonal are the powers  $P_t, t = \{1, \dots, T\}$ , allocated on each parallel eigen-mode of the channel with a limitation on the  $J = \text{Rank}(\mathbf{H})$ . The equation (2.41) can be maximized in order to obtain an adequate power allocation over the eigen modes [65, 29]:

$$\max_{P_j: \sum_{j=1}^J P_j \leq P} \sum_{j=1}^J \log_2 \left( 1 + \frac{P_j \gamma_j}{\sigma_z^2} \right) \quad (2.42)$$

After the Lagrangian maximization we have:

$$P_j = \left( \frac{1}{\lambda} - \frac{\sigma_z^2}{\gamma_j} \right)^+ \quad (2.43)$$

Power allocation among the channel eigen-modes is also a water-filling algorithm, this time for the MIMO scheme.

### MIMO channel capacity without CSIT and with CSIR

When no CSIT is available, the optimal allocation that can be made is equal power over the antennas. The covariance matrix is  $\mathbf{S}_x = \frac{P}{\sigma_z^2 T} \mathbf{I}_T$ . Replacing by the uniform power allocation covariance matrix, equation (2.36) becomes:

$$I(\mathbf{x}; \mathbf{y}) = \log_2 \det \left( \mathbf{I}_R + \frac{P}{\sigma_z^2 T} \mathbf{H} \mathbf{H}^H \right) \quad (2.44)$$

Using the singular value decomposition we have:

$$I(\mathbf{x}; \mathbf{y}) = \sum_{j=1}^{N_Z} \log_2 \left( 1 + \frac{P}{\sigma_z^2 T} \gamma_j \right) \quad (2.45)$$

The equation (2.45) permit to have an instantaneous capacity over a realization of the channel  $\mathbf{H}$ . While a mean capacity can be obtained by averaging with respect to the pdf of  $\mathbf{H}$ .

### MIMO outage channel capacity

In the design of broadcast or multicast systems, a useful quantity is the outage probability, defined as:

$$\mathbb{P}_{out} = \mathbb{P} \left( \mathbf{H} : \log_2 \det \left( \mathbf{I}_R + \frac{P}{\sigma_z^2 T} \mathbf{H} \mathbf{H}^H \right) < C_{out} \right) \quad (2.46)$$



Where a transmission  $C_{out}$  is a reference desired bit-rate necessary to obtain some service. An appropriate measure of efficiency of a given scheme is the probability that the obtained rate is smaller than the required one (i.e. that the channel is in "outage"). This is the definition of the outage probability, as defined by [48, 65, 29]. As seen above, the mutual information depends on the distribution of the channel eigenvalues. For large systems, the behavior of the singular values distribution has been heavily studied, and the random matrix theory give answers to many questions, as can be seen in [29] and the references cited inside.

### MIMO-OFDM channel capacity

The MIMO OFDM system model can be represented in frequency domain as  $N$  independent MIMO system with  $R \times T$  channel matrices, when we consider a sufficiently large cyclic prefix in the  $T$  transmit antenna [29, 63]. A detailed explanation can found in [63]. With the assumption that the OFDM system is properly designed, one sub-carrier of the MIMO OFDM system is described as:

$$\begin{pmatrix} y_1^{(n)} \\ \vdots \\ y_R^{(n)} \end{pmatrix} = \begin{pmatrix} h_{11}^{(n)} & \dots & h_{1T}^{(n)} \\ \vdots & \ddots & \vdots \\ h_{R1}^{(n)} & \dots & h_{RT}^{(n)} \end{pmatrix} \begin{pmatrix} x_1^{(n)} \\ \vdots \\ x_T^{(n)} \end{pmatrix} + \begin{pmatrix} z_1^{(n)} \\ \vdots \\ z_R^{(n)} \end{pmatrix} \quad (2.47)$$

or simply:

$$\mathbf{y}_{(n)} = \mathbf{H}_{(n)}\mathbf{x}_{(n)} + \mathbf{z}_{(n)} \quad (2.48)$$

Where  $\mathbf{y}_{(n)}$  is a complex vector that corresponds to the  $R$  signals received by the antennas on the sub-carrier  $n$ . The transmitter sends the complex vector  $\mathbf{x}_{(n)}$  on its  $T$

antennas. The transmitted signal is sent through the channel represented by matrix  $\mathbf{H}_{(n)}$  of size  $R \times T$ . Since, under the above mentioned assumptions, the structure is similar to (2.34) and (2.35); the formulas developed in the above section are fully valid.

### **Discussion on the MIMO Model**

Even more than in the SISO context is the channel state information at the receiver and the transmitter is important for the MIMO model, in order to obtain high data rates through spatial multiplexing techniques or reliable transmission through diversity techniques. Under ideal orthogonality, the MIMO OFDM system can be view as  $N$ -individual MIMO systems in parallel in the frequency domain.

## **2.2 Multi-User SISO communication system**

The previous sections dealt with OFDM systems, either in a SISO or a MIMO setting used for a point to point communication. We derived the link capacity for the SISO-OFDM model, and extended it to the single user MIMO model. Since our problem is to send information to multiple users, the need to understand how the models should be modified in order to accurately take the new situation into account.

This section reviews the model used for the multiuser case as well as the main results available in this context. In a multiuser setting one distinguishes between two main situations, depending on the direction of the communication : to the base station or from the base station, i.e. the uplink and the downlink. In information theory the downlink is known as broadcast channel (BC) and the uplink is known as the multiple access channel (MAC).

### 2.2.1 Channel capacity of MU-SISO broadcast channel

The broadcast channel is described in [17] in terms of flat fading channels. In the OFDM context, because of the orthogonality between the sub-carriers, we have  $N$  independent broadcast channels. The mathematical model for the OFDM case on each sub-carrier is:

$$y^{(\ell,n)} = h^{(\ell,n)}x^{(n)} + z^{(\ell,n)} \quad (2.49)$$

where  $y^{(\ell,n)} \in \mathbb{C}$  is the baseband received signal on the sub-carrier  $n$  of the user  $\ell$ . The signal to be broadcasted is  $x^{(n)} \in \mathbb{C}$  a complex baseband modulated symbol over the sub-carrier  $n$ . In a SISO context, this signal reaches user  $\ell$  after passing through  $h^{(\ell,n)} \in \mathbb{C}$  that is the Fourier transform of the impulse response of the time invariant channel of user  $\ell$  on sub-carrier  $n$ . The symbol meets a power constraint:  $E\{|x^{(n)}|^2\} \leq P_n$ .

Cover in [17] states that, in order to send a common information to all users one can just transmit the same signal with the power allowing to reach the capacity of the worst user. Another situation arises when one wants to send different signals to each user. This can be done by the use of superposition codes [17]. The easiest model allowing to solve the problem is the degraded broadcast channel [25]. Given a permutation function  $\pi(\cdot)$  that permits to accommodate the channels by the magnitude of their attenuation in decreasing order, the degraded case is defined at the situation where the transmit signal is physically degraded by the channel and the first receiver and it degrades more to the second receiver and so on, forming a Markov chain as:

$$x^{(n)} \rightarrow y^{(\pi(1),n)} \dots \rightarrow y^{(\pi(L),n)} \quad (2.50)$$

We say also that the broadcast channels is stochastically degraded when the channels are stochastically equivalent to a physically degraded broadcast channel. That is there exist a distribution from  $x^{(n)}$  to  $y^{(L,n)}$  such that:

$$p(y^{(1,n)}, \dots, y^{(L,n)} | x^{(n)}) = p(y^{(\pi(1),n)} | x^{(n)}) \prod_{\ell=2}^L p(y^{(\pi(\ell),n)} | y^{(\pi(\ell-1),n)}) \quad (2.51)$$

The capacity region of the degraded broadcast channel is well known [17, 25]. Given the channel gains ordered from the worst to the best user, with a decoding order:  $|h^{(\pi(1),n)}|^2 > \dots > |h^{(\pi(L),n)}|^2$  and the power constraint  $P_n$  on the sub-carrier  $n$ , the capacity region is[36]:

$$C_{BC} = \bigcup_{\sum_{\ell} P_{(\ell,n)} = P_n} \left\{ R : R_{\pi(\ell)} \leq \log_2 \left( 1 + \frac{|h^{(\pi(\ell),n)}|^2 P_{(\pi(\ell),n)}}{\sigma_{\mathbf{z}(\ell)}^2 + |h^{(\pi(\ell),n)}|^2 \sum_{j < \ell} P_{(\pi(j),n)}} \right) \right\} \quad (2.52)$$

The points of the region can be achieved with superposition coding and successive decoding [17, 25]. In this degraded setting, one must notice that the "good" users (the ones with good SNR) can also receive the signals that are intended to the users with poorer SNR. In other words, for embedded sources, good users will receive good quality signals, while "bad" users will still receive a signal, but with less quality.

### 2.2.2 Channel capacity of MU-SISO multiple access channel

The uplink is the situation when many users or subscribers wants to communicate with the base station. The model that is used to describe the Multiple Access Channel (MAC) is[36]:

$$y^{(n)} = \sum_{\ell} h^{(\ell,n)} x^{(\ell,n)} + z^{(n)} \quad (2.53)$$

This situation has been widely studied. Each user has a power constraint  $E \{|x^{(\ell,n)}|^2\} \leq P_{(\ell,n)}$  and the capacity region is given as follows:

$$C_{MAC} = \left\{ R : \sum_{\ell} R_{\ell} \leq \log_2 \left( 1 + \frac{1}{\sigma_z^2} \sum_{\ell} |h^{(\ell,n)}|^2 P_{(\ell,n)} \right) \right\} \quad (2.54)$$

We can see in (2.54) that the sum rate is bounded by a sub-modular rank function. This implies that the capacity region is a polymatroid, with  $L!$  vertices. Each vertices corresponds to a different permutation on the set of users  $\mathcal{L}$ . The decoding is done in such a way that the best user is decoded first, i.e.  $|h^{(L,n)}|^2 > \dots > |h^{(1,n)}|^2$

### 2.2.3 Duality of degraded Broadcast Channel and the Multiple Access Channel

Given a vector with channels gains  $\mathbf{H}_n = (|h^{(1,n)}|^2, \dots, |h^{(L,n)}|^2)$  there exists a relation between the capacity region of the degraded broadcast channel " $C_{BC}$ " and the capacity region of the multiple access channel " $C_{MAC}$ " [36]. Mainly the relationship can be exposed by:

$$C_{BC}(\mathbf{H}_n, P_n^{(BC)}) = \bigcup_{\sum_{\ell=1}^L P_{(\ell,n)}^{(MAC)} = P_n^{(BC)}} C_{MAC}(\mathbf{H}_n, P_{(1,n)}^{(MAC)}, \dots, P_{(L,n)}^{(MAC)}) \quad (2.55)$$

This relation between the capacity regions permits to establish a link between the MAC power allocation and the degraded broadcast channel power allocation. Further explanations can be found in [29, 36] and the references there in.

## 2.2.4 Discussion on Downlink and Uplink

The characterization of the general broadcast channel capacity region is still an open problem. However, assuming the channels to the users to be stochastically degraded, a capacity region can be found for the degraded broadcast channel with a power constraint. The multiple access channel has been widely studied, and one can establish a connection between the power allocation of both schemes. The corresponding expressions can be used in the context of OFDM systems by considering the sub-carriers to be orthogonal. The problem of a set of parallel subchannels was addressed treated by Tse in [67].

## 2.3 Multi-User MIMO

Following the previous subsection, we overview the multiuser MIMO case and the main results over this field. We start with an overview of the Broadcast Channel scheme and present briefly the Multiple Access Channel later.

### 2.3.1 Channel capacity of MU-MIMO Broadcast

The multiuser MIMO Broadcast Channel for user  $\ell$  on the sub-carrier  $n$  is modeled as followed:

$$\mathbf{y}_{(\ell,n)} = \mathbf{H}_{(\ell,n)}\mathbf{x}_{(n)} + \mathbf{z}_{(\ell,n)} \quad (2.56)$$

Where  $\mathbf{y}_{(\ell,n)} = (y_1^{(\ell,n)T} \dots y_R^{(\ell,n)T})^T$  is the received vector over the  $R$  antennas. The sent signal is  $\mathbf{x}_{(n)} = (x_1^{(n)T} \dots x_T^{(n)T})^T \sim \mathcal{CN}(0, S_{\mathbf{x}_{(n)}})$ , where  $S_{\mathbf{x}_{(n)}}$  is the covariance matrix of the signal to be transmitted, which is subject to a power constraint

$Tr(S_{\mathbf{x}_{(n)}}) \leq P_n$ , where  $P_n$  is the total power on the sub-carrier  $n$ . This signal is broadcasted to all the users and contains the information of interest for each user on sub-carrier  $n$ .

The MIMO broadcast channel is not degraded in general. Therefore, superposition coding is not used to achieve the capacity. The widely proposed technique is the Dirty Paper Coding (DPC) [15].

In 2001, an achievable region was derived by Yu and Cioffi [79]. The basis of this method is to decompose the broadcast channel into a series of single user channels with non-causal information and a precoding method is derived based on a Tomlinson-Harashima precoder [66, 31, 22].

Also based on DPC, Caire and Shamai [7, 8, 9] developed a MIMO approach with  $T$  antennas at the transmitter and  $L$  users, each one with a single antenna. They explore the possibility of transmit independent information through multi-antennas base station to a single antenna users. The transmitter decomposes the channel in an ordered set of interference channels, since this operation is made before to travel the channel is named a non-causal technique, as in [15]. The users are successively encoded based on the non-causal knowledge of the channel. The authors also explain that two users case is a special version of Marton's capacity region [40], that achieves the sum-rate of the system. Goldsmith present an overview of the advances over the subject until 2003 [30].

On 2006 Weingarten et al. propose an achievable capacity region for the multiuser broadcast channel case [73], using DPC. Considering an arbitrary encoding order  $\pi(\cdot)$ , where the user  $\pi(1)$  is encoding first until  $\pi(L)$ , the capacity is the union bound of the achievable rates that compose the vector  $\mathbf{R} = (R_1, \dots, R_L)$  over the set

$\mathcal{S} = \left\{ S_{\mathbf{x}^{(\ell,n)}} \succeq 0, \forall \ell \in \mathcal{L} : \text{Tr}(\sum_{\ell=1}^L S_{\mathbf{x}^{(\ell,n)}}) \leq P_n \right\}$ , containing the covariance matrices  $S_{\mathbf{x}^{(\ell,n)}}$  of each user, that respects the power constraints:

$$C_{BC}(H, P_n) = \bigcup_s \left\{ \mathbf{R} : R_\ell \leq \log_2 \frac{\det \left( \mathbf{I} + \mathbf{H}_{(\pi(\ell),n)} \left( \sum_{j \geq \ell} S_{\mathbf{x}^{(\ell,n)}} \right) \mathbf{H}_{(\pi(\ell),n)}^H \right)}{\det \left( \mathbf{I} + \mathbf{H}_{(\pi(\ell),n)} \left( \sum_{j > \ell} S_{\mathbf{x}^{(\ell,n)}} \right) \mathbf{H}_{(\pi(\ell),n)}^H \right)} \right\} \quad (2.57)$$

From the review of Gesbert et al. [27], one can understand that the results over the MU-MIMO scheme are mainly obtained using an Space Division Multiple Access (SDMA) point of view, with a precoding at the transmitter. Evaluating how many users can obtain a certain service turns out to involve a resource allocation problem. Spatial multiplexing of data streams can be done when users have a single antenna, but this situation may have a rank problem when Line of Sight (LOS) is present. The difficulty to obtain full-CSI necessitates to deal with partial-CSIT study.

The resource allocation of the MU-MIMO tries to take advantage of the CSIT by assigning properly the power  $P_{(\ell,n)}$  that will be used for the user  $\ell$  on the sub-carrier  $n$  [27]. The multiplexing gain is rank limited to  $T$ , meaning that the number of users served with  $P_{(\ell,n)}$  at any time is related to the number of antennas at the base station. In [78], Yu and Rhee explained that the optimal number of users with  $p_{(\ell,n)} > 0$  is upperbounded by  $T^2$ .

When a linear precoding technique is used, the number of users are limited by the number of degree of freedom at the base station, i.e.  $T$  [27]. The metric usually optimized by the schedulers are mainly the sum rate of the system or a specific per-user rate, while minimizing transmit power [27].



The maximization of the sum rate in the broadcast channel can be achieved by DPC [73], but is difficult to implement in practice. The two main lines to approach the capacity are: precoding methods, either linear or non-linear .

The linear precoding is a generalization of the SDMA scheme. The precoding is made at the base station, such that the receiver only decodes the intended signal. The received signal is:

$$\mathbf{y}_{(\ell,n)} = \mathbf{H}_{(\ell,n)} \sum_{j=1}^L \mathbf{W}_{(j,n)} \mathbf{u}_{(j,n)} + \mathbf{z}_{(\ell,n)} \quad (2.58)$$

$$\mathbf{y}_{(\ell,n)} = \mathbf{H}_{(\ell,n)} \mathbf{W}_{(\ell,n)} \mathbf{u}_{(\ell,n)} + \mathbf{H}_{(\ell,n)} \sum_{\substack{j=1 \\ j \neq \ell}}^L \mathbf{W}_{(j,n)} \mathbf{u}_{(j,n)} + \mathbf{z}_{(\ell,n)} \quad (2.59)$$

Here the transmitted signal,  $\mathbf{x}^{(n)} = \sum_{j=1}^L \mathbf{W}_{(j,n)} \mathbf{u}_{(j,n)}$ , is composed by the signal set  $\{\mathbf{u}_{(j,n)}\}_{\ell=1}^L$  of the users, prefiltered by the set of filters  $\{\mathbf{W}_{(\ell,n)}\}_{\ell=1}^L$ . Here  $\mathbf{u}_{(\ell,n)} \in \mathbb{C}^{S \times 1}$ , where  $S$  is the number of signal for the user  $\ell$  and  $\mathbf{W}_{(\ell,n)} \in \mathbb{C}^{T \times S}$ . The composed sent signal is  $\mathbf{x}^{(n)} \in \mathbb{C}^{T \times 1}$ . The objective is to design  $\mathbf{W}_{(\ell,n)}$ , such that the sum part of (2.59) becomes zero and finally the user can "see" only the intended signal:

$$\mathbf{y}_{(\ell,n)} = \mathbf{H}_{(\ell,n)} \mathbf{W}_{(\ell,n)} \mathbf{u}_{(\ell,n)} + \mathbf{z}_{(\ell,n)} \quad (2.60)$$

An example of the zero forcing precoding widely known is the block diagonalization method, that precancels the interference at the base station. [60, 37]

The non-linear precoding methods are based on the perturbation method [51] or on the spatial extension of the Tomlinson-Harashima precoding [27]. Those methods will not be reviewed in this thesis.

### 2.3.2 Channel capacity of MU-MIMO Multiple Access Channel

In the MU-MIMO MAC case we keep the notation considering that the base station has  $T$ -antennas and the user has  $R$ -antennas. For this case the mathematical model of the uplink channel is:

$$\mathbf{y}_{(n)} = \sum_{\ell=1}^L \mathbf{H}_{(\ell,n)}^H \mathbf{x}_{(\ell,n)} + \mathbf{z}_{(n)} \quad (2.61)$$

The base station receives  $\mathbf{y}_{(n)} \in \mathbb{C}^{T \times 1}$ , that is the combination of the received signals from the  $L$ -users. Where  $\mathbf{H}_{(\ell,n)} \in \mathbb{C}^{R \times T}$ , the signals sent by the users are  $\mathbf{x}_{(\ell,n)} \in \mathbb{C}^{R \times 1}$  with covariance matrix  $S_{\mathbf{x}_{(\ell,n)}}$ , subject to a power constraint over the antennas such that  $\text{Tr}(S_{\mathbf{x}_{(\ell,n)}}) \leq P_{(\ell,n)}$ .  $P_{(\ell,n)}$  is the power that the user  $\ell$  can distribute over the antennas on the sub-carrier  $n$ . Defining  $\mathbf{H}_n = (\mathbf{H}_{(1,n)}, \dots, \mathbf{H}_{(L,n)})$  and  $\mathcal{S} = \{S_{\mathbf{x}_{(\ell,n)}} \succeq 0, \forall \ell \in \mathcal{L} : \text{Tr}(S_{\mathbf{x}_{(\ell,n)}}) \leq P_{(\ell,n)}\}$ .

The achievable capacity region is given as:

$$C_{MAC}(\mathbf{H}_n, \mathcal{S}) = \left\{ \mathbf{R} : \sum_{\ell=1}^L R_{\ell} \leq \log_2 \det \left( \mathbf{I} + \frac{1}{\sigma_z} \sum_{\ell=1}^L \left( \mathbf{H}_{(\ell,n)}^H S_{\mathbf{x}_{(\ell,n)}} \mathbf{H}_{(\ell,n)} \right) \right) \right\} \quad (2.62)$$

The achievable capacity region is obtained by saying that the vector sum-rate over  $L$ -users is upper-bounded by the capacity with the power received from all the users. Since the users have an individual power constraint they have no reason to transmit at full power to have more capacity. In fact, this would be a waste of energy because the capacity is constrained by the other users [17, 29].

### 2.3.3 MU-MIMO BC and MAC duality

The duality between the MU-MIMO BC and MAC schemes is shown in [71]. The argument is similar to the scalar model presented early but using DPC:

$$C_{BC}(\mathbf{H}_n, P_n^{(BC)}) = \bigcup_{\sum_{\ell} P_{(\ell,n)}^{(MAC)} = P_n^{(BC)}} C_{MAC}(\mathbf{h}_{nn}, P_{(1,n)}^{(MAC)}, \dots, P_{(L,n)}^{(MAC)}) \quad (2.63)$$

Where  $\mathbf{H}_n = (\mathbf{H}_{(1,n)}, \dots, \mathbf{H}_{(L,n)})$  is the the channel matrix composed by the concatenation of the matrices of each user  $\ell$  over the sub-carrier  $n$ . The powers  $P_n^{(BC)}$  and  $P_{(\ell,n)}^{(MAC)}$  are defined in (2.57) and (2.62) respectively.

### 2.3.4 Discussion on Multi-User MIMO systems

The MIMO multiuser scheme has received great interest recently because of the promises of large achievable rates of this scheme compared to the SISO scheme. The main results are obtained using DPC schemes, which present an interesting technical challenge. The precoding solutions are reviewed on [27]. The quest of the achievable region and the duality present an alternative to calculate and maximize power allocation. The presented extension over  $n$ -parallel sub-channels put another interesting point over the power allocation issue, that it will be addressed later in Chapter 4.

## 2.4 Channel modeling

In the situation of interest, Channel State Information (CSI) is available at the transmitter. Since we intend to obtain performance evaluations for a realistic situation. We need a good channel modeling . In wireless communications the channel is less

predictable than in the wired situation; climatic factor, and environment characteristics like trees, buildings and hills, distort the signal sent by the transmitter on its way to the receiver. The distortions inflicted to the signal is currently named *fading* [56, 58] and we can distinguish two types of fading: *large-scale fading* and *small-scale fading*. Large-scale fading encompasses two phenomena: *path loss*, that is a deterministic phenomenon where the signal loses strength due to the distance and *shadowing* that is the product of successive attenuations due to large obstacles. Due to the variability of obstacles it is considered as being random. Small-scale fading or *fast fading* is a local phenomenon which happens when the receiver moves in short travel distance but the received signal strength fluctuates rapidly. The channel models are extensively addressed in [56, 58, 68].

### 2.4.1 Large-scale fading

The large scale fading encompasses two phenomena. The first one is the path loss, the signal power decreases due to the distance. Both empirical models and physical models exist for this phenomenon. The second one is the shadowing that is the power variation due to the big obstacles, considering the variability of the obstacles. The central limit theorem is invoked to model the phenomenon by a normal distributed random variable.

Formally the path loss is defined as the difference (in dB) between the effective transmitted power and the received power [56], expressed as follows.

$$PL[dB] = 10 \log \frac{P_t}{P_r} \quad (2.64)$$

Where  $P_t$  is the transmit power and  $P_r$  is the received power.

There are several models to model the path loss. We can classify these models among empirical and physical models [57]. Well known empirical models are the *power law model*, the *Okumura-Hata model* [32, 46] and the *COST231-Hata model*. On the other side, the most well known physical models are *free space propagation model*, *rooftop diffraction model*, and *flat edge model*.

The successive attenuations encountered by the signal have a multiplicative effect, which is additive in the decibel domain. If there is a sufficient number of diffraction paths on the way to the receiver, the *Central Limit Theorem* can be used to justify that these successive attenuations can be represented by a Gaussian random variable, actually called log-normal random variable since it Gaussian in the log domain. This random variable has a variance called *location variability* or Shadowing Factor denoted by  $SF$  (2.65) and (2.66) [58].

The path loss, denoted  $L(d)$ , is calculated in [53] using:

$$L(d) = L_{FS}(d) + SF, d \leq d_{BP} \quad (2.65)$$

$$L(d) = L_{FS}(d_{BP}) + 35 \log\left(\frac{d}{d_{BP}}\right) + SF, d > d_{BP} \quad (2.66)$$

$$L_{FS}(d) = 20 \log(d) + 20 \log(f) - 147.5 \quad (2.67)$$

Where  $L_{FS}(d)$  is the free space path loss at distance  $d$  and frequency  $f$ . The formula proposed by [53] considers a breakpoint distance  $d_{BP}$  above which the path loss increases with a slope of 3.5.

### 2.4.2 Small-scale fading

Abrupt variations on the signal strength at the receiver may arise when the user moves on a short distance. This is due to the effect of multiple signal paths, which cause interferences, varying when the phase changes. The interference is constructive when the signals are on phase and destructive when the phases are opposite from one signal to the other. The origin of the phenomenon is that the receiver belongs to an environment where there are multiple scatterers, and the signal arrives to him via multiple paths coming from various directions [56, 57, 58].

To characterize the small scale fading there exist many empirical models, all of them specified by a Power Delay Profile (PDP). The parameters that compose the PDP are the relative delay from the first path and the average power of the path in dB.

As an example we take the multipath model below, which is extensively used in this thesis [41].

Two parameters permits to have a design criterion and a comparison between different models, the mean excess delay and the Root Mean Square (RMS) delay spread. Let  $\tau_p$  the delay of the path  $p$  and  $P(\tau_p)$  the average linear (not dB) power of the path  $p$ . The mean excess delay is defined as:

$$\bar{\tau} = \frac{\sum_p P(\tau_p)\tau_p}{\sum_p P(\tau_p)} \quad (2.68)$$

The RMS delay spread is defined as:

| Path | Delay (ns) | Average relative Power (dB) |
|------|------------|-----------------------------|
| 1    | 0          | -4.9                        |
| 2    | 10         | -5.1                        |
| 3    | 20         | -5.2                        |
| 4    | 40         | -0.8                        |
| 5    | 70         | -1.3                        |
| 6    | 100        | -1.9                        |
| 7    | 140        | -0.3                        |
| 8    | 190        | -1.2                        |
| 9    | 240        | -2.1                        |
| 10   | 320        | 0.0                         |
| 11   | 430        | -1.9                        |
| 12   | 560        | -2.8                        |
| 13   | 710        | -5.4                        |
| 14   | 880        | -7.3                        |
| 15   | 1070       | -10.6                       |
| 16   | 1280       | -13.4                       |
| 17   | 1510       | -17.4                       |
| 18   | 1760       | -20.9                       |

Table 2.1: Power Delay Profile Model E [41]

$$\tau_{RMS} = \sqrt{\bar{\tau}^2 - (\bar{\tau})^2} \quad (2.69)$$

$$\text{where } \bar{\tau}^2 = \frac{\sum_p P(\tau_p) \tau_p^2}{\sum_p P(\tau_p)} \quad (2.70)$$

The RMS delay spread  $\tau_{RMS}$  is a good indicator of the system error performance. By instance for the table 2.1,  $\tau_{RMS} = 0.24 \times 10^{-6}[s]$  that is much less than the guard interval from the parameters that we choose,  $0.8 \times 10^{-6} [s]$ .

### 2.4.3 Channel Model

The channel matrix  $\mathbf{H}$  of equation (2.25) is derived from the Fourier transform of the complex baseband equivalent impulse response with multipath fading:

$$h(\tau, t) = \sum_i \beta_i(t) e^{-j\theta_i(t)} \delta(\tau - \tau_i(t)) \quad (2.71)$$

as

$$H(f, t) = \int_{-\infty}^{\infty} h(\tau, t) e^{-j2f\pi\tau} d\tau \quad (2.72)$$

$$= \sum_i \beta_i(t) e^{-j(2f\pi\tau_i(t) + \theta_i(t))} \quad (2.73)$$

$$H(f) = \sum_i \beta_i e^{-j(2f\pi\tau_i + \theta_i)} \quad (2.74)$$

The parameters describing the channel are:  $\beta_i(t)$  the complex valued channel gain,  $\tau_i(t)$  the delay, and  $\theta_i(t)$  a phase shift that can be encountered in the channel, uniformly distributed in  $[0, 2\pi]$ ; and the subindex  $i$  corresponds to the  $i$ -th path. In (2.74), the channel parameters are considered to be time invariant. The complex valued channel gain  $\beta_i = \sqrt{\frac{1}{L(d)}} G_i$  is composed of a constant path loss  $L(d)$  (large scale fading) and a complex valued fading gain  $G_i$  (small scale fading) [57]. The path loss is due to the distance "d" between the access point and the user [21, 57, 56, 53]. The complex valued channel gain  $G_i$ , is the attenuation of the path taken by the signal with delay  $\tau_i$ .

We take empirical values for  $g_i$  and  $\tau_i$  from the fading channel model parameters given by [41]. Obviously, one can find many other models, such as the cluster model in [49], but the model we use is one of the most classical ones, which corresponds to a standard situation. We choose the *Model E*, designed for Non Line of Sight(NLOS) environments with a RMS delay spread of 250 [ms].

Having parameterized  $H(f)$  (2.74), we sample  $f$  at frequency spacing  $f_s$  (Table 2.2)  $N$



times. By doing so, we obtain the channel values of  $N$  complex baseband sub-carriers  $\{H^{(n)}\}$ ,  $n = \{1, \dots, N\}$ . Then we construct the channel matrix as  $\mathbf{H} = \text{diag}\{\{H^{(n)}\}\}$ . From [3] we identify the sub-carriers that are not used in the standard for carrying information and finally, only those 52 carriers that are used to transport data are candidates for power allocation.

For our simulations we took the parameters of 802.11a/n standard, the main ones being summarized in Table 2.2,[3][53].

Table 2.2: 802.11a/n Parameters

| Parameters                   |                       |
|------------------------------|-----------------------|
| NSubcarriers:                | 64 (52 used for data) |
| Subcarrier spacing $f_s$ :   | 312,5 kHz.            |
| RF Carrier Frequency:        | 5,180 GHz             |
| Channel Bandwidth:           | 20 MHz                |
| Transmit power ( $P$ )       | 100 mW                |
| Noise power ( $\sigma_z^2$ ) | 0.31622 pW            |

To model the MIMO channel (2.47), we compute (2.74) on each path between the antennas parameterized with the model of [41] , then we sample  $f$  at frequency spacing  $f_s, N$  times. Like before, we obtain the  $N$  sub-carrier complex baseband equivalent values, now on each path between all antennas. Once we have those values we merge then sub-carrier by sub-carrier to build matrix (2.47).

The following simulations are valid for delays smaller than the guard interval. Beyond that value, the orthogonality between the sub-carriers is lost and the system model involving parallel channels is no longer valid.

## Chapter 3

# Multicast or Broadcast using MU-SISO OFDM systems

The situation where the same signal has to be sent to a number of wireless receivers arises more and more often, due to the increasing use of wireless internet including TV. Classically, this is done either by establishing several one to one communications, which is obviously a waste of resources, or by establishing a broadcast service, addressing potentially all users of a given area. However, the broadcast service cannot be tuned to a specific set of users, and also results in a waste of power in a number of circumstances. This could be avoided if the transmitter knew the parameters (CSI) of the users willing to attend the service, in a situation similar to "multicast". This chapter provides the tools that are necessary to evaluate the performance improvement brought by wireless multicast over the classical broadcast situation, and provides numerical evaluations when the transmission is done over realistic OFDM channels.

This chapter evaluates the improvements brought by the knowledge of the channel

at the transmitter (multicast situation) over the broadcast situation in realistic situations. In other terms, we provide means of evaluation the situations where multicast would be useful in wireless OFDM systems. It is shown that this strongly depends on the number of users (obviously), but also on their distance to the transmitter.

The so called *wireless multicast* defined above, is close to the *broadcast channel* as known in information theory. There is a slight difference in both situations : the broadcast channel in information theory solves a coding problem in order to sent different information to the various users present in the system The option of sending also a common signal is seldom considered. In the common understanding of "broadcast", one is interested only in transmitting a common information to all users. This paper addresses a somewhat intermediate situation : the common signal is of interest, but when additional rate is available to some users, we know that it can be used to obtain better quality signals through layered coding [?], which can be useful for video, for example. Therefore, we have chosen the sum-rate of all receivers as a criterion for optimization, while the improvements are measured in terms of the percentage of throughput increase per user.

To solve the problem, we propose a power allocation algorithm for maximizing the sum-rate capacity in multiuser SISO-OFDM system. We use numerical simulations to illustrate our results in the power allocation algorithm over different scenarios and many realizations of channels. Using the histogram and statistics of the ratio of the optimized capacity versus equal power allocation capacity permits to give a tool to compare and decide whether multicast is really of interest compared to broadcast.

The system under study is similar to the broadcast channel (BC) studied by information theory and consists of one transmitter and  $L > 1$  receivers. All he terminals

are assumed to be equipped with a single antenna. Our objective is to investigate the power allocation problem at the transmitter in the OFDM scenario, where the transmitter uses  $N$ -orthogonal sub-carriers to send its message to the receivers. Our performance criterion is the sum-rate capacity for the multiuser SISO-OFDM situation. The received signal of user  $\ell \in \{1, \dots, L\}$  can be expressed by:

$$\mathbf{y}_\ell = \mathbf{H}_\ell \mathbf{x} + \mathbf{z}_\ell, \quad (3.1)$$

where  $\mathbf{x} = (x^{(1)}, \dots, x^{(N)}) \sim \mathbb{C}\mathcal{N}(0, S_{\mathbf{x}})$  represents the input vector of  $N$  OFDM symbols and  $S_{\mathbf{x}}$  is the covariance matrix of vector  $\mathbf{x}$ . It is a diagonal matrix of elements  $S_{\mathbf{x}} = \text{diag}\{p_n\}$ ,  $n \in \{1, \dots, N\}$ , with  $p_n$  representing the power allocated to the  $n$ -th subcarrier. The overall available transmit power is constrained as follows:

$$\sum_{n=1}^N p_n \leq P.$$

Matrix  $\mathbf{H}_\ell$  is the  $N \times N$  channel gain matrix, which is also diagonal and its entries are the Fourier transform of the channel impulse described on the background  $\mathbf{H}_\ell = \text{diag}\{h^{(\ell, n)}\}$  and is perfectly known at the transmitter. Vector  $\mathbf{z}$  denotes the AWGN at the receiver  $\mathbf{z}_\ell \sim \mathbb{C}\mathcal{N}(0, S_{\mathbf{z}})$  (all receivers are assumed to have the same noise variance).

### 3.1 System sum-capacity

Since we want to transmit the same information to multiple receivers with limited power at the transmitter, we are interested in maximizing the mutual information between the transmitter and the  $L$  receivers. First consider the simple case of two users ( $L = 2$ ). The mutual information between the input  $\mathbf{x}$  and the system outputs  $(\mathbf{y}_1, \mathbf{y}_2)$  reads:

$$I(\mathbf{x}; (\mathbf{y}_1, \mathbf{y}_2)) = \sum_{\mathbf{x}} \sum_{\mathbf{y}_1} \sum_{\mathbf{y}_2} p(\mathbf{x}, \mathbf{y}_1, \mathbf{y}_2) \log \frac{p(\mathbf{x}, \mathbf{y}_1, \mathbf{y}_2)}{p(\mathbf{x})p(\mathbf{y}_1, \mathbf{y}_2)} \quad (3.2)$$

The receivers are assumed to use the same decoding scheme which is realistic in a scenario the users are subscribed to receive the same data.

The mutual information also reads:

$$I(\mathbf{x}; (\mathbf{y}_1, \mathbf{y}_2)) = I(\mathbf{x}; \mathbf{y}_1) + I(\mathbf{x}; \mathbf{y}_2) - I(\mathbf{y}_1; \mathbf{y}_2) \quad (3.3)$$

, and this value is the sum of the individual mutual information subtracted by the mutual information between the receivers.

However, given that we are mainly interested in transmitting the same information to all receivers in a layered coding situation, and given that the receivers are assumed independent and un-cooperative, our criterion simply becomes:

$$C = I(\mathbf{x}; \mathbf{y}_1) + I(\mathbf{x}; \mathbf{y}_2) \quad (3.4)$$

We can generalize this to the case of  $L > 2$  independent receivers and obtain the required criterion as the sum of the individual mutual information:

$$I(\mathbf{x}; (\mathbf{y}_1, \dots, \mathbf{y}_L)) = \sum_{\ell=1}^L I(\mathbf{x}; \mathbf{y}_\ell) \quad (3.5)$$

The system capacity is the mutual information in (3.5) maximized over the set of possible transmit power allocation policies:

$$C = \max_{\mathbf{x}: \text{Tr}(S_{\mathbf{x}}) \leq P} \sum_{\ell=1}^L I(\mathbf{x}, \mathbf{y}_\ell) \quad (3.6)$$

Our problem can be re-written as a convex optimization problem with linear constraints [6]:

$$\min_{\{p_n\}_n} \left\{ - \sum_{\ell=1}^L \sum_{n=1}^N \log \left( \frac{p_n}{\gamma_n^{(\ell)}} + 1 \right) \right\} \quad (3.7)$$

$$\text{Subject to } \begin{cases} \sum_{n=1}^N p_n = P \\ -p_n \leq 0, \end{cases} \quad (3.8)$$

$$(3.9)$$

where  $\gamma_n^{(\ell)} = \frac{\sigma_z^2}{|h^{(\ell,n)}|^2}$  for all  $n$  and all  $\ell$ .

By Lagrangian optimization it is found that the optimal power allocation depends on a parameter  $\lambda \geq 0$ :

$$\forall n, \sum_{\ell=1}^L \frac{-1}{p_n + \gamma_n^{(\ell)}} + \lambda = 0 \quad (3.10)$$

where  $\lambda$  is chosen such that the power constraint is met:  $\sum_{n=1}^N p_n^* = P$ .

We can see that if  $L = 1$  the solution of (3.10) is the well known *water-filling* solution [17]. However, in our multi-user case finding a closed-form solution for the power allocation is not possible. The solution is obtained via a numerical solution, as will be seen in the next section.

## 3.2 SISO optimal power allocation algorithm

First define the following functions:

$$f(\lambda) = \sum_{n=1}^N p_n(\lambda) - P \quad (3.11)$$

and

$$\forall n, F_n(p_n, \lambda) = \sum_{\ell=1}^L \frac{-1}{p_n + \gamma_n^{(\ell)}} + \lambda \quad (3.12)$$

The objective is to find the solution to the system:

$$\left\{ \begin{array}{l} f(\lambda) = 0 \\ \forall n, F_n(p_n(\lambda), \lambda) = 0 \end{array} \right. \quad (3.13)$$

We analyze an equation of the type  $F_n(p_n(\lambda), \lambda) = 0$ . For this purpose we calculate the partial derivative of  $F_n(p_n(\lambda), \lambda)$  with respect  $p_n$ .

$$\frac{\partial F_n(p_n, \lambda)}{\partial p_n} = \sum_{\ell=1}^L \frac{1}{(p_n + \gamma_n^{(\ell)})^2}; \quad (3.14)$$

In what follows, we analyze the function  $F_n(p_n, \lambda)$  interval by interval with respect to  $p_n$ .

We must first find the critical points of the functions  $F_n(\cdot)$ , that is all points where the function tends to infinity.

- $F(p_n, \lambda)$  tends to infinity when  $p_n \rightarrow -\gamma_n^{(\ell)}$ ,  $\ell = \{1, \dots, L\}$  Users. If we assume that the values  $\gamma_n^{(\ell)}$  are in increasing order that is:

$$\gamma_n^{(1)} < \gamma_n^{(2)} < \dots < \gamma_n^{(L-1)} < \gamma_n^{(L)} \quad (3.15)$$

The critical points are:

$$-\gamma_n^{(L)} < -\gamma_n^{(L-1)} < \dots < -\gamma_n^{(2)} < -\gamma_n^{(1)} \quad (3.16)$$

Considering the fact that, when  $p_n \rightarrow \pm\infty$  the function  $F(p_n, \lambda) \rightarrow \lambda$

- The domain of validity of the function is divided into several homogeneous

intervals, namely:

$$\begin{aligned} & ] -\infty, -\gamma_n^{(L)}[ \cup ] -\gamma_n^{(L)}, -\gamma_n^{(L-1)}[ \cup \dots \\ & \cup ] -\gamma_n^{(2)}, -\gamma_n^{(1)}[ \cup ] -\gamma_n^{(1)}, +\infty[ \end{aligned}$$

Based on properties of the first derivative we can conclude the following, on each interval:

- $] -\infty, -\gamma_n^L[$ , when  $p_n \rightarrow -\infty$ , the derivative is positive and when  $p_n$  approach  $-\gamma_n^k$  from the left, the derivative is positive too. Inside this interval the function is monotonically increasing.
- $] -\gamma_n^L, -\gamma_n^{L-1}[$ , when  $p_n \rightarrow -\gamma_n^k$  from the right, the derivative is positive and when  $\sigma_i^2$  approach  $-\gamma_n^{L-1}$  from the left, the derivative is positive too. At this interval the function is monotonically increasing. In the other intervals that have the same structure the function is monotonically increasing.
- $] -\gamma_n^1, +\infty[$ , when  $p_n \rightarrow -\gamma_n^1$  from the right, derivative is positive and when  $p_n \rightarrow \infty$  from the left, the derivative is positive. Inside this interval the function is also monotonically increasing.

There is a single interval where we can verify that  $p_n > 0$ , that is the interval:  $] -\gamma_n^{(1)}, +\infty[$ . Since the derivative is positive in all intervals, the function is monotonically increasing therefore if the function goes to 0, ( $F(p_n, \lambda) = 0$ ), for some  $p_n(\lambda)$ , this value is unique.

Therefore, any algorithm searching for zeros of functions, conveniently initialized, will provide the correct solution. In our programs, we used 'fzero' from MATLAB to solve this problem. The optimization parameters are  $p_n$  and  $\lambda$ , for which search



windows are to be defined with care. These algorithms will converge to the right solution if we choose the interval  $[p_{01}, p_{02}] \subset ] - \gamma_i^1, +\infty[$  that allows  $F(p_{01}, \lambda)$  and  $F(p_{02}, \lambda)$  to have different signs. This interval must be compatible with the choice of the interval  $[\lambda_{01}, \lambda_{02}]$  to search  $\lambda$ , since we use 'fzero' to find  $\lambda$  too.

It is easily seen that choosing  $p_{01} = -\gamma_i^{(1)}$  as the lower interval value, and a value larger than the total power that can be allocated to one channel as the upper value  $p_{02} = P$  will ensure to have a correct search domain for the individual powers.

First we set the criterion to set  $[p_{01}, p_{02}] \subset ] - \gamma_i^{(1)}, +\infty[$ . Although we know that  $p_{0i} > 0$ , we will use  $p_{01} = -\gamma_i^{(1)}$  as the lower interval value in order to ensure the 'fzero' convergence conditions. The upper value must be a value larger than the total power allocated to one channel, therefore, a safe value is  $p_{02} = P$ , i.e. assume that the total power can be allocated to a single subcarrier.

The search window for the Lagrangian parameter is defined as  $[\lambda_{01}, \lambda_{02}]$ . If we consider the interval that we set before. Knowing the values of  $p_{01}$  and  $p_{02}$  we can calculate  $\lambda_{01}$  and  $\lambda_{02}$  using fzero too.

$$\text{if } p_n \rightarrow 0 \text{ then(3.10) becomes } \lambda = \sum_{\ell=1}^L \frac{1}{\gamma_n^{(\ell)}} \quad ; \quad n = \{1, \dots, N\} \quad (3.17)$$

$$\text{if } p_n \rightarrow \infty \text{ then(3.10) becomes } \lambda = 0 \quad ; \quad n = \{1, \dots, N\} \quad (3.18)$$

Then for  $\lambda_{01}$  we have the following set of values:

$$\lambda_{01} \in \left\{ \sum_{\ell=1}^L \frac{1}{\gamma_1^{(\ell)}}, \sum_{\ell=1}^L \frac{1}{\gamma_2^{(\ell)}}, \dots, \sum_{\ell=1}^L \frac{1}{\gamma_N^{(\ell)}} \right\} \quad (3.19)$$

we must choose which user has the best sum value of channels, that is:

$$\lambda_{01} = \max_i \left\{ \sum_{\ell=1}^L \frac{1}{\gamma_i^{(\ell)}} \right\}, \quad i = 1, \dots, N. \quad (3.20)$$

To obtain the value of  $\lambda_{02}$  using the second criteria, consider the case where all power  $P$  could be allocated to a single subcarrier, that is:

$$\lambda_{02} \in \left\{ \sum_{\ell=1}^L \frac{1}{\gamma_1^{(\ell)} + P}, \sum_{\ell=1}^L \frac{1}{\gamma_2^{(\ell)} + P}, \dots, \sum_{\ell=1}^L \frac{1}{\gamma_N^{(\ell)} + P} \right\} \quad (3.21)$$

And we choose the best value as in (3.20):

$$\lambda_{02} = \max_i \left\{ \sum_{\ell=1}^L \frac{1}{\gamma_i^{(\ell)} + P} \right\}, \quad i = 1, \dots, N. \quad (3.22)$$

which also ensures the problem to have a solution in the search domain.

### 3.3 Numerical results

The instrument that we use to compare multicast vs classical broadcast (equal power allocation) is the histogram of the obtained sum rates. This allows us to compare the frequency, over a large number of samples (5000), of optimized and non-optimized capacity values. We set a channel model, fix users (distance, number of users) and generate the samples. We start with one user in the system and we increase the number and do histograms for all situations.

**At 100[m] the results are** With 1 user in the system the optimized power allocation is 20.55 % better in mean than the broadcast capacity. The mean of the optimized capacity is 2.05 *Bit/s/Hz*, while the most frequent event is 0.43 *Bit/s/Hz*. When we increase the number of users, optimal power allocation policy does not improve

a lot on the broadcast scheme. Already with 5 users in the system, the mean of the improvement is 0.96 %. We can conclude, that at such distance, uniform power allocation of the power over the sub-carriers is sufficient. However, a definite conclusion can be drawn only by looking at coverage, since it will be shown below that the largest improvement is always obtained for small rates, which are proportionally improved more than large rates. In other words, users far from the base station will benefit more from the optimization.

**At 200[m] the results are** With 1 user in the system the percentage of sum rate increase is 62.69% (in mean) when we do power allocation; the mean for the optimized capacity is near 0.52 *Bit/s/Hz*, while the most frequent event is 0.05 *Bit/s/channel* use. When the number of users increases until 5, the mean in terms of percentage increase moves abruptly to 9.81%, while the mean in terms of optimized capacity moves slowly to 0.45 *Bit/s/Hz*. With 10 users in the system we are below the 4.04 % of percentage increase, with 0.44 *Bit/s/Hz* with optimized capacity in mean. When we augment the number of users beyond 10 users, the most reasonable transmission scheme is the use the uniform power allocation policy.

**At 300[m] the results are** With 1 user in the system the percentage increase is, in mean, close to 107.26% with 0.2 *Bit/s/Hz*. When we increase from 2 to 5 users the percentage increase remains between 61.47% and 28.01%, decreasing from 0.17 to 0.15 *Bit/s/Hz* in mean. If we have 10 users in the system, the power allocation still provides 14.96 % of percentage increase, with 0.14% *Bit/s/Hz*. With 15 users, the

percentage increase is 9.95 % and the optimized capacity gives 0.14 Bit/s/channel use. We can see in Fig. 3.3(a) the histogram of the percentage increase and in the Fig. 3.3(b) the distribution of the optimized capacity per user in this scenario.

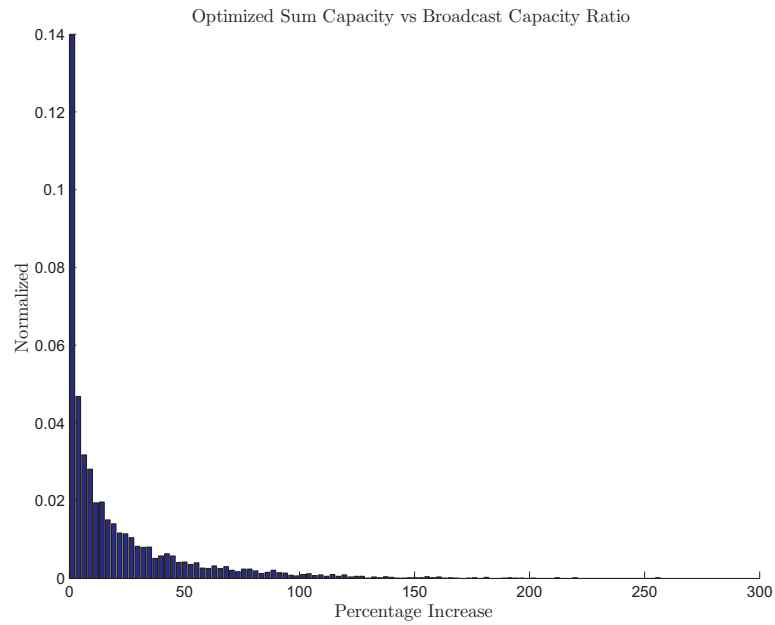
**At 400[m] the results are** When we have 1 user in the system the percentage increase is 142.14% better than the equal power repartition with a mean of 0.1 *Bit/s/Hz*. With 2 users, the percentage increase falls near to 90.95% and the capacity per user is close to 0.08 *Bit/s/Hz*. With 5 users, we have 47.62 % of percentage increase with 0.07 *Bit/s/Hz*. Beyond 5 users the optimization does not seem to be useful.

**At 500[m] the results are** Even though the values of percentage increase is close to 167.52% for 1 user, the transmission with optimization offers only 0.05 *Bit/s/Hz*. When the number of users increases, between 2 to 5 users the percentage increase is in the range of 114.98% to 65.26% with 0.04 *Bit/s/Hz*. The power allocation presents good performance in the sense to maintain reliable communication, but the quantity of bits per transmission is quite small as 0.03 Bits per subcarrier for 10 user in the system, with 41.89% percentage increase.

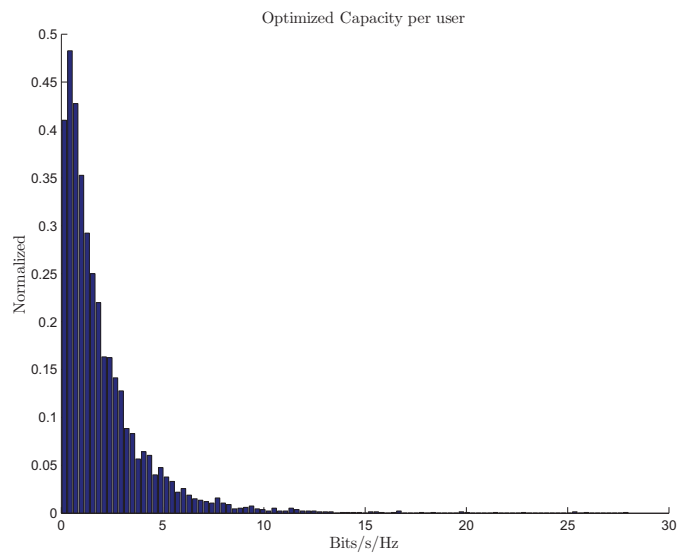
### 3.4 Conclusion

In this chapter we derive an optimal power allocation algorithm that permits to optimally distribute power over the transmitted OFDM symbol, in the multiuser case.

Simulation results show that our algorithm perform a good improvements compared to the uniform power allocation, in terms of capacity. Obviously, when the number of users increases, optimization is expected to be less and less useful. However, it can be observed that noticeable improvements are obtained for the worst users in a cell (the ones far from the access point) with a frontier at about 5 users... above this number, equal power allocation seems to be the simplest choice, with almost no loss of performance. This conclusion has anyway to be confirmed in terms of coverage (see last chapter).

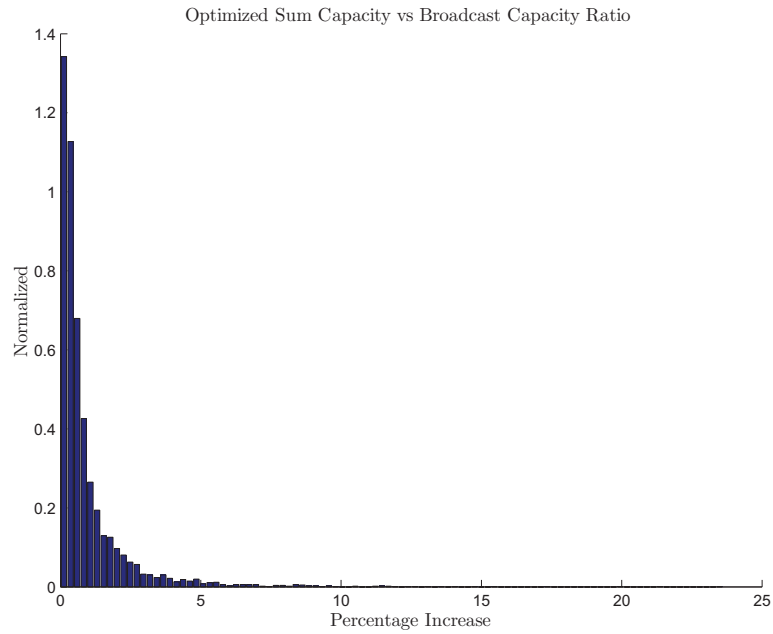


(a) Percentage increase

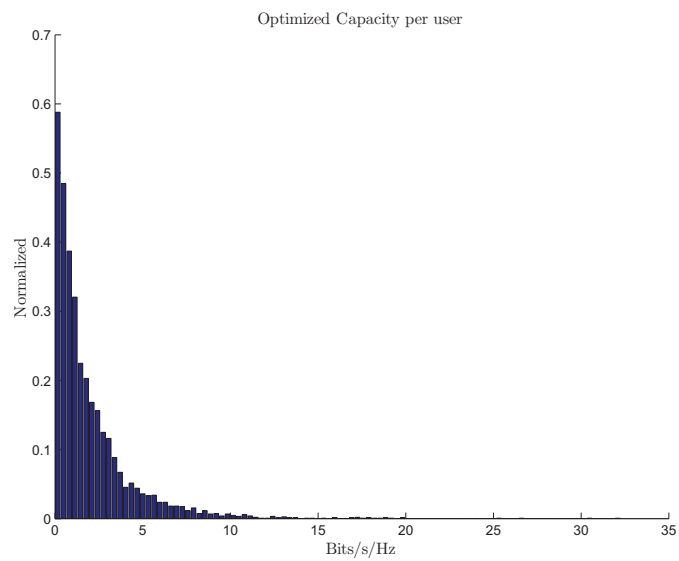


(b) Capacity in Bit/s/Hz

Figure 3.1: Histograms for 1 User at 100 [m] from access point

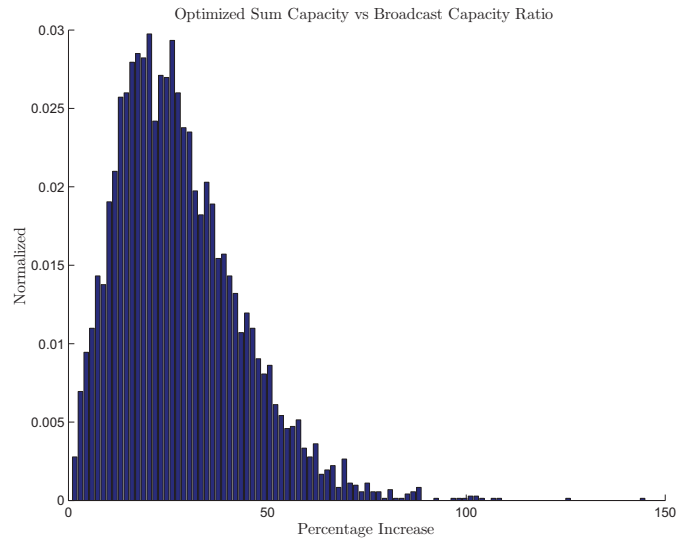


(a) Percentage increase

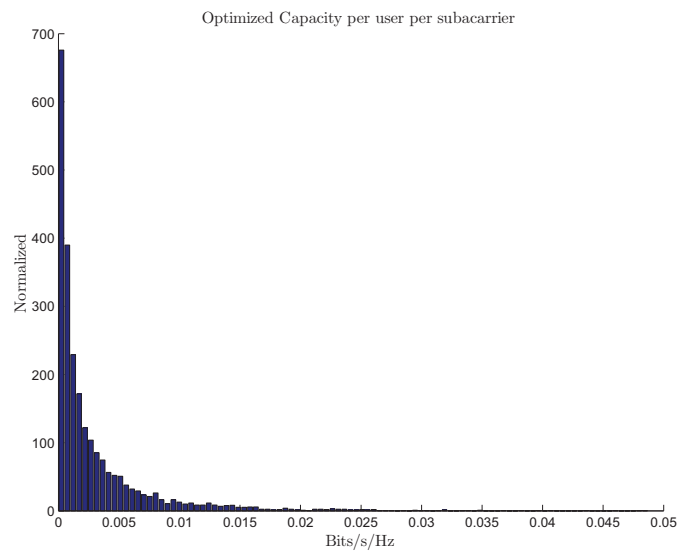


(b) Capacity in Bit/s/Hz

Figure 3.2: Histograms for 5 User at 100 [m] from access point



(a) Percentage increase



(b) Capacity in Bit/s/Hz

Figure 3.3: Histograms for 5 User at 300 [m] from access point



## Chapter 4

# Power allocation in MU-MIMO OFDM systems

The previous chapter addressed the case of SISO - OFDM, in the sense that both transmitter and receiver had a single antenna and multiple sub-carriers. Now we turn our attention to MIMO-OFDM (Multiple Input Multiple Output - OFDM), using multiple antennas and multiple sub-carriers at the transmitter and the receivers.

This situation deserves some comments, which will allow to precise what can be expected from the study. It has been seen in sections 2.1.2 and 2.3 that capacity improvements were mostly obtained in the MIMO context by Channel State Information available at the Transmitter. Therefore, the classical "broadcast", intending to send some common signal to an unknown set of (possibly many) users does not seem to be really relevant with MIMO transmitters and receivers, which would not benefit from the "internal" power allocation inside each MIMO channel. Therefore, the gains of the "multicast" situation over equal power allocation are expected to be large in almost all cases. However, it has already been explained that MIMO channels cannot

be considered as being degraded, which prevents general solutions to be available. We have chosen to work in a situation where the transmitter benefits from CSIT to perform linear precoding, which brings strong constraints on the respective number of antennas at transmitter and receivers. Therefore, the set of possible situations in this chapter is restricted, but the results clearly shows that improvements brought by CSIT are present in all feasible cases.

This is the reason for the lack of symmetry in the title of this chapter compared to the previous one: the main output is the power allocation algorithm, and it will be seen that it is of interest versus "equal power allocation" in all cases. However, this "equal power allocation" cannot really be denoted as "MIMO broadcast", since it cannot fully benefit from the MIMO setting. Whether a traditional broadcast is feasible while benefiting from the many antennas available is still an open problem, to our knowledge.

## 4.1 Notations and problem statement

In this chapter,  $t$  is the index for the transmit antenna,  $t = \{1, \dots, T\}$ ,  $T$  being the total number of transmit antennas. Index  $r$  is the index for the receiver antenna,  $r = \{1, \dots, R\}$ , while  $R$  is the total number of receive antennas. The received signal of user  $\ell$  on subcarrier  $n$  is:

$$\mathbf{y}_{(\ell,n)} = \mathbf{H}_{(\ell,n)} \mathbf{x}^{(n)} + \mathbf{z}_{(\ell,n)} \quad (4.1)$$

Where  $\mathbf{y}_{(\ell,n)} = (y_1^{(\ell,n)T} \dots y_R^{(\ell,n)T})^T$  is the received vector over the  $R$  antennas, here  $(\cdot)^T$  is transpose operator. The signal to be transmitted is  $\mathbf{x}^{(n)} = (x_1^{(n)T} \dots x_T^{(n)T})^T \sim$

$\mathbb{C}\mathcal{N}(0, S_{\mathbf{x}^{(n)}})$ , where  $S_{\mathbf{x}^{(n)}}$  is the covariance matrix of the signal, which is subject to a power constraint such that  $Tr(S_{\mathbf{x}^{(n)}}) \leq P_n$ , where  $P_n$  is the total power on sub-carrier  $n$ . This signal is broadcasted to all users on sub-carrier  $n$ . The precoding method we have chosen is block diagonalization by means of zero-forcing matrices on the downlink [60, 13, 27, 38, 12]. See chapter 2

The method is applied at the base station in each subcarrier for the users of the system. The broadcasted signal is constructed as follows:

$$\mathbf{x}^{(n)} = \mathcal{W}^{(n)} \mathbf{u}^{(n)} \quad (4.2)$$

where  $\mathbf{x}^{(n)} \in \mathbb{C}^{T \times 1}$ ,  $\mathcal{W}^{(n)} \in \mathbb{C}^{T \times LS}$  and  $\mathbf{u}^{(n)} \in \mathbb{C}^{LS \times 1}$ . The matrix  $\mathcal{W}^{(n)} = (\mathbf{W}_{(1,n)} \dots \mathbf{W}_{(L,n)})$  contains the set of pre-filter sub-matrices  $\{\mathbf{W}_{(\ell,n)}\} \in \mathbb{C}^{T \times S}$  and the vector  $\mathbf{u}^{(n)} = (\mathbf{u}_{(1,n)}^T \dots \mathbf{u}_{(L,n)}^T)^T$ , contains the concatenation of intended S-symbols vector  $\{\mathbf{u}_{(\ell,n)}\} \in \mathbb{C}^{S \times 1}$  to be sent to the L-users.

The MIMO-channel matrix,  $\mathbf{H}_{(\ell,n)}$ , from the base station to user  $\ell$  on sub-carrier  $n$  is given by

$$\mathbf{H}_{(\ell,n)} = \begin{pmatrix} h_{11}^{(\ell,n)} & \dots & h_{1T}^{(\ell,n)} \\ \vdots & \ddots & \vdots \\ h_{R1}^{(\ell,n)} & \dots & h_{RT}^{(\ell,n)} \end{pmatrix} \quad (4.3)$$

whose entries  $h_{ij}^{(\ell,n)}$  are the fading coefficients from the transmit antenna  $j$  to the receiver antenna  $i$ . The fading are modelled considering path model, shadowing and multi-path fading as explained at Section 2.4.3.

$\mathbf{z}_{(\ell,n)} = (z_1^{(\ell,n)T} \dots z_R^{(\ell,n)T})^T \sim \mathbb{C}\mathcal{N}(0, S_{\mathbf{z}^{(n)}})$  is the AWGN noise vector present at the receiver. We consider that the noise is uncorrelated between antennas and users.

Then the covariance noise matrix is  $S_{\mathbf{z}^{(n)}} = \sigma^2 \mathbf{I}_R$ .

In order to simplify the analysis, we divide (4.1) by  $\sigma$ . Now we have a normalized system where the covariance noise matrix is  $\mathbf{I}_R$  and we consider that  $\mathbf{H}_{(\ell,n)} = \frac{1}{\sigma} \mathbf{H}_{(\ell,n)}$ .

## 4.2 Block diagonalization

Block diagonalization is a well known method in the literature [60, 13, 27, 38, 12], it permits to send coded information to multiple users just like in a single-user MIMO system. This is made possible by an appropriate precoding done at the base station using eigenvalue decomposition of the known channels values to construct an orthogonal precoding matrix. The method is applied for each data user, superposed and broadcasted. The users can recover the data by a variety of signal detection methods [12].

Our purpose in this chapter is to estimate how many users can be accepted in the multicast system while maintaining a noticeable improvement in capacity over a uniform power transmission among all transmit antennas and subcarriers.

Since  $\mathbf{x}^{(n)}$  is broadcasted, user  $\ell$  on the subcarrier  $n$  receives  $\mathbf{y}_{(\ell,n)}$  on  $R$  antennas, see (4.1). So (4.1) can be rewritten as:

$$\mathbf{y}_{(\ell,n)} = \mathbf{H}_{(\ell,n)} \sum_{j=1}^L \mathbf{W}_{(j,n)} \mathbf{u}_{(j,n)} + \mathbf{z}_{(\ell,n)} \quad (4.4)$$

or better

$$\mathbf{y}_{(\ell,n)} = \mathbf{H}_{(\ell,n)} \mathbf{W}_{(\ell,n)} \mathbf{u}_{(\ell,n)} + \mathbf{H}_{(\ell,n)} \sum_{\substack{j=1 \\ j \neq \ell}}^L \mathbf{W}_{(j,n)} \mathbf{u}_{(j,n)} + \mathbf{z}_{(\ell,n)} \quad (4.5)$$

The user  $\ell$ , in order to recover his data, need to set the sum part of (4.5) to zero. If  $\mathbf{W}_{(\ell,n)}$  is well design according to this criterion, it becomes:

$$\mathbf{y}_{(\ell,n)} = \mathbf{H}_{(\ell,n)} \mathbf{W}_{(\ell,n)} \mathbf{u}_{(\ell,n)} + \mathbf{z}_{(\ell,n)} \quad (4.6)$$

Assume that the symbols sent to user  $\ell$  are contained in vector  $\mathbf{u}_{(\ell,n)}$  of size  $S$  symbols, i.e.  $\mathbf{u}_{(\ell,n)} \in \mathbb{C}^{S \times 1}$  for any user. The block vector composed by the concatenation of all the symbols to be transmitted form  $\mathbf{u}^{(n)} \in \mathbb{C}^{LS \times 1}$ , a linearly independent block vector. Since we precode with  $\mathcal{W}^{(n)} \in \mathbb{C}^{T \times LS}$  to merge all the symbols in  $\mathbf{x}^{(n)}$ , we need that  $\mathcal{W}^{(n)}$  has  $LS$  linear independent precoders. That is  $\text{rank}(\mathcal{W}^{(n)}) = LS$ . We know that  $\text{rank}(\mathcal{W}^{(n)}) \leq \min(T, LS)$ , so the condition is that the number of transmit antennas must be equal or greater than the product of the total number of user by the size of the symbol, i.e.  $T \geq LS$ .

With a fixed number of antennas  $T$ , the precoder matrix  $\mathbf{W}_{(\ell,n)}$  maps the symbols to the antennas, and the corresponding signals are sent through the channel  $\mathbf{H}_{(\ell,n)}$ . Then the product  $\mathbf{H}_{(\ell,n)} \mathbf{W}_{(\ell,n)}$  needs to have  $R$  linear independent block rows in order to transmit  $S$  linearly independent symbols. That is  $\text{rank}(\mathbf{H}_{(\ell,n)} \mathbf{W}_{(\ell,n)}) = R$ . Then  $\text{rank}(\mathbf{H}_{(\ell,n)} \mathbf{W}_{(\ell,n)}) \leq \min(\text{rank}(\mathbf{H}_{(\ell,n)}), \text{rank}(\mathbf{W}_{(\ell,n)}))$ . We know that  $\text{rank}(\mathbf{H}_{(\ell,n)}) = R$  and  $\text{rank}(\mathbf{W}_{(\ell,n)}) = S$ , so  $\text{rank}(\mathbf{H}_{(\ell,n)} \mathbf{W}_{(\ell,n)}) \leq \min(R, S)$ . Now to satisfy  $\text{rank}(\mathbf{H}_{(\ell,n)} \mathbf{W}_{(\ell,n)}) = R$ , we need that  $R \geq S$ .

To design  $\mathbf{W}_{(\ell,n)}$  we define a block matrix  $\mathbf{H}_{(\bar{\ell},n)} \in \mathbb{C}^{(L-1)R \times T}$  that stacks all matrices of the system except the one of interest  $\ell$ . We want that the sum part of (4.5) becomes zero, that is  $\mathbf{W}_{(\ell,n)} \in \text{Ker}(\mathbf{H}_{(\bar{\ell},n)})$ . The condition to design  $\mathbf{W}_{(\ell,n)}$  is that the rows of  $\mathbf{H}_{(\bar{\ell},n)}$  are linearly independent, so the  $\text{rank}(\mathbf{H}_{(\bar{\ell},n)}) = (L-1)R$ . Since  $\text{rank}(\mathbf{H}_{(\bar{\ell},n)}) \leq \min((L-1)R, T)$ , to satisfy the rank condition we need that

$T \geq (L - 1)R$ .

We define the Singular Value Decomposition (SVD) of  $\mathbf{H}_{(\bar{\ell},n)}$  as follows:

$$\mathbf{H}_{(\bar{\ell},n)} = \mathbf{U}_{(\bar{\ell},n)} \boldsymbol{\Sigma}_{(\bar{\ell},n)} [\mathbf{V}_{(\bar{\ell},n)}^{(1)} \mathbf{V}_{(\bar{\ell},n)}^{(0)}]^T \quad (4.7)$$

The columns of  $\mathbf{V}_{(\bar{\ell},n)}^{(0)} \in \mathbb{C}^{T \times T - \text{rank}(\mathbf{H}_{(\bar{\ell},n)})}$  form a basis in the null space of  $\mathbf{H}_{(\bar{\ell},n)}$ . Then any linear combination of  $\mathbf{V}_{(\bar{\ell},n)}^{(0)}$  is useful to design  $\mathbf{W}_{(\ell,n)}$ , as follows:

$$\mathbf{W}_{(\ell,n)} = \mathbf{V}_{(\bar{\ell},n)}^{(0)} \boldsymbol{\sigma}_{(\ell,n)} \quad (4.8)$$

Where  $\boldsymbol{\sigma}_{(\ell,n)} \in \mathbb{C}^{T - \text{rank}(\mathbf{H}_{(\bar{\ell},n)}) \times S}$ , is an arbitrary matrix subject to a power constraint to send the intended vector symbol  $\mathbf{u}_{(\ell,n)}$ , such that  $\mathbf{P}_{(\ell,n)} = \boldsymbol{\sigma}_{(\ell,n)} \boldsymbol{\sigma}_{(\ell,n)}^H$ . Now  $\mathbf{P}_{(\ell,n)} \in \mathbb{C}^{T - \text{rank}(\mathbf{H}_{(\bar{\ell},n)}) \times T - \text{rank}(\mathbf{H}_{(\bar{\ell},n)})}$ .

At the receiver, equation (4.6) can be rewritten as (4.9):

$$\mathbf{y}_{(\ell,n)} = \mathbf{H}_{(\ell,n)} \mathbf{V}_{(\bar{\ell},n)}^{(0)} \boldsymbol{\sigma}_{(\ell,n)} \mathbf{u}_{(\ell,n)} + \mathbf{z}_{(\ell,n)} \quad (4.9)$$

The total rate received by user  $\ell$  is:

$$R_\ell = \sum_{n=1}^N \log_2 \det \left( \mathbf{H}_{(\ell,n)} \mathbf{V}_{(\bar{\ell},n)}^{(0)} \mathbf{P}_{(\ell,n)} \mathbf{V}_{(\bar{\ell},n)}^{(0)H} \mathbf{H}_{(\ell,n)}^H + \mathbf{I}_R \right) \quad (4.10)$$

And the throughput (Sum rate) expression of the system is:

$$\sum_{\ell=1}^L \sum_{n=1}^N \log_2 \det \left( \mathbf{H}_{(\ell,n)} \mathbf{V}_{(\bar{\ell},n)}^{(0)} \mathbf{P}_{(\ell,n)} \mathbf{V}_{(\bar{\ell},n)}^{(0)H} \mathbf{H}_{(\ell,n)}^H + \mathbf{I}_R \right) \quad (4.11)$$

### 4.3 Sum-rate maximization

Considering that we have power constraint over the  $L$ -users and the  $N$ -subcarriers, the sum-rate maximization problem is:

$$\begin{aligned}
& \max \quad \sum_{\ell=1}^L \sum_{n=1}^N \log_2 \det \left( \mathbf{H}_{(\ell,n)} \mathbf{V}_{(\ell,n)}^{(0)} \mathbf{P}_{(\ell,n)} \mathbf{V}_{(\ell,n)}^{(0)H} \mathbf{H}_{(\ell,n)}^H + \mathbf{I}_R \right) \\
& \text{subject to} \quad \sum_{\ell=1}^L \sum_{n=1}^N \text{Tr}(\mathbf{P}_{(\ell,n)}) \leq P \\
& \quad \mathbf{P}_{(\ell,n)} \succeq 0; \quad \ell = 1, \dots, L, \quad n = 1, \dots, N.
\end{aligned} \tag{4.12}$$

Following [38], we can rewrite (4.12) as (4.13), considering  $\mathbf{G}_{(\ell,n)} = \mathbf{H}_{(\ell,n)} \mathbf{V}_{(\ell,n)}^{(0)}$ :

$$\begin{aligned}
& \max \quad \sum_{\ell=1}^L \sum_{n=1}^N \log_2 \det \left( \mathbf{G}_{(\ell,n)} \mathbf{P}_{(\ell,n)} \mathbf{G}_{(\ell,n)}^H + \mathbf{I}_R \right) \\
& \text{Subject to} \quad \sum_{\ell=1}^L \sum_{n=1}^N \text{Tr}(\mathbf{P}_{(\ell,n)}) \leq P \\
& \quad \mathbf{P}_{(\ell,n)} \succeq 0; \quad \ell = 1, \dots, L, \quad n = 1, \dots, N.
\end{aligned} \tag{4.13}$$

According to [81] and [6], this is a convex optimization problem, and the KarushKuhn-Tucker (KKT) conditions are necessary and sufficient to characterize the solution.

The Lagrangian of (4.13) is:

$$\begin{aligned}
& \mathcal{L}(\{\mathbf{P}_{(\ell,n)}\}, \lambda, \{\mathbf{Q}_{(\ell,n)}\}) = \\
& \sum_{\ell=1}^L \sum_{n=1}^N \log_2 \det \left( \mathbf{G}_{(\ell,n)} \mathbf{P}_{(\ell,n)} \mathbf{G}_{(\ell,n)}^H + \mathbf{I}_R \right) \\
& - \lambda \left( \sum_{\ell=1}^L \sum_{n=1}^N \text{Tr}(\mathbf{P}_{(\ell,n)}) - P \right) + \sum_{\ell=1}^L \sum_{n=1}^N \text{Tr}(\mathbf{Q}_{(\ell,n)} \mathbf{P}_{(\ell,n)})
\end{aligned} \tag{4.14}$$

To satisfy the constraints on (4.13), we define the slack variable  $\lambda$  and the slack matrices  $\{\mathbf{Q}_{(\ell,n)}\}$ . These last ones ensure the positiveness of the solution  $\mathbf{P}_{(\ell,n)}$  over

the total power constraint  $P$ .

The KKT conditions of the problem can be obtained via results of [42] and [39] to obtain :

$$\begin{aligned}
 & \bullet \mathbf{G}_{(\ell,n)}^H (\mathbf{I}_R + \mathbf{G}_{(\ell,n)} \mathbf{P}_{(\ell,n)} \mathbf{G}_{(\ell,n)}^H)^{-1} \mathbf{G}_{(\ell,n)} = \\
 & \quad \lambda \mathbf{I}_{T-\text{rank}(\mathbf{H}_{(\bar{\ell},n)})} + \mathbf{Q}_{(\ell,n)} \\
 & \bullet \text{Tr}(\mathbf{Q}_{(\ell,n)} \mathbf{P}_{(\ell,n)}) = 0 \\
 & \bullet \lambda \geq 0 \\
 & \bullet \mathbf{Q}_{(\ell,n)}; \quad \ell = \{1, \dots, L\}, n = \{1, \dots, N\}.
 \end{aligned} \tag{4.15}$$

From  $\nabla_{\mathbf{P}_{(\ell,n)}} \mathcal{L}(\{\mathbf{P}_{(\ell,n)}\}, \lambda, \{\mathbf{Q}_{(\ell,n)}\}) = 0$ , we derive (??) and we can obtain the matrix  $\mathbf{P}_{(\ell,n)}$ , as follows:

$$\mathbf{P}_{(\ell,n)} = (\lambda \mathbf{I}_{T-\text{rank}(\mathbf{H}_{(\bar{\ell},n)})} + \mathbf{Q}_{(\ell,n)})^{-1} - \mathbf{G}_{(\ell,n)}^{-1} \mathbf{G}_{(\ell,n)}^{-H} \tag{4.16}$$

Denoting  $J = T - \text{rank}(\mathbf{H}_{(\bar{\ell},n)})$  and since  $\mathbf{G}_{(\ell,n)} \mathbf{G}_{(\ell,n)}^H \in \mathbb{C}^{J \times J}$  and  $\mathbf{Q}_{(\ell,n)} \in \mathbb{C}^{J \times J}$  are commuting matrices, they can share the same eigenvectors. So they can be eigen-decomposed as  $\mathbf{G}_{(\ell,n)} \mathbf{G}_{(\ell,n)}^H = \mathbf{U}_{(\ell,n)} \Gamma_{(\ell,n)} \mathbf{U}_{(\ell,n)}^H$  and  $\mathbf{Q}_{(\ell,n)} = \mathbf{U}_{(\ell,n)} \Delta_{(\ell,n)} \mathbf{U}_{(\ell,n)}^H$ . Replacing the later in (4.16) we obtain:

$$\mathbf{P}_{(\ell,n)} = \mathbf{U}_{(\ell,n)} [(\lambda \mathbf{I}_J + \Delta_{(\ell,n)})^{-1} - \Gamma_{(\ell,n)}^{-1}] \mathbf{U}_{(\ell,n)}^H \tag{4.17}$$

Using the complementary slackness (??), we have:

$$[(\lambda \mathbf{I}_J + \Delta_{(\ell,n)})^{-1} - \Gamma_{(\ell,n)}^{-1}] \Delta_{(\ell,n)} = 0 \tag{4.18}$$

As  $\Delta_{(\ell,n)} = \text{diag}(\delta_{(\ell,n)_1}, \dots, \delta_{(\ell,n)_J})$  and  $\Gamma_{(\ell,n)} = \text{diag}(\gamma_{(\ell,n)_1}, \dots, \gamma_{(\ell,n)_J})$ . A by



scalar element expression can be written:

$$[(\lambda + \delta_{(\ell,n)_j})^{-1} - \gamma_{(\ell,n)_j}^{-1}] \delta_{(\ell,n)_j} = 0 \quad (4.19)$$

Due to the KKT conditions (??) and (4.15), we can say that  $\delta_{(\ell,n)_j} \geq 0$  and  $\gamma_{(\ell,n)_j} \geq \lambda + \delta_{(\ell,n)_j}$ . If  $\delta_{(\ell,n)_j}$  is close to zero, for  $j = \{1, \dots, J\}$ , we can express the power assigned to user  $\ell$  on subcarrier  $n$  as:

$$\mathbf{P}_{(\ell,n)} = \mathbf{U}_{(\ell,n)} \text{diag} \left[ \left( \frac{1}{\lambda} - \frac{1}{\gamma_{(\ell,n)_1}} \right)^+, \dots, \left( \frac{1}{\lambda} - \frac{1}{\gamma_{(\ell,n)_J}} \right)^+ \right] \mathbf{U}_{(\ell,n)}^H \quad (4.20)$$

With  $(u)^+ = \max(u, 0)$  denoting the function that considers the positive part.

Including (4.20) in the power constraints (4.13), we obtain:

$$\sum_{\ell=1}^L \sum_{n=1}^N \sum_{j=1}^J \left( \frac{1}{\lambda} - \frac{1}{\gamma_{(\ell,n)_j}} \right)^+ \leq P \quad (4.21)$$

the eigenvalue water-filling among the  $L$ -users, over the  $N$ -subcarriers and the  $J$ -modes of transmission, for the zero-forcing pre-coding. This result is a direct outcome of the previous work in [60, 38].

It has to be noted that the implementation of (4.21) is simpler than the SISO optimal power allocation in chapter 3, because it is now directly in the simple structure of the classical water-filling.

## 4.4 Numerical results

As seen from the above explanation, the design of zero-forcing pre-coders in multi-user MIMO involves many design constraints. The first one is the condition required to construct the precoder, that is  $T \geq LS$ . Follow, the quantity of reception antennas  $R \geq S$ . And the existence of the orthogonal precoder is  $T \geq (L-1)R$ . Our simulated Multiuser-MIMO systems, respect the constraints given by the MIMO structure. The number of antennas at the reception are equal of the dimension of the transmitted signal on the subcarrier  $n$ , that is  $R = S$ . It follows that  $T \geq LR$ . We consider a realistic scenario where  $T = 8$ . The constraints lead us to separate the system in comparable sub-system in terms of quantity of user and the number of receive antennas. The table 4.1 summarizes the results for mean distances of 100, 200, and 300 meters. The table are separate by comparable sub-systems because the number of antenna. When the users has 1 antenna, the MIMO multiuser base station ensure up to 8 users in the system with zero-forcing precoding method. If we add an antenna to each receiver, the MIMO multiuser base station can accept up to 4 users respecting the constraints. When each receiver has 3 or 4 antennas, the system can be composed up to 2 users. The results in the columns of the table 4.1 are *the percentage increase of the capacity (% Inc.)* in mean, it describes how much better is the sum capacity with power optimization than the sum capacity with uniform power distribution. The other column shows how many bits can be allocated by subcarriers (B\S.c.) in mean.

**MIMO System with 8 Transmit antennas and 1 Receive antenna** This type of system is also known as MISO (Multiple Input Single Output), we can immediately observe that the percentage of rate increase is much larger than the one obtained in

the case of SISO communications. As an example, 504,42% better with 5 users and the possibility of allocating 9,13 Bits per subcarrier in mean within a distance of 100 meters in mean. This is clearly due to the MIMO setting, in which uniform power allocation among the eigenvectors is far from being optimal. The Multiuser setting comes on top of this problem. In this case, "equal power allocation" should not be considered as being equivalent to "classical broadcast" situation.

When the numbers of users increase, the capacity decreases because the energy must be shared among other users coming in the system. On the other hand when the distance increases, the percentage of improvement due to power allocation also increases, but the capacity decreases accordingly. This phenomenon was already observed in the SISO case.

**MIMO System with 8 Transmit antenna and 2 Receive antennas** Due to the constraints imposed by the design of zero-forcing method, this MIMO system can accept up to 4 users. The results are shown in the table 4.1. The capacity increase is less in mean than the one with same users in the previous case. But at 300 meters even if the percentage increase is less, the method ensures more Bits per subcarrier in mean. The normalized histogram of Fig. 4.1(a) shows the p.d.f. of the percentage increase, from that histogram we can see that 68% of the realizations are close to the mean (700,74) with a standard deviation of 195,56. Fig. 4.1(b) shows the p.d.f. of the capacity per subcarrier, then we can see that although the mean on the samples are 2,14 Bits per subcarrier, the mode is 0,17 Bits per subcarrier.

In the case where the users have 3 and 4 antennas, the percentage increase in sum capacity is less since there are two users. At 300 meters, with two users with 3 antennas we have 0,32 bits per sub-carrier in mean, while if the users have 4 antennas

this capacity is 0,33 bits per sub-carrier. The capacity if the two users have 1 antenna is 0,26 bits per sub-carrier.

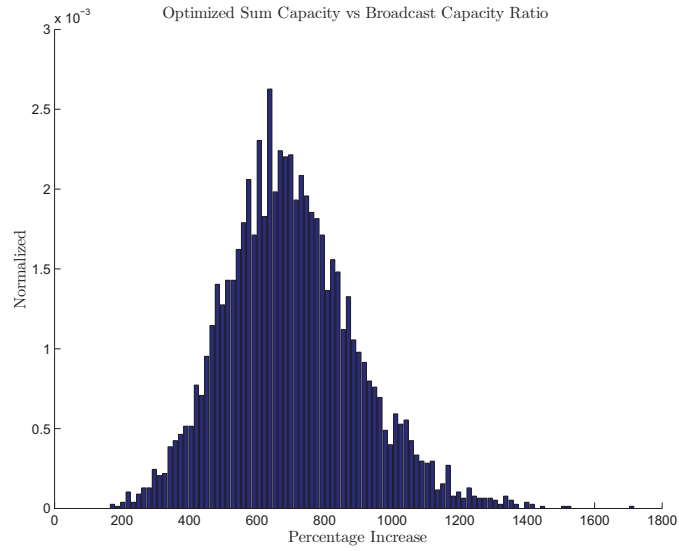
Table 4.1: Multiuser MIMO Results

| $\ell$ Ant | 100 meters |        | 200 meters |        | 300 meters |        |
|------------|------------|--------|------------|--------|------------|--------|
|            | % Inc.     | B\S.c. | % Inc.     | B\S.c. | % Inc.     | B\S.c. |
| 1 1        | 269,40     | 24,31  | 581,58     | 7,49   | 787,73     | 0,37   |
| 2 1        | 317,45     | 17,59  | 775,74     | 5,21   | 1121,57    | 0,26   |
| 3 1        | 370,57     | 13,92  | 941,15     | 3,98   | 1404,39    | 0,20   |
| 4 1        | 428,16     | 11,39  | 1113,37    | 3,13   | 1690,82    | 0,16   |
| 5 1        | 504,42     | 9,13   | 1310,71    | 2,37   | 2005,65    | 0,12   |
| 6 1        | 607,15     | 7,20   | 1573,75    | 1,82   | 2418,25    | 0,09   |
| 7 1        | 765,68     | 5,46   | 1981,08    | 1,35   | 3067,02    | 0,07   |
| 8 1        | 1108,16    | 3,49   | 2868,99    | 0,84   | 4497,37    | 0,04   |
| 1 2        | 160,64     | 18,00  | 337,29     | 4,97   | 458,05     | 0,47   |
| 2 2        | 208,00     | 12,01  | 500,40     | 3,19   | 724,26     | 0,31   |
| 3 2        | 279,49     | 8,23   | 700,74     | 2,14   | 1042,34    | 0,21   |
| 4 2        | 431,87     | 5,03   | 1099,58    | 1,27   | 1657,00    | 0,12   |
| 1 3        | 112,14     | 14,90  | 242,09     | 3,93   | 333,08     | 0,55   |
| 2 3        | 169,61     | 8,73   | 415,45     | 2,25   | 603,27     | 0,32   |
| 1 4        | 84,10      | 13,01  | 190,59     | 3,39   | 265,98     | 0,64   |
| 2 4        | 157,54     | 6,89   | 389,57     | 1,76   | 567,50     | 0,33   |

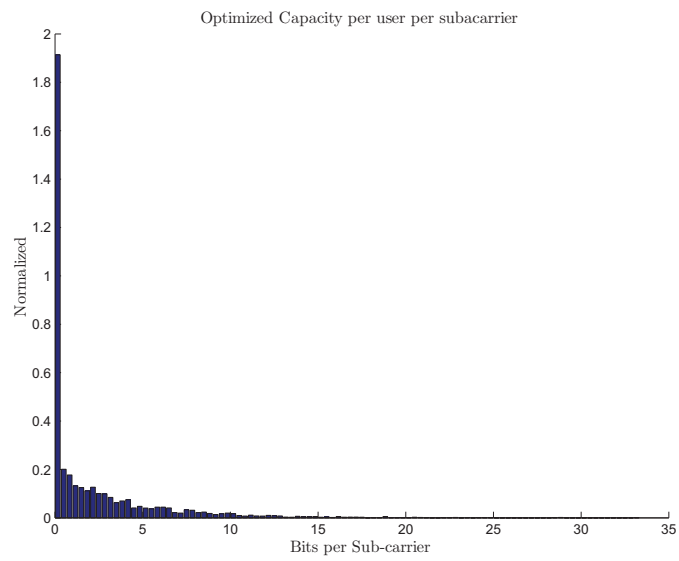
## 4.5 Conclusion

In this chapter we extended the work made by Kaviani [38], from the MU-MIMO to the MU-MIMO OFDM case. We developed an algorithm based on zero forcing precoding. Taking all constraints into account, we considered several feasible cases, which are representative of all feasible situations. Clearly, this set of linearly precoded MIMO systems cannot accommodate a large number of users. It can be observed that, the overall improvement is quite large. It can also be clearly seen that this kind of "broadcast" always correspond to savings compared to the establishment of several point to point communications, even if we take into account the fact that in the

multiuser case, the optimisation is less efficient than in the single user case.



(a) Percentage increase



(b) Capacity in Bit per Subcarrier

Figure 4.1: Histograms for 3 User at 200 [m] from access point

# Chapter 5

## OFDM Realistic Coverage

The final aim of this work is to decide when wireless multicast brings some advantage over classical broadcasting. The comparisons made in the previous chapters already bring some light to this problem. However, classical broadcast (in contrast with its information theoretic counterpart) is designed in a very specific way, which should be taken into account for the comparison. In such a situation the transmitter has no hope that the transmitted signal will be received by all users, because the randomness of channels makes some of them really untractable. In such case, the only way to take these events into account is via outage capacity: a broadcast channel is always designed in such a way that  $x$  % of the users are certain to obtain a given rate. This is clearly linked to the definition of "outage capacity" as defined in the background chapter.

In practical situations, the estimation of the coverage of an access point or base station is done via a huge number of simulations. However, recently, techniques known as "stochastic geometry" were proposed [62], which allow to solve analytically such problems in simple cases. This chapter intends to extend the known techniques for

OFDM channels, and it will be shown that analytical solutions are not fully feasible, and that only numerical solutions are obtained. This is anyway faster than the many simulations usually required.

Obviously, the percentage of users meeting the given bitrate constraint depend on their location. Therefore, we assume that the users are distributed according to a certain spatial point process. It allows us to consider the spatial distribution of the users around the base station, from which we deduce the distribution of the capacity. Then, for a typical user, we compute a coverage area where a minimum/fixed capacity is guaranteed with a certain probability. This corresponds to an outage probability on the capacity. This outage probability may also be interpreted as the proportion of users for which this fixed capacity will be offered, which is precisely the desired design criterion for broadcast transmission. This whole chapter deals with SISO-OFDM transmissions.

Our solution involves some approximations to obtain semi-analytical results, therefore, a first set of numerical results checks that the different approximations of the distributions (channels, capacity of a given channel, etc.) involved in the computation of the final capacity are accurate. Then, the extrapolated capacity is compared to simulations, in order to check if our optimization is correct over this scenario, meaning that the required percentage of users indeed meets the desired bit-rate.

## 5.1 OFDM coverage modeling

The goal is to find a closed-form expression to calculate the coverage, and have an impartial instrument to say if the multicast optimization is still useful under a spatial distribution of the users, with an outage criterion in mind.



Let  $\mathbb{P}(C \geq C_{out})$  denote the outage probability. It is the probability that the capacity of a typical user, denoted  $C$ , is greater than a predetermined value  $C_{out}$  [29, 68]. Given a capacity requirement  $C_{out}$  and an outage probability, we can calculate the maximal coverage, i.e. the maximal distance where users can be distributed while statistically meeting these two constraints. We recall the capacity formula for the OFDM case:

$$C = \frac{1}{N} \sum_{n=1}^N \log_2 \left( 1 + \frac{|h^{(n)}|^2 p_n}{\sigma_z^2} \right) \quad [bits/s/Hz] \quad (5.1)$$

The complex subcarrier gain  $h^{(n)}$  is expressed in the frequency domain. It is modeled by (2.74), evaluated at frequency  $f_n$ . Therefore, the complex channel gain is expressed as:

$$h^{(n)} = \sum_{i=1}^I \beta_i e^{-j(2\pi f_n \tau_i + \theta_i)} \quad (5.2)$$

Where  $\beta_i$  is the product of the path loss gain  $\sqrt{\frac{1}{L(D)}}$  and the complex gain of the path  $g_i$ :  $\beta_i = \sqrt{\frac{1}{L(D)}} \cdot g_i$ . We can express it as:

$$h^{(n)} = \sqrt{\frac{1}{L(D)}} \sum_{i=1}^I g_i e^{-j(2\pi f_n \tau_i + \theta_i)} \quad (5.3)$$

The multipath part of this expression can be written as:

$$g^{(n)} = \sum_{i=1}^I g_i e^{-j(2\pi f_n \tau_i + \theta_i)} \quad (5.4)$$

Given that the path gains  $\{g_i\}$  are Rayleigh distributed with the parameter  $\sigma_i$  and the phase  $\theta_i$  are uniformly distributed on the interval  $[0, 2\pi]$ , we define  $\bar{g}_i = g_i e^{-j\theta_i}$

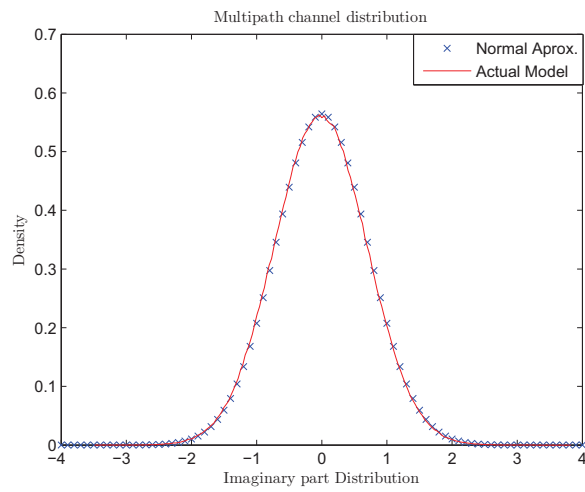
as a single random variable with a complex Gaussian distribution with zero mean and variance  $\sigma_i^2$ . The random variables  $\{\bar{g}_i\}_{i=1,\dots,I}$  form a sequence of independent complex Gaussian random variables with zero mean and different variances. The real and imaginary parts are assumed to be independent. The multipath part thus reduces to:

$$g^{(n)} = \sum_{i=1}^I \bar{g}_i e^{-j2\pi f_n \tau_i} \quad (5.5)$$

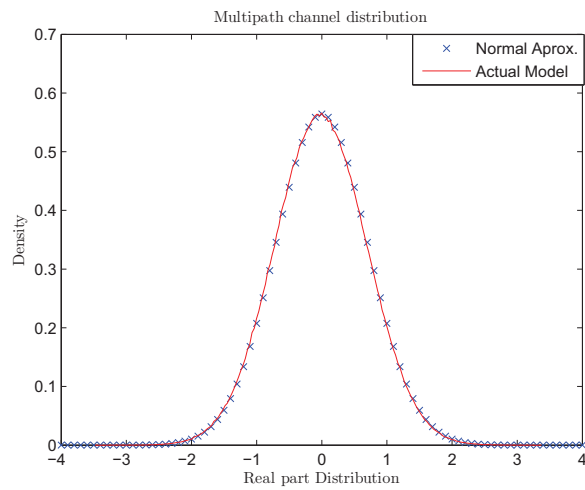
And the complex channel gain  $h^{(n)}$  can be viewed as:

$$h^{(n)} = \sqrt{\frac{1}{L(D)}} g^{(n)} \quad (5.6)$$

The first step towards characterizing properly the capacity is to first evaluate the probability density function of the channel  $h^{(n)}$ . We can see that  $g^{(n)}$  is a combination of different random variables, all of them with zero mean, but of various variances. Under this situation the central limit theorem does not apply, because the involved random variables have different variances. However, in order to simplify our next computations, we will make a Gaussian approximation of  $g^{(n)}$ . In fact, for the considered model, the *model E* described in [41], we can empirically show by simulation that the real and imaginary parts of  $g^{(n)}$  are very close to Gaussian distributions. We illustrate in Figure 5.1 on the next page the distribution of imaginary and the real part of  $g^{(n)}$  for this model. In this figure we can appreciate the actual model in red line and the approximated by the complex Gaussian function in cross blue line. The curves are almost superimposed, and the complex normal distribution seems to be a good approximation for our purpose.



(a) Imaginary Multipath Distribution



(b) Real Multipath Distribution

Figure 5.1: Multipath Channel Distribution

Therefore, in the rest of this chapter, we assume that the random variables  $g^{(n)}$  follow complex normal distributions. Hence, the probability distribution function of  $g^{(n)}$  is approximated by:

$$f_{g^{(n)}}(z) = \frac{1}{\pi \sum_{i=1}^I \sigma_i^2} \exp \left\{ -\frac{\bar{z}z}{\sum_{i=1}^I \sigma_i^2} \right\} \quad (5.7)$$

which will be useful for a proper characterization of the capacity distribution.

### 5.1.1 Outage probability

Unfortunately, analytical computation of the capacity pdf is not tractable for our model. Instead, we approximate it with a known distribution. Parameters of this distribution will be deduced from mean and variance of the capacity. Therefore, in this section, we compute mean and variance of the capacity for our model.

If we retake the formula (5.1) and put inside the channel expression (5.6) we obtain:

$$C = \frac{1}{N} \sum_{n=1}^N \log_2 \left( 1 + \frac{1}{L(D)} |g^{(n)}|^2 \frac{P_n}{\sigma_z^2} \right) \quad \text{bits/s/Hz} \quad (5.8)$$

The random variables that compose the equation of the capacity (5.8) are the distance  $D$  and the complex channel gains  $g^{(n)}$ .

The distance  $D$  is the distance between a typical user and the base station. We assume that users are distributed in an observation window. In our numerical evaluation, it consists in a ball with radius  $R$ . Within this ball, users location can follow any distribution. Here we consider that users are independently and uniformly distributed in this window. Since the base station is at the center of this ball, the pdf of the distance from a user to the BS is given by:

$$f_D(d) = \frac{2d}{R^2} \quad (5.9)$$

where  $d$  belongs to  $[0, R]$ .

Recall that the multipath complex channel gain  $g^{(n)}$  has  $f_{g^{(n)}}(z)$  as probability density function (5.7).

The computation of the mean capacity is straightforward. It is given by:

$$\mathbb{E}[C] = \frac{1}{N} \sum_{n=1}^N \mathbb{E} \left[ \log_2 \left( 1 + \frac{1}{L(D)} |g^{(n)}|^2 \frac{p_n}{\sigma_z^2} \right) \right] \quad (5.10)$$

$$= \frac{1}{N} \sum_{n=1}^N \int_0^R \int_{\mathbb{C}} \log_2 \left( 1 + \frac{1}{L(d)} |z|^2 \frac{p_n}{\sigma_z^2} \right) f_{g^{(n)}}(z) f_D(d) dz \quad dd \quad (5.11)$$

For the variance of the capacity, we get:

$$Var(C) = \sum_{n=1}^N Var(C_n) + 2 \sum_{n=1, i>n}^{N-1, N} Cov(C_i, C_n) \quad (5.12)$$

where  $C_n$  is the capacity over one subcarrier.

Considering that the channels can have a correlation between the subcarriers, the covariances are not nil. This correlation is due to the random variables  $\bar{g}_i$  (see formula (5.5)) which are the same for all the channels.

The covariance  $Cov(C_i, C_n)$  has the form:

$$Cov(C_i, C_n) = \int_0^R \int_{\mathbb{C}} \int_{\mathbb{C}} c_n(z^n, d) c_i(z^i, d) f_{g^{(n)}, g^{(i)}}(z^{(n)}, z^{(i)}) f_D(d) dz^{(n)} dz^{(i)} dd \quad (5.13)$$

where  $c_n(z^n, d)$  is the capacity of the subcarrier  $n$  for a given sample of  $g^n$  (equals to  $z^n$ ) and a realization of the distance  $D$  ( $d$ ).  $f_{(g^{(n)}, g^{(i)})}(z^{(n)}, z^{(i)})$  is the joint probability density function of the random variables  $(g^n, g^i)$ .

If we assume that the vector  $(g^{(n)}, g^{(i)})$  is still normal complex, the joint distribution is:

$$f_{(g^{(n)}, g^{(i)})}(z^{(n)}, z^{(i)}) = \frac{1}{\pi^2 \det(\Gamma)} \exp \left\{ \frac{\sum_{i=1}^I \sigma_i^2}{\det(\Gamma)} \left( z^{(n)} \overline{z^{(n)}} + z^{(i)} \overline{z^{(i)}} \right) - 2 \operatorname{Re}(\gamma_{n,i} z^{(i)} \overline{z^{(n)}}) \right\} \quad (5.14)$$

with  $\det(\Gamma) = \left( \sum_{i=1}^I \sigma_i^2 \right)^2 - |\gamma_{n,i}|^2$  and

$$\gamma_{n,i} = \sum_{u=1}^l \sigma_u^2 \exp \{ -j2\pi(f_n - f_i)\tau_u \} \quad (5.15)$$

The joint distribution above is obtained under the assumption that  $(g^{(n)}, g^{(i)})$  is a normal complex distribution, and is function of variance, covariance, etc. of these two random variables [69, 54].

As we can see the mean and the variance of the capacity have not a kind form. These integrals must be calculated numerically.

### 5.1.2 Modeling the capacity pdf

Let  $f(E[C], \operatorname{Var}[C], x)$ , the probability density function of the capacity parameterized with the mean  $E[C]$  and the variance  $\operatorname{Var}[C]$ . To calculate the outage probability under the given scenario, we use the following formula:

$$\begin{aligned} \mathbb{P}(C \geq C_{out}) &= 1 - \mathbb{P}(C \leq C_{out}) \\ &= 1 - \int_0^{C_{out}} f(E[C], \operatorname{Var}[C], x) dx \end{aligned} \quad (5.16)$$

Once the mean and variance of the capacity are obtained, we will compare the shape of the actual pdf obtained by simulation with a well known function, in order to find the best fit. A good candidates are the log-normal probability distribution.

By instance  $f(E[C], \operatorname{Var}[C], x)$  can be the log-normal probability density function.

It can be used to approach the empirical probability density function of the capacity under a realistic environment. This function has the following form:

$$f(E[C], Var[C], x) = \frac{1}{x\sigma_V} \exp\left(-\frac{(\ln(x) - \mu_E)^2}{2\sigma_V}\right) \quad (5.17)$$

$$\text{With } \mu_E = \ln\left(\frac{E[C]^2}{\sqrt{Var[C] + E[C]^2}}\right) \quad (5.18)$$

$$\text{and } \sigma_V = \ln\left(\frac{Var[C]}{E[C]^2} + 1\right) \quad (5.19)$$

where the parameters  $\mu_E$  and  $\sigma_V$  are deduced from mean and variance of the capacity  $C$ . Once we have (5.17) parameterized, we can calculate numerically  $C_{out}$  from (5.16). The mean  $E[C]$  (5.10) and the  $Var[C]$  (5.12) were calculated using numerical integration. We took the probabilistic distribution (5.9) with  $R = 200$ . We use the parameters of the model E [41] to model the pdf of the fading channel, and parameterize (5.7). For the path loss, equations (2.65) and (2.66) are considered, taking in account the distance breakpoint. Using these parameters, the calculated mean has value:  $E[C] = 0.4529$  and the variance:  $Var[C] = 0.8827$ . On the other hand, in order to have values to compare, we perform an empirical test generating samples, the empirical mean is 0.4525 and the variance of the samples is 0.9996. The difference are essentially due to the iterations needed to perform the integrations. The log-normal distribution is parameterized with this mean and this variance and the pdf is shown in figure 5.2. The curve in *blue* is the pdf of the empirical random variable, made with many samples. The curve in *magenta*, is the log-normal pdf but parameterized with the empirical values of the mean and variances of the samples. And finally, the *black* curve shown is parameterized with the computed values using the theoretical pdf. It appears that the curves are quite different on the peak of the

distributions, but the distribution tails are very close to each others.

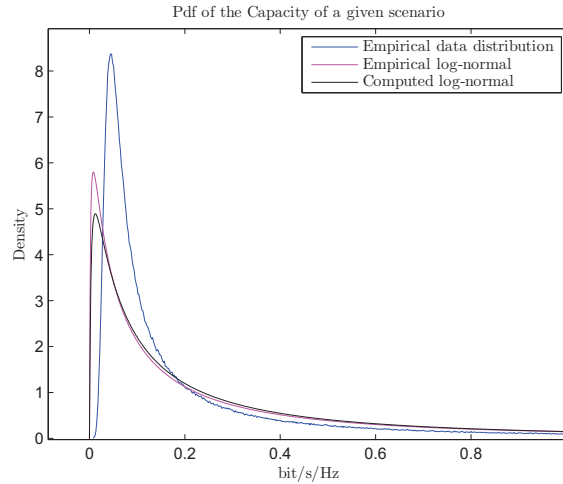


Figure 5.2: PDF of the capacity of a given scenario

The formula (5.16) can be used in different ways. It gives the distribution of the capacity offers to broadcast communications when the parameters (mean and variance capacity) are given. It can also be used to parameterize the system in order to achieve a certain quality of service: fix the maximum radio range  $R$  of the BS to ensure a capacity  $C_{out}$  with a certain probability, etc. In the next section we show numerical results that can be found performing many realizations.

## 5.2 Numerical results

The simulation considers two different levels of noise, that are on the order of magnitude of what can be found in practical situations, i.e. an SNR between 10 and 15  $dB$ . The simulations are performed under the assumption that the users are uniformly distributed over a ball of radius  $R = 200$  [m]. To aim a SNR close to 10 $dB$  we set



the noise with a power of  $1.0 \times 10^{-12}$  [W]. And to aim a SNR close to 15dB we set the noise with a power of  $1.0 \times 10^{-13}$  [W]. We perform the simulations using our optimization algorithm for both cases and compare with the non optimized case. We set the  $\mathbb{P}(C \geq C_{out}) = 0.95$  and we calculate  $C_{out}$ . The target here is to check how the optimization criterion (sum capacity) matches the broadcast optimization criterion (outage capacity) . Also we see if the extrapolation by a known pdf are useful in order to establish a design criterion for the broadcast channel situation.

### 5.2.1 Numerical results at 10 dB

Figure 5.3 shows the results and presents the followed concepts:

- The capacity outage  $C_{out}$  where the probability is 95 % for broadcast scheme, Brown - Circle.
- The capacity outage  $C_{out}$  where the probability is 95 % for optimized scheme, Dark Red - Star.
- The mean Broadcast capacity where probability is over 95 % , Cyan - Cross.
- The mean Optimized capacity where probability is over 95 % , Pink - Square.
- The mean of the Broadcast capacity (100 %), Yellow - triangle.
- The mean of the Optimized capacity (100 %), blue - Diamond.
- Log-Normal based computed Outage Capacity, Blue-Green - Plus.
- Log-Normal based empirical Outage Capacity, Red - Dash.

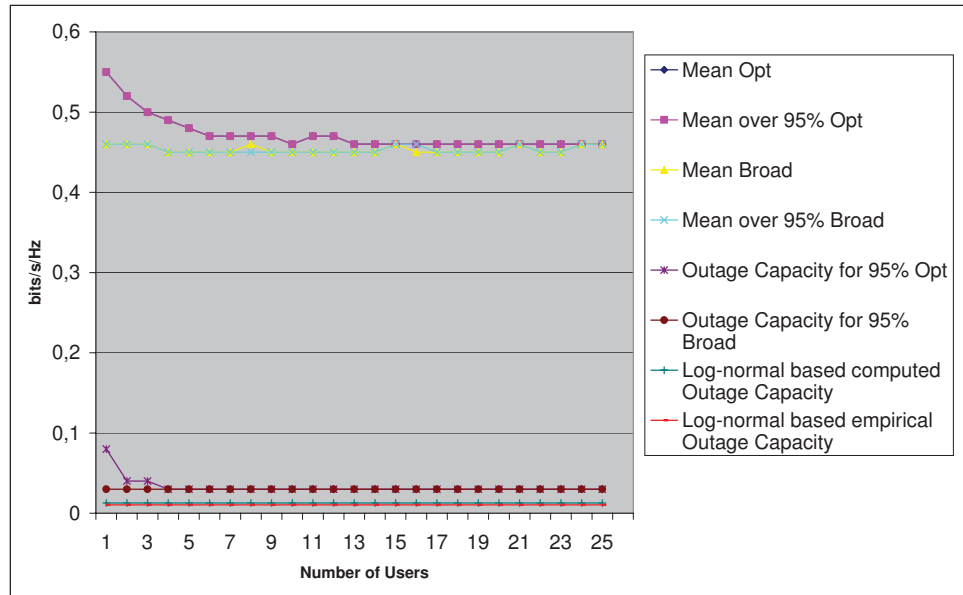


Figure 5.3: Mean capacity, Outage capacity for 95 % and Mean over 95 % for SNR 10 dB

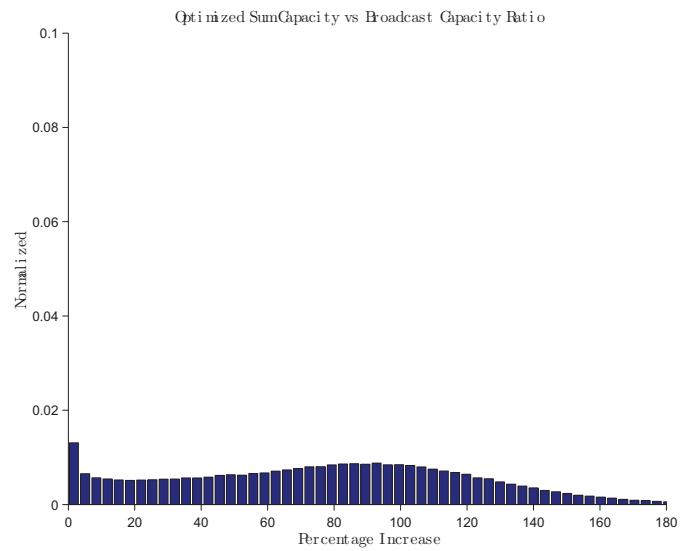
At first glance we can see that the capacity gain in mean is weak. From Figure 5.3, we can see 20 % of increase in one user and 13 % when we have 2 users. The mean of the sub-set that is over 95 % of probability is equal with the one with all the samples. The mean of the optimized capacity shows weak improvement between one and eight users. The outage capacity of the samples is near 0.03  $[bits/s/Hz]$ . We try to approximate the actual pdf by a log-normal pdf. When we parameterize the log-normal pdf with the mean and the variance of the samples, the log-normal based empirical outage capacity is 0.0103  $[bits/s/Hz]$ . And when we parameterize with

the mean and the variance obtained computing  $E[C]$  and  $Var[C]$ , the log-normal based computed capacity is 0.0127 [bits/s/Hz].

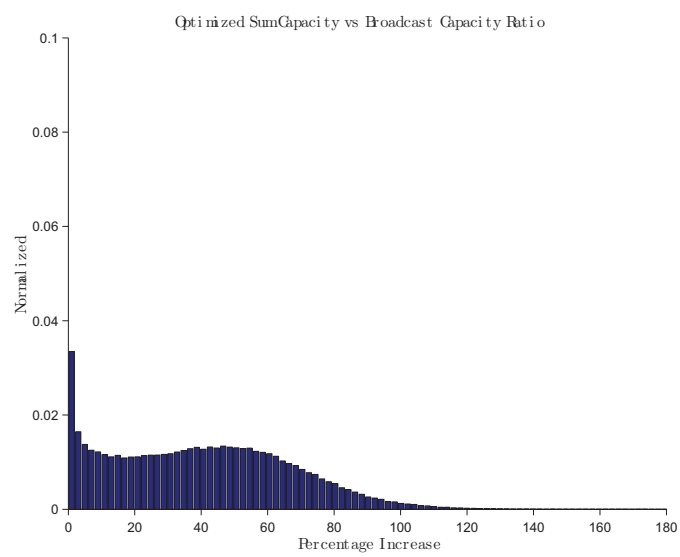
On the other hand, we consider the *percentage increase histograms* (Figure 5.4 on the next page). It is computed for each sample as:

$$\left(\frac{\textit{Optimized Capacity}}{\textit{Broadcast Capacity}} - 1\right) \cdot 100$$

Figure 5.4 on the next page shows the distribution of this percentage increase. A percentage increase of 0% means that the optimized and broadcast capacity are the same (the ratio is 1). We can observe that for approximately 30% of the samples, there is a percentage increase superior to 100%, meaning that the optimized capacity is at least two times greater than the broadcast one. Also, it is worth noting that for one user the mean percentage increase is 72 %. The difference with the results shown in Figure 5.3 may be explained by the fact that these improvements mainly concerns users with small capacity keeping mean capacity quite constant. The later can be appreciated comparing the histograms in Figure 5.5 on page 144, for one user. It clearly appears that the distribution of the capacity is different for the first part (approximately for capacity less than 0.5 bit/s/Hz), and similar for higher capacities. More precisely, for one user the optimized mean capacity is 0.55 bits/s/Hz, the broadcast mean capacity is 0.46 bits/s/Hz. If we compare the means we have 20 % of increase between the means. For 2, 3, 4 and 5 users this comparison gives 13 %, 8.7 %, 8.8 % and 6.66 % respectively.

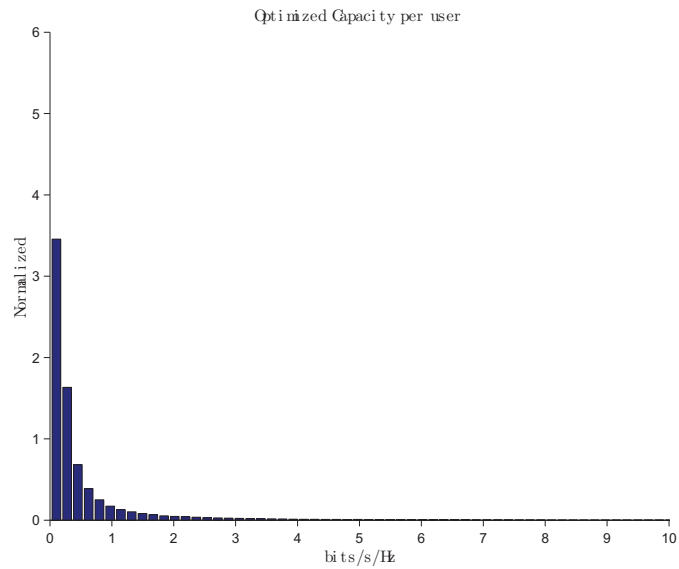


(a) 1 User

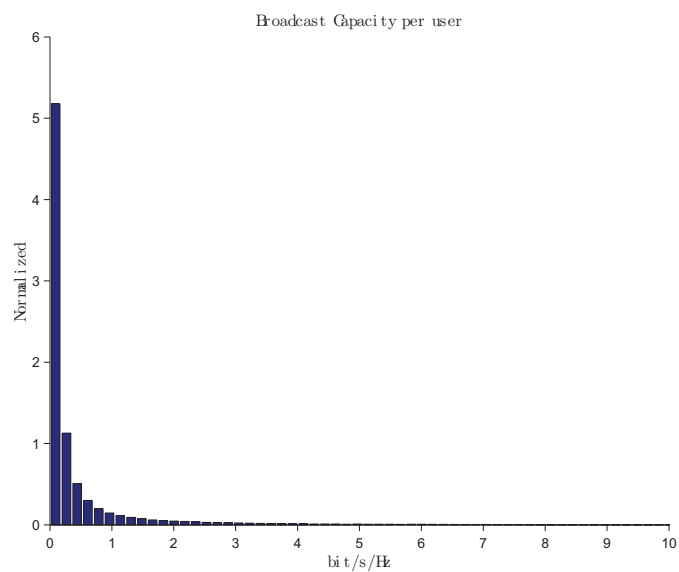


(b) 2 User

Figure 5.4: Percentage increase at 10 dB



(a) Optimized capacity one user



(b) Broadcast capacity one user

Figure 5.5: Optimized and Broadcast Capacity for one user at 10 dB

## 5.2.2 Numerical results at 15 dB

The Figure 5.6 on the next page, shows the results and present the followed concepts:

- The capacity outage  $C_{out}$  where the probability is 95 % for broadcast scheme, Brown - Circle.
- The capacity outage  $C_{out}$  where the probability is 95 % for optimized scheme, Dark Red - Star.
- The mean broadcast capacity where probability is over 95 % , Cyan - Cross.
- The mean optimized capacity where probability is over 95 % , Pink - Square.
- The mean of the broadcast capacity (100 %), Yellow - triangle.
- The mean of the optimized capacity (100 %), Blue - Diamond.
- Log-Normal based computed outage capacity, Blue-Green - Plus.
- Log-Normal based empirical outage capacity, Red - Dash.

Over the figure we can see that the optimized capacity mean is practically equal to the mean over the subset that is over the 95 % of probability. The same happens with the broadcast mean. The gain in percentage is 20 % for one user. The gain in capacity is maximum with one user and decreases quickly. With six users, there is no more reason to perform optimization. The broadcast outage capacity is equal to 0.15 bits/s/Hz, the accuracy of this value has a bias and is due to the number of samples used (200.000); an other set with 2.000.000 of samples give a value of 0.2763 [bits/s/Hz]. Extrapolating with the log-normal distribution, we found that the log-normal based empirical outage capacity has 0.22 [bits/s/Hz]. And when we

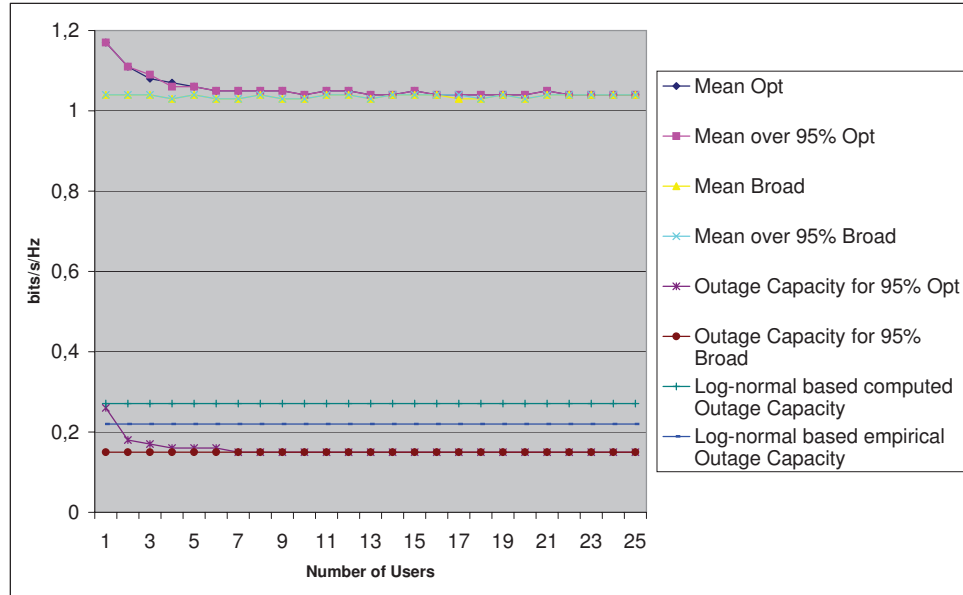


Figure 5.6: Mean capacity, Outage capacity for 95 % and Mean over 95 % for SNR 15 dB

parameterize with the mean and the variance obtained computing  $E[C]$  and  $Var[C]$ , the log-normal based computed capacity is  $0.27[bits/s/Hz]$ . In this case the log-normal distribution seems to be a good pdf to extrapolate the outage capacity. In Figure 5.6, we can see that the gain in percentage is 20 % for one user. But if we do the *percentage increase histograms* (Figure 5.7 on page 149 ), we observe that the mean of increase is 34 %. The means for the percentage increase for 2, 3, 4 and 5 users are 15.28%, 8.99%, 5.99% and 4.33%, respectively.

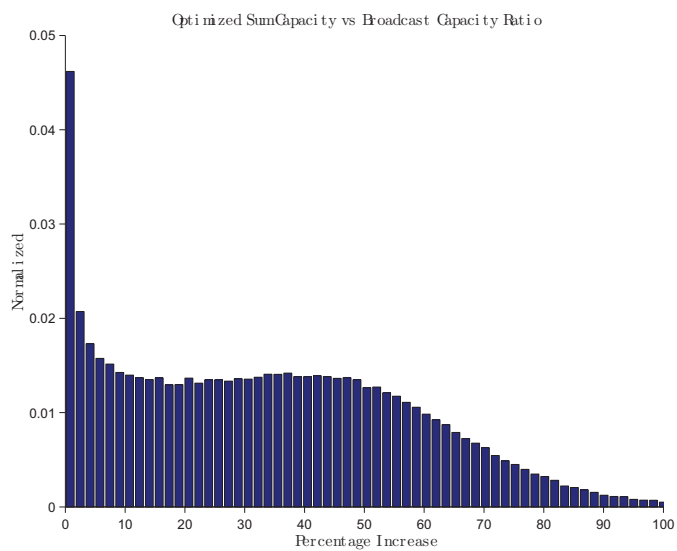
### 5.3 Conclusion

In this chapter we explore the capacity of the OFDM system with new elements. We consider that the user are distributed uniformly over a ball with a fixed radius from the base station. Following the goal of characterizing the outage probability, we derive expressions for the mean and the variance of the capacity under the studied scenario. These two quantities could be used to extrapolate the capacity distribution. From this distribution, the broadcast can be designed in order to ensure a certain quality of service. For example, the system can be tuned in order to ensure to a certain proportion of users and in a certain radio range a given capacity. Comparisons between the optimized and the classical broadcasts have shown that there is not a significant improvement in average. The mean capacity increases of 20 % for one user and decreases slowly with the number of users. Nevertheless, a deeper study of this improvement shows that for a major part of the users there is an important increase. But, it concerns users with small capacity that explains the poor improvement in average. However, this is an issue of practical importance, since the largest improvement is provided to the users with the smallest quality of service...

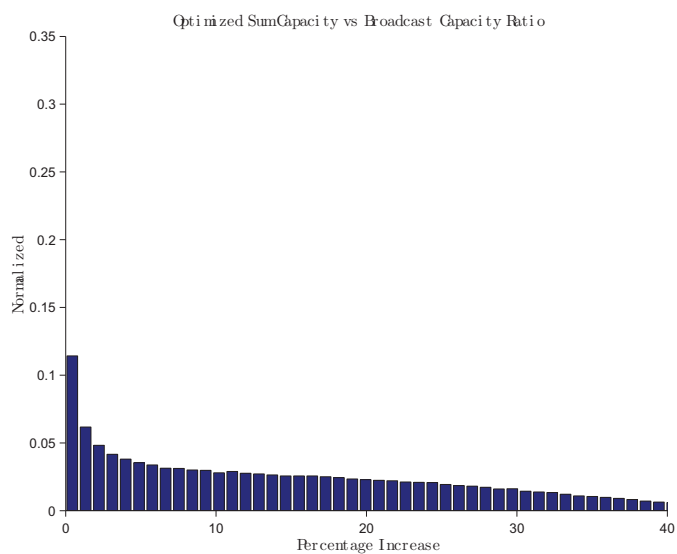
A topic that could extend this work would consist in comparing the capacity improvement with different spatial distributions. Indeed, it appeared clearly that the distance between the users and the BS impacts the capacity gain of the optimized case. Spatial distributions where the users are far from the BS should greatly increase the benefit of an optimized allocation power, whereas distributions where the users are gathered near the BS should lead to cases where this optimization is almost useless. It could be particularly interesting to collect real users spatial distributions and real scenarios, to have better insight of the situations where multicast is really worth the



additional complexity needed for the optimization.



(a) 1 User



(b) 2 User

Figure 5.7: Percentage increase at 15 dB

# Chapter 6

## Summary and Conclusions

The main subject of this thesis is the usefulness of the power allocation on a downlink OFDM communication where one aims at transmitting a common signal to all users, complemented by possible additional information, just like in layered source coding.

We first review SISO and MIMO OFDM schemes, with special emphasis on orthogonality. A special attention is put on the capacity of these schemes. Since our target is to obtain conclusions useful for practical situations, we focus on a description of the realistic parameters involved in channel modeling. This will also be useful in the final chapter on stochastic geometry. We first propose a power allocation at the transmitter in the MU-SISO case and extend our study to MU-MIMO OFDM scheme in the linear precoding case. Finally, we revisit the MU-SISO power allocation scheme with a stochastic geometry point of view, trying to find a closed-form expression evaluating the coverage area of an access point, in order that the users receive at least a minimum rate, given an outage probability constraint.

Such a study requires knowledge on many aspects, which are addressed in a background part.

Knowing that OFDM is a technique that provides strengths to the data transmission over the wireless medium, we first study how such system works. The orthogonality is obtained by the distribution of the signal over an orthogonal base, that permit to transform a wideband frequency selective channel into many narrowband parallel channels. This technique is widely used to face the impairments induced by scattered environments. The capacity for the SISO scheme is recalled, with an emphasis given to the classical waterfilling algorithm which allows to allocate optimally the power among the subcarriers. A state of the art is made on the MIMO case, and the corresponding capacity is reviewed. A characteristic of the MIMO case is that it exploits spatial diversity and multiplexing gain. The focus is put on the multiplexing gain since is the property that will be used in the MU-MIMO power allocation. The multiuser case is still an subject of interest in communication theory. We review different approaches such as Costa's "writing on dirty paper" for the MU-SISO scheme and the "Zero-Forcing" method for the MU-MIMO. We also put a glance on how we will simulate a realistic channel, taking in account the large scale fading and the fast fading channels in our model. We took also realistic parameters used on actual devices, to have a fine sight onto the actual performance.

Our contributions are of three kinds and concern the extension of known results to resource allocation to the multi-user case:

Since the flexibility of the OFDM allows to develop simple practical resource allocation algorithms, we propose a simple power allocation algorithm in the MU-SISO case. Even if this algorithm has no explicit form as the waterfilling algorithm, it has a very simple structure, and guaranteed convergence. Simulations demonstrate that our algorithm performs a substantial capacity improvement compared to the uniform

power allocation. We perform a statistical study and perform the histogram of the capacity obtained by the users in terms of their distance to the access point. As expected, when the number of user grows, the optimization does not gives much improvement, and uniform power allocation is the best option. However, for reasonable number of users (typically up to at least 5), sum-rate improvements are obtained, at very little cost. it has to be noted that the largest improvements are for "bad" users", which is a very interesting characteristic: this allows more users to join the communication.

The MU-MIMO case presents constraints that makes the problem difficult to handle. The diversity and the multiplexing gain present wide subject of study over the field. We study the main lines on the background and decide to extend the work of Kaviani [38] to the OFDM case. We develop an power allocation algorithm under the constraint tht the transmitter implements a linear zero forcing precoder. The constraints put by the dimensionality of the MIMO scheme limits the number of users that can simultaneously be addressed. These constraints involve the number of antenna, either on the transmitter or on the receiver and the number of simultaneous users. Overall, for all feasible situations, the power optimization algorithm provides substantial improvements over equal power allocation..

The coverage question is finally discussed. The probability density distribution of the location of the user and the channel are taken into account. The goal was obtain a characterization of the pdf of the capacity in order to calculate the outage capacity given an outage probability constraint. We derive expressions for the mean and the variance of the capacity under the studied scenario. An interesting topic to explore is use the mean and the variance to parameterize a known pdf function that

can be close to the empirical distribution of the capacity. That will allow, with two single parameters, to set a quick evaluation on at which data rate we can transmit on a given environment. We perform numerical simulations. The simulations does not give results that permit to distinguish clearly if the optimization is good or not. Mainly because the bad realizations mask the good ones, and the interpretation of the results are fuzzy. By other hand, a good comparison can be made using the means of the realizations.

# Bibliography

- [1] Ieee standard for local and metropolitan area networks part 16: Air interface for broadband wireless access systems, May 29 2009.
- [2] 3GPP. 3gpp ts 36.300 v8.5.0; technical specification group radio access network; e-utra and e-utran overall description : stage 2 (release 8), December 2008.
- [3] 80211nIEEE. Ieee standard for information technology–telecommunications and information exchange between systems–local and metropolitan area networks–specific requirements part 11: Wireless lan medium access control (mac) and physical layer (phy) specifications amendment 5: Enhancements for higher throughput, oct. 2009.
- [4] J.A.C. Bingham. Multicarrier modulation for data transmission: an idea whose time has come. *Communications Magazine, IEEE*, 28(5):5–14, may 1990.
- [5] K. Bouchireb and P. Duhamel. Transmission schemes for scalable video streaming in a multicast environment. In *Wireless Communications and Mobile Computing Conference, 2008. IWCMC '08. International*, pages 419–424, aug. 2008.
- [6] Stephen Boyd and Lieven Vandenberghe. *Convex Optimization*. Cambridge University Press, March 2004.

- [7] G. Caire and S. Shamai. On achievable rates in a multi-antenna broadcast downlink. *38th Annu. Allerton Conf. Communication, Control and Computing*, Oct 2000.
- [8] G. Caire and S. Shamai. On achievable rates in a multi-antenna gaussian broadcast channel. In *Proc. IEEE Int Information Theory Symp*, 2001.
- [9] G. Caire and S. Shamai. On the achievable throughput of a multiantenna gaussian broadcast channel. *IEEE Transaction on information theory*, 49(7):1691–1706, July 2003.
- [10] G. Caire, P. D. Torino, and E. Biglieri. Capacity of multi-antenna block-fading channels. In *Proc. Communication Theory Mini-Conf*, pages 11–15, 1999.
- [11] Robert W. Chang. Synthesis of band-limited orthogonal signals for multichannel data transmission. *Bell Systems Technical Journal*, 45:1775–1796, December 1966.
- [12] Y.S. Cho, J. Kim, W.Y. Yang, and C.G. Kang. *MIMO-OFDM Wireless Communications with MATLAB*. John Wiley & Sons, 2010.
- [13] Lai-U Choi and R. D. Murch. A transmit preprocessing technique for multiuser mimo systems using a decomposition approach. 3(1):20–24, 2004.
- [14] Jr. Cimini, L. Analysis and simulation of a digital mobile channel using orthogonal frequency division multiplexing. *Communications, IEEE Transactions on*, 33(7):665 – 675, jul 1985.
- [15] Max Costa. Writing on dirty paper. *IEEE Transactions on Information Theory*, 29(3):439–441, May 1983.



- [16] Thomas M. Cover. Broadcast channels. *IEEE Transactions on Information Theory*, IT-18(1):2–14, January 1972.
- [17] Thomas M. Cover and Joy A. Thomas. *Elements of Information Theory*. Wiley, second edition, July 2006.
- [18] T.M. Cover. Comments on broadcast channels. *Information Theory, IEEE Transactions on*, 44(6):2524–2530, October 1998.
- [19] Wilbur B. Davenport and William L. Root. *An Introduction to the Theory of Random Signals and Noise*. McGraw-Hill Book Company, 1958.
- [20] Vinko Erceg, Larry J. Greenstein, Sony Y. Tj, Seth R. Parkoff, Ajay Gupta, Boris Kulic, Arthur A. Julius, and Renee Bianchi. An empirically based path loss model for wireless channels in suburban environments. *IEEE Journal on Selected Areas in Communications*, 17:1205–1211, 1999.
- [21] Vinko Erceg, K. V. S. Hari, M.S. Smith, and Daniel S Baum. Channel models for fixed wireless applications. *Contribution to IEEE 802.16.3*, july 2001.
- [22] Robert F.H. Fischer, Christoph Windpassinger, Alexander Lampe, and Johannes B. Huber. Space-time transmission using tomlinson-harashima precoding. In *Proceedings of 4. International ITG Conference on Source and Channel Coding(SCC)*, pages 139–147, Berlin, Germany, January 2002.
- [23] G. J. Foschini and M. J. Gans. On limits of wireless communications in a fading environment when using multiple antennas. *Wireless Personal Communications*, 6:311–335, 1998.

- [24] Gerard J. Foschini. Layered space-time architecture for wireless communication in a fading environment when using multi-element antennas. *Bell Labs Tech. J.*, 1(2):41–59, 1996.
- [25] R.G. Gallager. Capacity and coding for degraded broadcast channels. *Probl. Peredachi Inf.*, 10(3):3–14, July-Sept 1974.
- [26] A. A. El Gamal. Capacity of the product and sum of two unmatched broadcast channels. *Probl. Peredachi Inf.*, 16:3–23, 1980.
- [27] D. Gesbert, M. Kountouris, R. W. Heath, Chan-Byoung Chae, and T. Salzer. Shifting the mimo paradigm. 24(5):36–46, 2007.
- [28] Ramy H. Gohary and Timothy N. Davidson. On power allocation for parallel gaussian broadcast channels with common information. *EURASIP Journal on Wireless Communications and Networking*, 2009.
- [29] A. Goldsmith. *Wireless Communications*. Cambridge University Press, September 2005.
- [30] A. Goldsmith, S.A. Jafar, N. Jindal, and S. Vishwanath. Capacity limits of mimo channels. *Selected Areas in Communications, IEEE Journal on*, 21(5):684 – 702, june 2003.
- [31] H. Harashima and H. Miyakawa. Matched-transmission technique for channels with intersymbol interference. *Communications, IEEE Transactions on*, 20(4):774 – 780, aug 1972.
- [32] M. Hata. Empirical formula for propagation loss in land mobile radio services. *IEEE Transactions on Vehicular Technology*, 29:317–325, 1980.

- [33] Roger A. Horn and Charles R. Johnson. *Matrix Analysis*. Cambridge University Press, February 1990.
- [34] Jiho Jang and Kwang B. Lee. Transmit power adaptation for multiuser ofdm systems. *Selected Areas in Communications, IEEE Journal on*, 21(2):171–178, 2003.
- [35] Nihar Jindal. *Multi-User Communication Systems: Capacity, Duality, and Cooperation*. PhD thesis, Stanford University, July 2004.
- [36] Nihar Jindal, Sriram Vishwanath, and Andrea Goldsmith. On the duality of multiple-access and broadcast channels. In *Channels, Allerton Conference on Commun., Control, and Computing*, pages 3–5, 2001.
- [37] M. Joham, W. Utschick, and J.A. Nossek. Linear transmit processing in mimo communications systems. *Signal Processing, IEEE Transactions on*, 53(8):2700 – 2712, aug. 2005.
- [38] S. Kaviani and W. A. Krzymien. On the optimality of multiuser zero-forcing precoding in mimo broadcast channels. In *Proc. IEEE 69th Vehicular Technology Conf. VTC Spring 2009*, pages 1–5, 2009.
- [39] Jan R. Magnus and Heinz Neudecker. *Matrix differential calculus with applications in statistics and econometrics*. John Wiley & Sons, 2nd edition, 1999.
- [40] K. Marton. A coding theorem for the discrete memoryless broadcast channel. *Information Theory, IEEE Transactions on*, 25(3):306 – 311, may 1979.
- [41] J. Medbo and P. Schramm. Channel models for hiperlan/2 in different indoor scenarios, 1998.

- [42] T. Minka. Old and new matrix algebra useful for statistics, 1997.
- [43] A.F. Molisch. *Wireless Communications*. Wiley - IEEE. John Wiley & Sons, 2005.
- [44] Richard van Nee and Ramjee Prasad. *OFDM for Wireless Multimedia Communications*. Artech House, Inc., Norwood, MA, USA, 2000.
- [45] Loutfi Nuaymi. *WiMAX: Technology for Broadband Wireless Access*. Wiley-Blackwell, January 2007.
- [46] Y. Okumura, E. Ohmori, T. Kawano, and K. Fukuda. Field strength and its variability in vhf and uhf land mobile service. *Rev. Elec. Comm. Lab*, 16:825, September-October 1968.
- [47] Alan V. Oppenheim, Ronald W. Schaffer, and John R. Buck. *Discrete-Time Signal Processing (2nd Edition) (Prentice-Hall Signal Processing Series)*. Prentice Hall, 2 edition, January 1999.
- [48] L. H. Ozarow, S. Shamai, and A. D. Wyner. Information theoretic considerations for cellular mobile radio. 43(2):359–378, 1994.
- [49] Patrice Pajusco. Propagation channel models for mobile communication. *Comptes Rendus Physique*, 7(7):703 – 714, 2006. Towards reconfigurable and cognitive communications.
- [50] A. Paulraj, R. Nabar, and D. Gore. *Introduction to Space-Time Wireless Communications*. Cambridge University Press, 2003.

- [51] Christian B. Peel, Bertrand M. Hochwald, and A. Lee Swindlehurst. A vector-perturbation technique for near-capacity . . . *IEEE TRANS. COMMUN*, 53(1):195–202, 2005.
- [52] A. Peled and A. Ruiz. Frequency domain data transmission using reduced computational complexity algorithms. In *Acoustics, Speech, and Signal Processing, IEEE International Conference on ICASSP '80.*, volume 5, pages 964 – 967, apr 1980.
- [53] Eldad Perahia and Robert Stacey. *Next Generation Wireless LANs: Throughput, Robustness, and Reliability in 802.11n*. Cambridge University Press, 2008.
- [54] Bernard Picinbono. Second-order complex random vectors and normal distributions. *IEEE Transactions on Signal Processing*, 44(10):2637–2640, October 1996.
- [55] John G. Proakis and Masoud Salehi. *Digital Communications*. Mc Graw-Hill, fifth edition, 2008.
- [56] Theodore Rappaport. *Wireless Communications: Principles and Practice*. Prentice Hall PTR, Upper Saddle River, NJ, USA, second edition, 2002.
- [57] Simon R. Saunders. *Antennas and Propagation For Wireless Communication Systems*. Wiley, 1999.
- [58] John S. Seybold. *Introduction to RF Propagation*. Wiley, 2005.
- [59] Claude E. Shannon. A mathematical theory of communication. 1948.

- [60] Q. H. Spencer, A. L. Swindlehurst, and M. Haardt. Zero-forcing methods for downlink spatial multiplexing in multiuser mimo channels. 52(2):461–471, 2004.
- [61] A. Steiner and S. Shamai. The broadcast approach in communications systems. In *Electrical and Electronics Engineers in Israel, 2008. IEEEI 2008. IEEE 25th Convention of*, pages 006 –010, dec. 2008.
- [62] Dietrich Stoyan, Wilfrid S. Kendall, and Joseph Mecke. *Introduction to Stochastic Geometry*. John Wiley & Sons, 1987.
- [63] G.L. Stuber, J.R. Barry, S.W. McLaughlin, Ye Li, M.A. Ingram, and T.G. Pratt. Broadband mimo-ofdm wireless communications. *Proceedings of the IEEE*, 92(2):271 – 294, feb 2004.
- [64] Andrew Tanenbaum. *Reseaux*. Pearson Education France, Paris, 4 edition, 2003.
- [65] I. Emre Telatar. Capacity of multi-antenna gaussian channels. *EUROPEAN TRANSACTIONS ON TELECOMMUNICATIONS*, 10:585–595, 1999.
- [66] M. Tomlinson. New automatic equaliser employing modulo arithmetic. *Electronics Letters*, 7(5-6):138–139, 1971.
- [67] D. N. Tse. Optimal power allocation over parallel gaussian broadcast channels. In *Proc. Symp. IEEE Int Information Theory 1997*, 1997.
- [68] David Tse and Pramod Viswanath. *Fundamentals of Wireless Communications*. Cambridge University Press, New York, NY, USA, 2005.
- [69] A. van den Bos. The multivariate complex normal distribution-a generalization. *IEEE Transactions on Information Theory*, 41(2):537–539, March 1995.

- [70] E. van der Meulen. A survey of multi-way channels in information theory: 1961-1976. *Information Theory, IEEE Transactions on*, 23(1):1–37, 1977.
- [71] S. Vishwanath, N. Jindal, and A. Goldsmith. Duality, achievable rates, and sum-rate capacity of gaussian mimo broadcast channels. *Information Theory, IEEE Transactions on*, 49(10):2658 – 2668, oct. 2003.
- [72] Sriram Vishwanath, Nihar Jindal, and Andrea Goldsmith. On the capacity of multiple input multiple output broadcast channels. In *In Proceedings of Int. Conf. Commun*, pages 1444–1450, 2002.
- [73] H. Weingarten, Y. Steinberg, and S. Shamai. The capacity region of the gaussian multiple-input multiple-output broadcast channel. 52(9):3936–3964, Sept. 2006.
- [74] Hanan Weingarten. On the compound mimo broadcast channel. In *in Proceedings of Annual Information Theory and Applications Workshop UCSD*, 2007.
- [75] S. Weinstein and P. Ebert. Data transmission by frequency-division multiplexing using the discrete fourier transform. *Communication Technology, IEEE Transactions on*, 19(5):628 –634, october 1971.
- [76] J. Winters. On the capacity of radio communication systems with diversity in a rayleigh fading environment. *Selected Areas in Communications, IEEE Journal on*, 5(5):871 – 878, jun 1987.
- [77] Cheong Y. Wong, R. S. Cheng, K. B. Lataief, and R. D. Murch. Multiuser ofdm with adaptive subcarrier, bit, and power allocation. *Selected Areas in Communications, IEEE Journal on*, 17(10):1747–1758, 1999.

- [78] W. Yu and W. Rhee. Degrees of freedom in wireless multiuser spatial multiplex systems with multiple antennas. *IEEE Transactions on Communications*, pages 1747–1753, 2006.
- [79] Wei Yu and J. M. Cioffi. Trellis precoding for the broadcast channel. *Proceedings of the IEEE globecom*, page 133844, November 2001.
- [80] Wei Yu and J. M. Cioffi. Sum capacity of gaussian vector broadcast channels. *IEEE Transactions on information theory*, 50(9):1875–1892, Sept. 2004.
- [81] Wei Yu, W. Rhee, S. Boyd, and J. M. Cioffi. Iterative water-filling for gaussian vector multiple access channels. In *Proc. IEEE Int Information Theory Symp*, 2001.